

RIGA TECHNICAL UNIVERSITY

Faculty of Power and Electrical Engineering

Institute of Power Engineering

Shaker Jassem Gatan

Doctoral Student of the Study Programme “Power and Electrical Engineering”

**A NEW DESIGN OF M.V – VACUUM CIRCUIT
BREAKER – WITH AUXILIARY UNITS
DAMPING TECHNIQUES FOR SOFT
INTERRUPTER APPLICATIONS**

Doctoral Thesis

Scientific supervisor
Associated Professor Dr. sc. ing.
ANDREJS PODGORNOVS

Riga 2019

INTRODUCTION

The dissertation is made with the intention for develop an optimization methodology to create a static switching interrupter-for medium voltage application. Based on the designing and modification of Petersen Reactor Coils Automatic Tuning & inserting of LTT Thyristors for damping technique -main task.

Because of RTU university does not have M.V Laboratory for making sample(s) or verifying of the processes on switching Interrupter. Moreover, the dissertation is analysis of the existing samples for the real experiments. For an instance, some researching papers from the Institute of Electrophysical Apparatus -St. Petersburg, Los Alamos National Laboratory, Behlike Power Electronics LLC -Hamburg / Germany and others.

The work is written in English and Latvian – 103 pages long. Its parts which are, introduction ,3 chapters with main conclusions and four scientific appendixes ,118 scientific information sources including several of industrial samples for both of international academic universities and global industrial firms.

Introduction, the topically of the work was studying, fabricating and analysis the existing of “Petersen Reactor Coils Automatic Tuning” for damping of arcing currents and chopping currents by inserting of a set of LTT Lighted triggered thyristors.

1st chapter- the terminology issues are described as followings:

- Sample of the existing vacuum interrupter, MATLAB Switching experiment test and one sample achievement for simplifying of my dissertation.
- Create switching parameters, with some descriptions in the characteristics both of capacitive currents interrupter and inductive currents interrupter.For the purpose of more understanding of technical behavior inside interrupter.
- One prototype was proved that the commutation transition processes di/dt & du/dt of the materials, switching time process I_{ss} .
- Fabricated of the radial magnetic field to being rotate as the basic theory of Petersen coil for implementing my thesis.

2nd chapter includes of the followings:

- Collecting of data sheets in details for contacting metallurgical materials of vacuum interrupter in M.V applications.
- Classification of vacuum arcs – G.R Mitchel -IEEE standard.
- Calculating of joule heating inside vacuum Interrupter.
- Basically, my thesis depends on Harris model as prototype.
- Mathematical Fourier transformation model, an intervene among arcing currents, chopping currents and transients when come together as negative consequences occurred.

- Calculating of maximum values of chopping currents-experimental tests as a real test on one of the existing Petersen coils with ABB, last 2016 on Norway.
- Calculating of NSD discharging switching times.

3rd chapter contains

- Designing and fabricating stages of Petersen Reactor Coil Automatic Tuning.
- Inserting of LTT experiment test.
- Synthesis of mathematical model, my proposal for damping process.
- One single line diagram proposed, MATLAB experiment damping test.

In the last part – main conclusions – with four Appendices- the most important part which describes the pioneers whom were constructing of many samples and highlighted them in short recommendations. Finally, this novelty was only analysis of the other researchers for prove my dissertation.

CONTENTS

I. MEDIUM VOLTAGE SWITCHING PARAMETERS

1.1 Switching parameters	06
1.2 Switching characteristics and multiple voltage escalation	07
1.3 Capacitive current Interrupter.....	09
1.4 Inductive current Interrupter.....	12
1.5 Experiment test one – Transition Rate of di/dt	16
1.6 Experiment test two – Formation of Radial Magnetic Field	19
1.7 Conclusions	22

II. CONTACTING MATERIALS OF M.V SWITCHING

2.1 Analysis of technical materials inside vacuum interrupter.....	23
2.2 Types of vacuum arcs	25
2.3 Calculating of Joule heating in vacuum interrupter.....	29
2.4 Synthesis of mathematical model	31
2.5 Electrode effects and break- down	32
2.6 Transient over voltages formula	35
2.7 Mathematical Fourier transformation model.....	39
2.8 Experiment test for calculating of chopping currents.....	42
2.9 Calculating of NSD discharging times – Experiment Test	46
2.10 Conclusions	49

III. DESIGN CIRCUIT & MATHEMATICAL APPLICATIONS

3.1 Hypothesis of static vacuum Interrupter	50
3.1.1 Analysis the designing of the existing Petersen Coil Automatic Tuning.....	50
3.1.2 Fabricating of Petersen Coil -Anode & cathode Coils.....	50
3.1.3 Inserting of LTT damping circuit.....	57
3.1.4 Synthesis of mathematical model.....	58
3.1.5 Synthesis of MATLAB/Simulink models.....	61
Appendices.....	63
Appendix 1 – Damping Mathematical Application	63
Appendix 2 – Splitting of Arcing Currents – Power Electronics -Experiment Test.....	69
Appendix 3 – Pulse Power Equipment by LTT Thyristor	81
Appendix 4 – Transition of Switching Rates du/dt & di/dt for Snubber Application.....	85
References	95

SCOPE OF RESEARCH

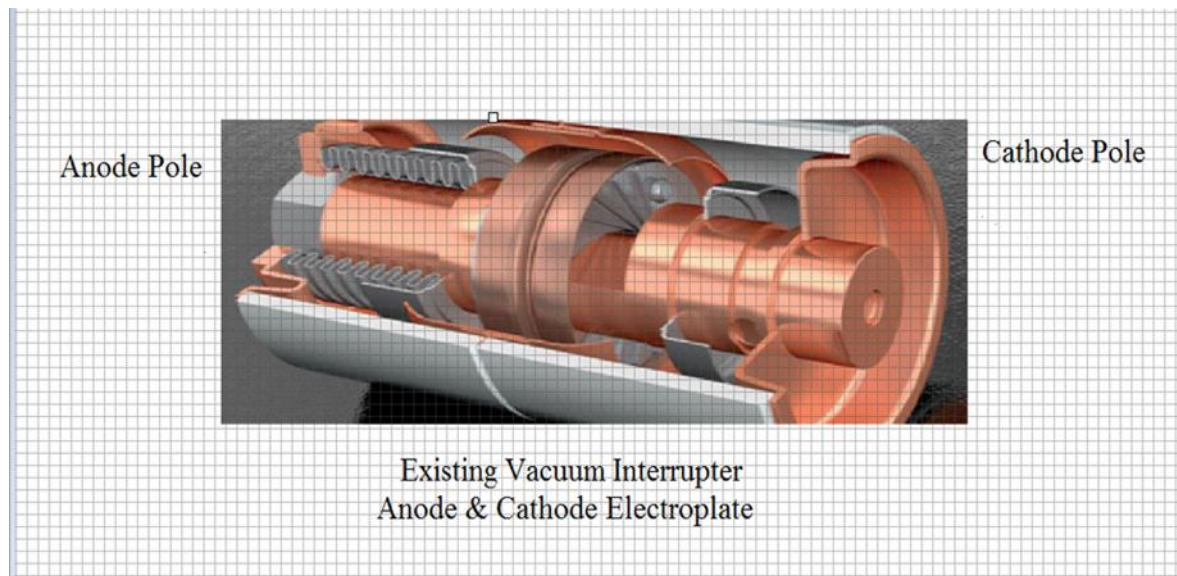


Fig 1.1 Vacuum circuit breaker under researching project for soften interrupter

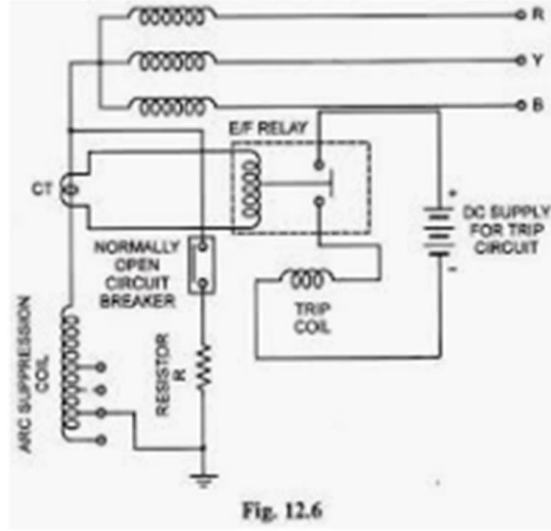


Fig 1.2 Petersen Reactor Coil under fabricating of industrial researching project
[Fabricating Petersen Reactor Coils – modifying steps by inserting of LTT damping process]
[My proposed theory]

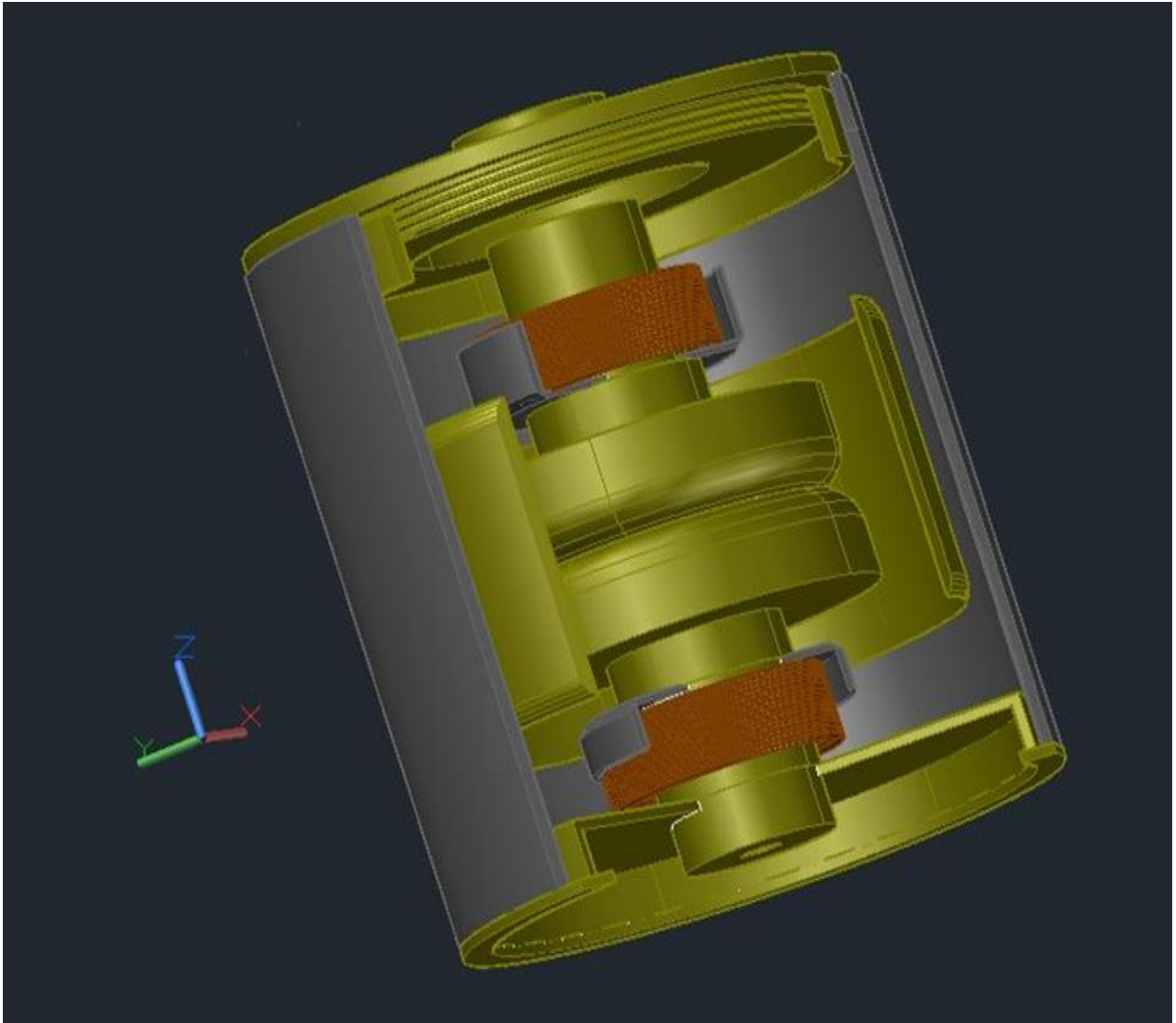


Fig.1.3 Fabricated Petersen Reactor Coils - Anode Pole & Cathode Pole
[The purpose of the axial magnetic field rotates instantaneously during interrupter
Processing of Arcing currents & chopping current]

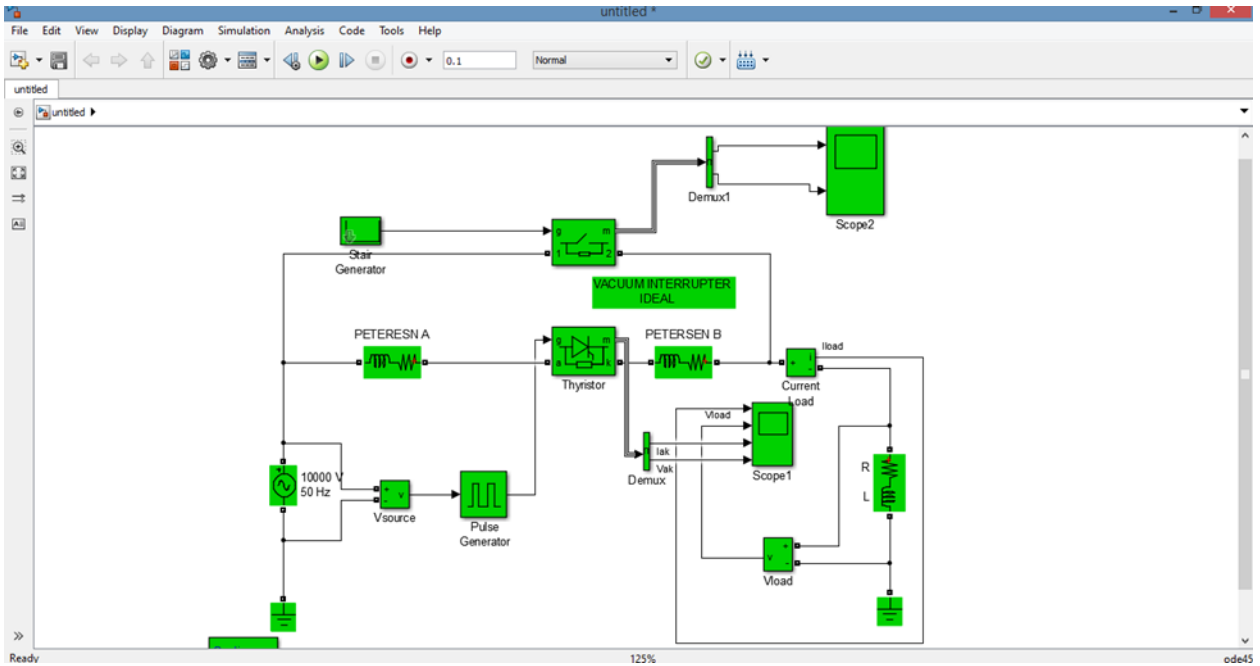


Fig.1.4 MATLAB/ Simulink: Fabricated Petersen Reactor Coil Automatic Tuning -Anode Pole & Cathode Poles including of Inserting Rectifying LTT set for attenuating inside cathode Petersen Coil.

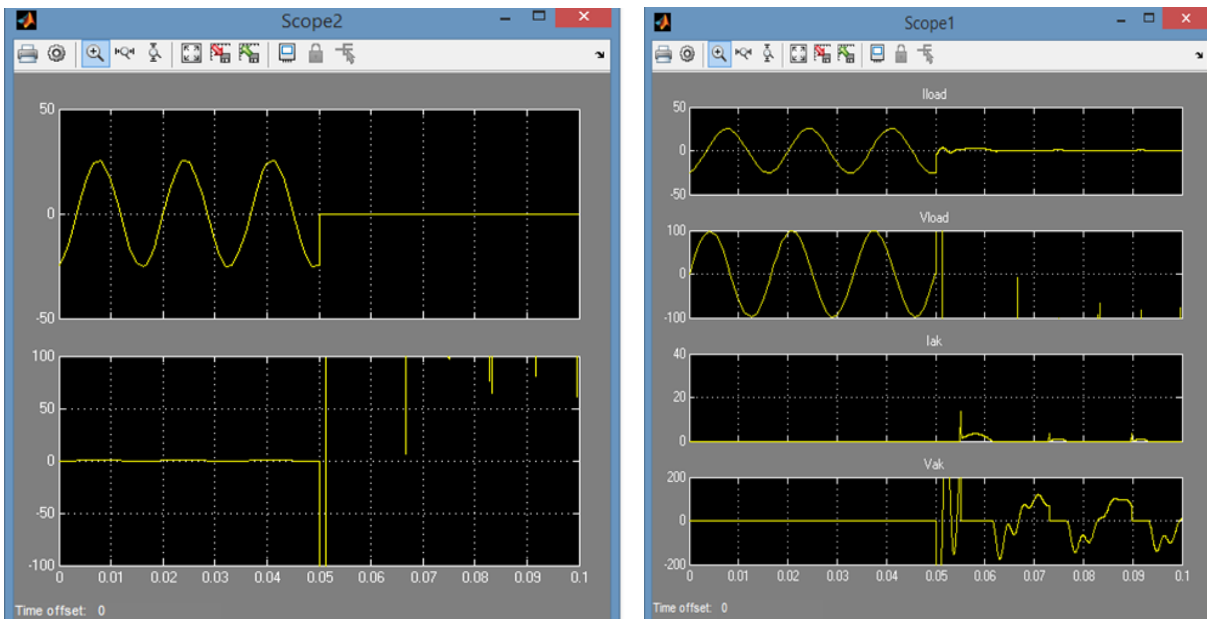


Fig. 1.5 Analysis of switching Interrupter times -MATLAB Verifying of time switching interrupter- Harris model

I. MEDIUM VOLTAGE SWITCHING PARAMETERS

The main reason of each insulation damages in medium voltage machines is the repeating of medium voltage switching processing interrupter –in addition there are further grounding discharging occurrences “Ecto- parasites and Endo parasites capacitors” either highly- rate- of rise of arcing currents or as voltage escalation in the vacuum itself:

1.1. Switching parameters

All the switching interrupter mechanism has three negative parameters which must be controlled to ensure safe application of vacuum circuit breaker;

- A) Arcing currents
- B) Chopping currents.
- C) Transient voltage rates & changing the frequency.

The over voltage magnitude is a straightforward concept; as the amplitude of any over voltage increases, the probability of breakdown in air, or the breakdown of solid insulation increases. Transient voltages rate –of –rise are important because very fast rising transients can cause the overvoltage to be non-uniformly distributed in Motors/Transformer windings. For example, a voltage transient within $0.2\mu\text{s}$, rise time may result in 80% to 100% of a voltage surge appearing across the first coil of a multi-coil motor windings [2][3][5] .

If there were 6 coils in a winding, the turns of first coil could be stressed 6 times higher than if the transient was slow rising . Consequently, a surge whose magnitude is well below could damage the inter-turn insulation of the first coil of the windings. An important factor to consider is that, even if the non-uniform distribution in a winding does not actually result in a failure of the inter-turn insulation repetitive fast –rising transients can gradually degrade insulation to the possible point of failure over a long period of time.

The multiple reignition –Impulses (static phenomenon) can cause winding insulation to be subjected to fast –transients more frequently with vacuum switchgear several times per switching event –than with other types of switchgear. It is therefore, important to determine those applications where fast transients could cause problems, and to take appropriate measures to control the voltage rate-of-rise in those applications.

In discussion of switching transients, there are three different frequencies which are describe the phenomena;

In the first step is the source power frequency -50Hz.

In the second when the normal load transient over voltage, normally in the range from (150 Hz & 400Hz), it generates inside vacuum tube due to endo parasites because the mechanical switching malfunction creates disturbances in the transition process.

The third factor has also to be more considered, namely the capacitors which generate between the lines and to ground, normally they are very dangerous phenomenon when the vacuum interrupting process, Ecto -parasites. “I am calling here stray capacitance” [9].

This normal voltage frequency is governed by the effective inductance of the load and the effective capacitance from load terminal to ground; this capacitance may have three components – terminal bushing to ground capacitance, cable capacitance, and a surge capacitor if one is providing at load.

The forth is that due to high frequency reignitions. Note that in all systems, irrespective of what type of breaker – vacuum circuit breaker – is used, high frequency currents are caused to flow whenever the breaker reignitions or prestrikes.

The value of frequency is determined by the effective capacitance at the load and the effective inductance of the cable between breaker and load. When a reignition, restrike, or prestrike occurs in the vacuum device, the collapse of voltage across the breaker injects a voltage surge into the cable/load system. This surge is reflected at the load terminal, returns to the source/breaker end of the system, and travels back and forth along the cable and all inductive loads many times until attenuated by losses [10].

The frequency of the current is related to the travel/return frequency of reflected surge propagated back and along the cable; the frequency is directly proportional to cable length, modified by resistive and reflective attenuation losses. Typical value of high frequency vary in the range over 2MHz for 25meters of cable giving 0.2 μ s rise time, to over 50KHz for 750 meters to cable with almost 10 μ s rise-time [11][12].

1.2 Switching characteristics and multiple voltage escalation

When a switching interrupts the current at power frequency, the current does not come to zero smoothly directly that will be raised to the value abruptly with the arc becomes unstable causing the current to be interrupted abruptly and prematurely. Furthermore, the original frequency was not be stable; some researchers shown that the next poles-L2&L3 would be raising *150Hz and 400 Hz* during chopping process such an event is called a current chop and this phenomenon is referred to as current chopping.

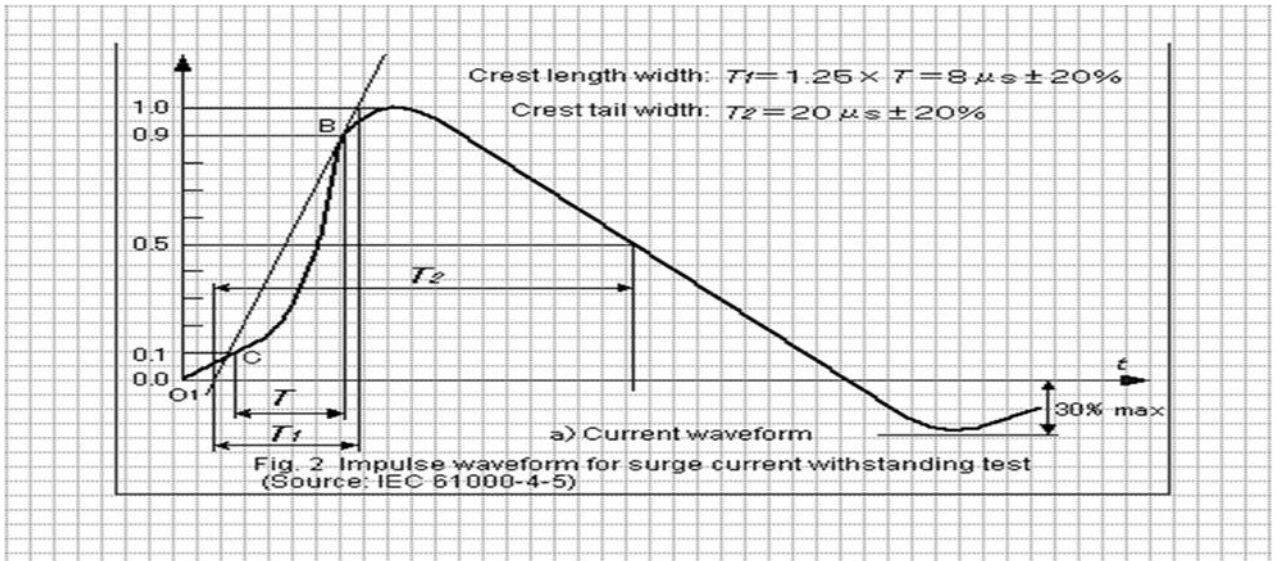


Fig 1.6 Switching of voltage wave shape ;1.2/50μs [General Specification]

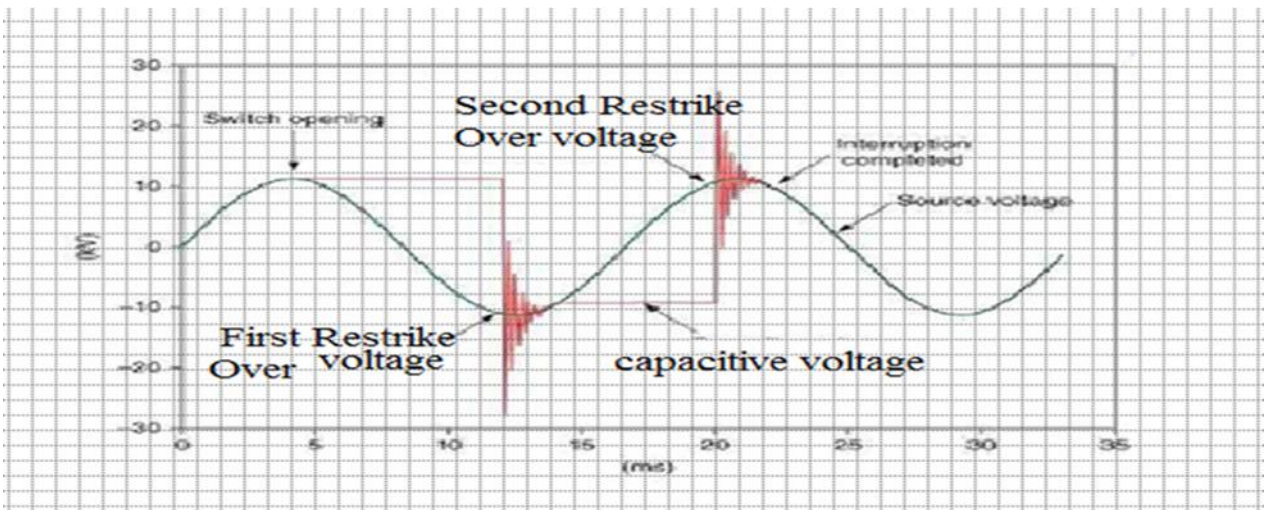


Fig. 1.7 Restrikes of over voltages [Negative occurrence inside vacuum interrupter]

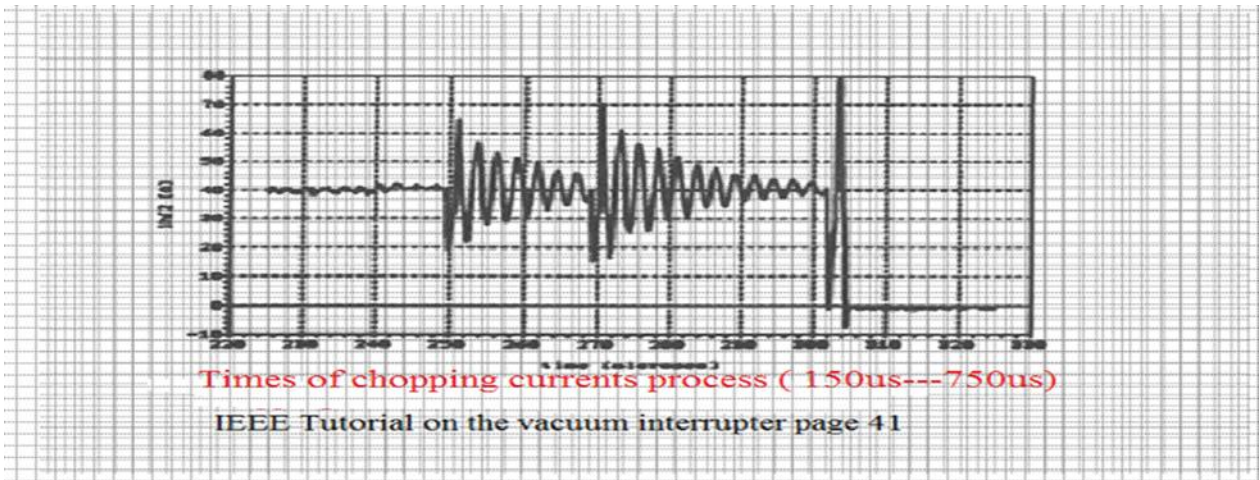


Fig. 1.8 Chopping currents Phenomenon inside interrupter[Novelty]
Oscillating phenomenon among arcing currents and chopping currents

1.3 Capacitive current Interrupter

Capacitive current arises in a number of situations: Current that is drawn by overhead lines the load of which is not connected (unloaded lines). This current is usually very small (in the order of 10 A). Current that is drawn by unloaded cables. The value of this current depends much on the length of the connected cable circuits. As an order of magnitude values of several tens of amperes are normally encountered. Current drawn by capacitor banks used for voltage stability reasons and/or power factor correction. This current is usually much higher than in the situations above (a few hundred of amperes).

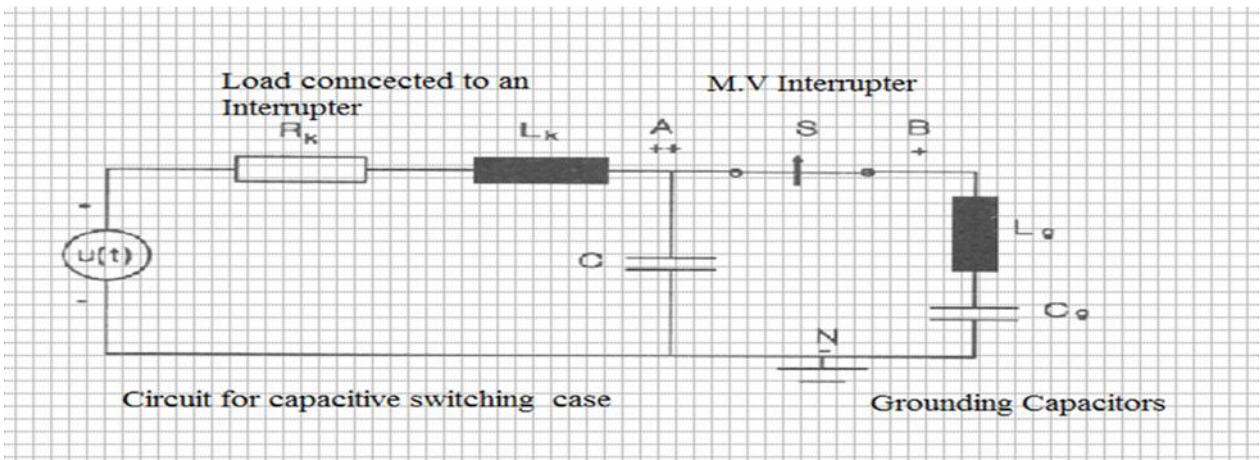


Fig.1.9 Circuit for capacitive switching load

Because the interruption of (the small) capacitive current is not a severe duty in itself, the current can easily be interrupted when the contact distance is small, or in other words, at short arcing times. This is in contrast to the interruption of short-circuit current, in which case a

(sometimes considerable) minimum contact distance (or minimum arcing time) is necessary to accomplish the interruption [23][100] .

A small contact distance at interruption of current implies that the full contact distance in open position is not yet reached when the maximum of recovery voltage is stressing the circuit breaker. Therefore, a breakdown of the contact gap can occur. Such a breakdown - due to the full 2pu-per unit system ; recovery voltage over the not yet fully opened contact gap - is commonly called "restrike", provided that the breakdown occurs later than 1/4 of the power frequency period. In case the breakdown occurs earlier than 1/4period, the breakdown is called "reignition".

Restrikes are highly unwanted, because they can generate over voltages and produce steep voltage fronts that can influence secondary parts of the installation, if not properly designed from an EMC point of view. Also, damage to the breaker is not excluded, although SF6 breakers (puncture of the nozzle) are more prone to damage by restrike events than vacuum breakers. In the case of a restrike, high-frequency currents result, due to the discharge of the capacitive load (C_g in fig.1.4) over the equivalent circuit inductance L_k . Also, current components of higher frequency are present Since vacuum interrupters have an excellent capability to interrupt such a high-frequency current, it is probable that after only a few loops this current is interrupted, giving rise to the situation as depicted in fig.1.5. Does the vacuum interrupter interrupt the high-frequency current after an odd number of loops?

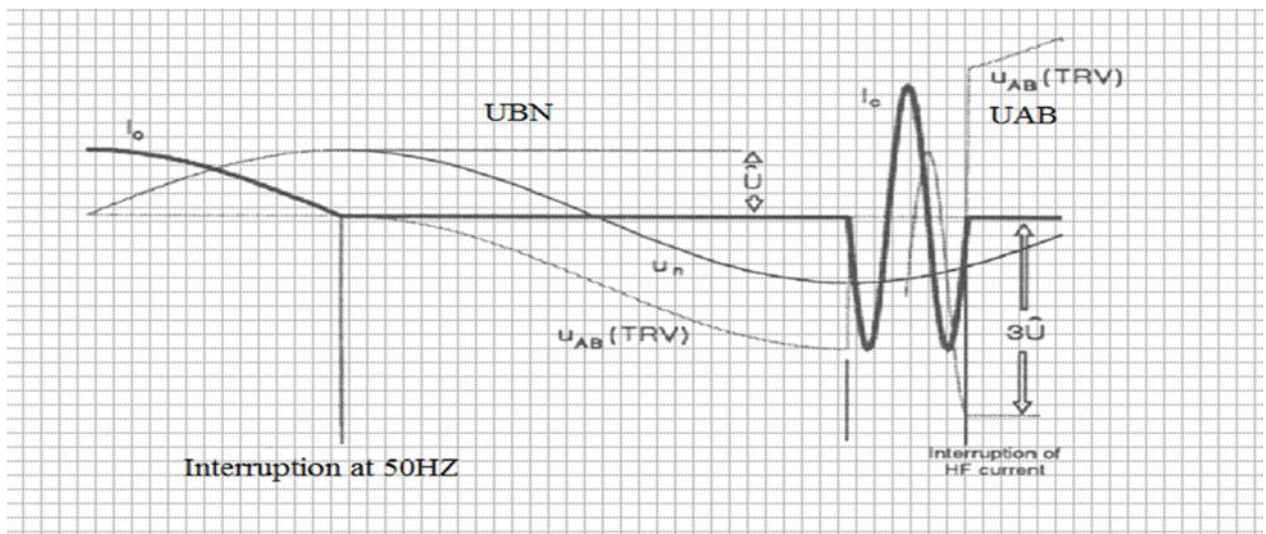


Fig. 1.10 Transient over voltages of capacitive current[Inside vacuum interrupter]

than the trapped voltage on the capacitive load is augmented to 3 pu (see fig.1.5) yielding a voltage of 4 pu. over the interrupter one loop of power frequency current later. New restrike near this instant causes a new reignition current, but now with twice the amplitude, leaving now 5pu trapped on the load capacitor when again interrupted after an odd number of loops. In theory, very

large over voltages can be generated, but to damping and leakage of charge the situation is less dramatic in real networks. This scenario of "voltage escalation", though very improbable to occur exactly along the line of sequences as sketched above, is more likely to occur in the application of vacuum interrupters than with interrupters based on other technologies (oil, SF6), due to the vacuum interrupters' excellent ability to interrupt high-frequency current. For this reason, "vacuum" is often termed a hard interrupter in contrast to the "softer" SF6 and oil interrupters. Energizing a capacitor bank will cause large transient current - the so-called inrush current - to flow starting at the moment of breakdown (pre-strike) of the approaching contacts.

This current will flow until galvanic touch of the contacts causing a thermal stress of the contacts in vacuum that is depending on the rate of change (di/dt) of this current. At low values of di/dt the inrush current will not reach a high value during the relatively short period of restriking (order of a ms normally in vacuum) . Is the value of di/dt high, then a high current corresponding to a high arcing energy is present between the closing contacts, easily leading to welding of the (very clean) vacuum contact.

In most cases the opening mechanism is designed to break such a weld, but sharp metallic protrusions, always remain. The action of the arc that follows at the opening of the contact is beneficial, as it burns away or re melts (parts) of these protrusions. In cases though of no arc at all (cold opening) or small current interruption, such an electric smoothing or polishing of the contacts fails to appear degrading the insulation of the gap due to the presence of remnants of the energizing operation important factors thus are: rate of rise (or frequency) of current magnitude of inrush current duration of pre-arcing period (depending on system voltage and state of the vacuum interrupters' contacts) .By applying synchronous switching(closing the interrupter at sufficient velocity and at system voltage minimum) the prestrike can be greatly reduced .interrupted current frequency of operation In fig.1.6, a comparison is made of various current wave shapes that stress the contact system during the prestrike period [7][8].

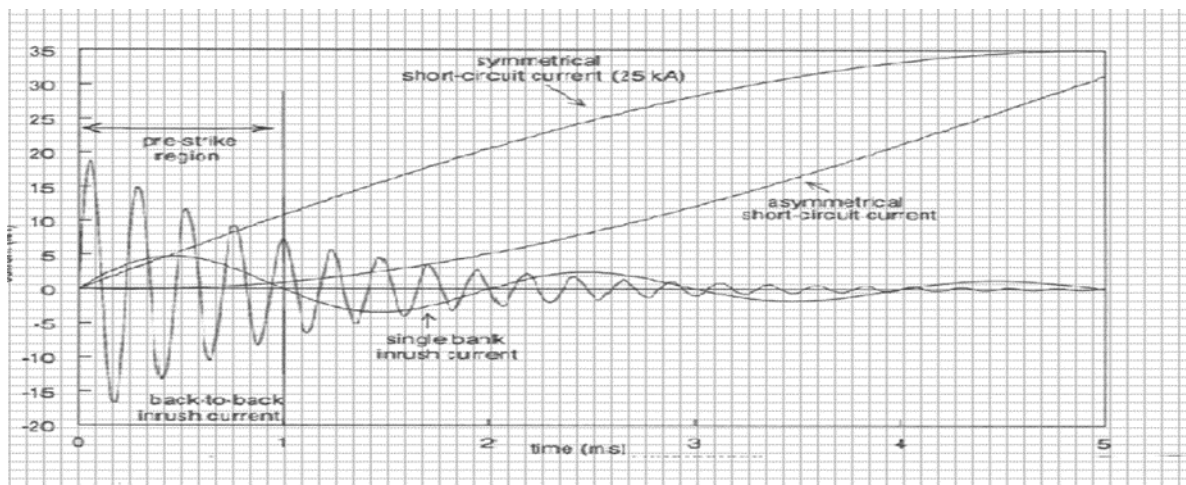


Fig. 1.11 Arcing currents measurement IEEE tutorial

1.4 Inductive current Interrupter

Current chopping is the interruption of an AC current shortly before natural (sinusoidal) current zero. As a result, current will be not interrupted at $i = 0$ but at $i = I_0$ with I_0 the chopping current. For the circuit to be interrupted, under certain conditions current chopping can cause over voltages. This can easily be understood by realizing that in the circuit to be interrupted, a magnetic energy $\frac{1}{2}LI_0^2$ will remain trapped, with L the inductance of that circuit. The essential equivalent circuit is given in fig. 1.7

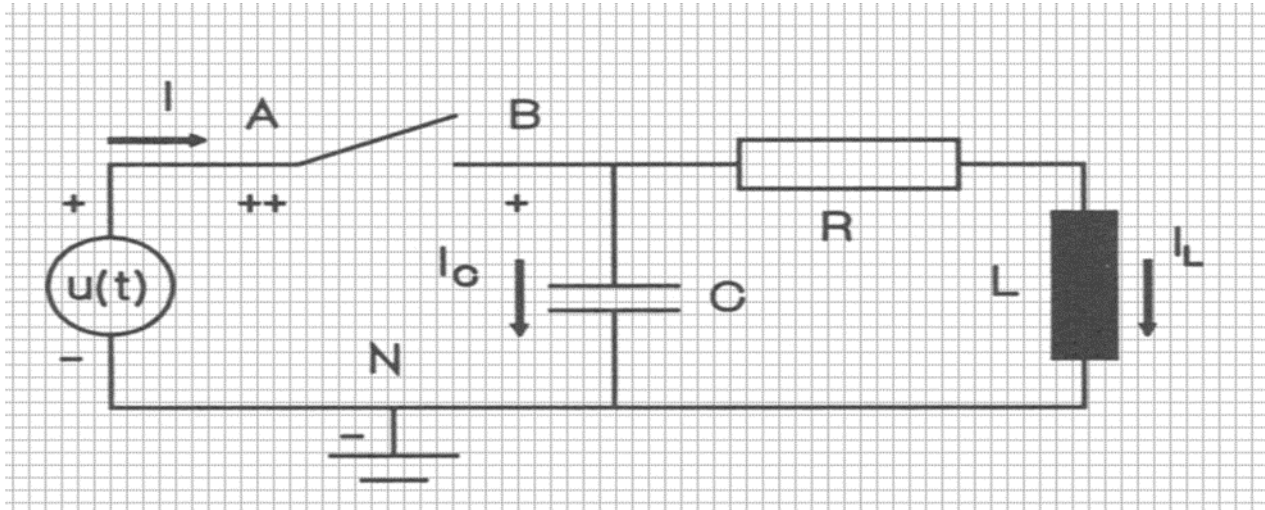


Fig. 1.12 Basic measurement of circuit an inductive switching interrupter [IEEE tutorial]

This allows a simple estimation of the overvoltage produced by a chopping vacuum interrupter. After interruption of the current the residual energy (E_r) stored in the load (RLC circuit in fig.1.7) is present in the load inductance (L) and in the (parasitic) capacitance (C), charged to the crest voltage U of the source $u(t)$ in the (worst) case the interrupted current is purely inductive.

$$E_r = \frac{1}{2} * L * I_0^2 + \frac{1}{2} C U^2 \dots \dots (1.1)$$

After interruption, the energies stored in L and C start to oscillate causing in a certain moment the total energy E_r to be present in the capacitance only, leading to a voltage U'_t over the load:

$$E_r = \frac{1}{2} C * U_t'^2 + \frac{1}{2} L * I_0^2$$

$$U_t' = \sqrt{U^2 + \frac{L * I_0^2}{C}} = \sqrt{U^2} + \sqrt{(Z_0 * I_0)^2} \dots (1.2)$$

with Z_0 the surge impedance of the load characterizing the circuit's response to switching transients.

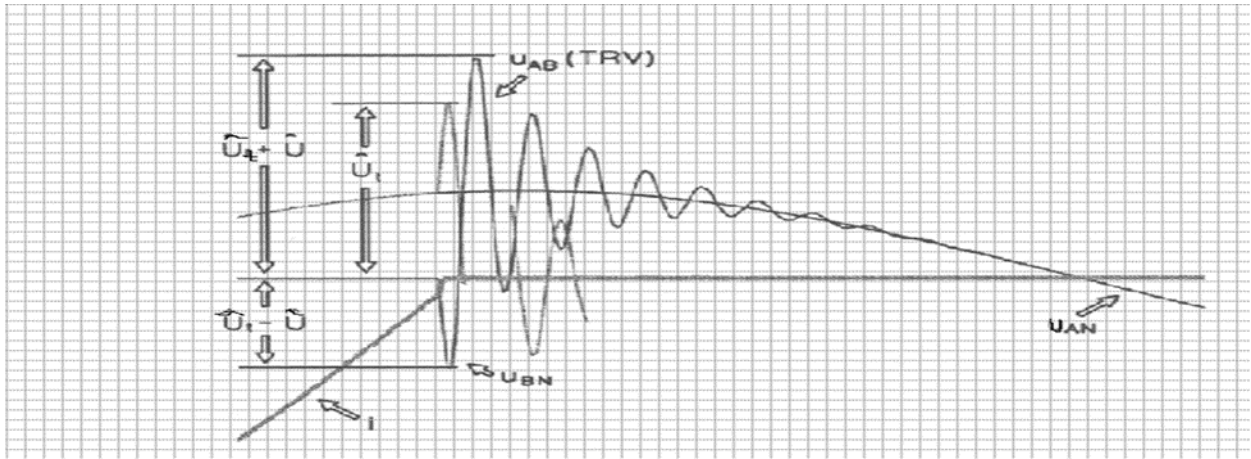


Fig. 1.13 Transient voltages du to current chopping[IEEE tutorial]

Fig.1.8 shows the wave shapes of the transient recovery voltage (TRV) over the interrupter (U_{AB}), and the voltage over the load (U_{BN}). As can be seen, the maximum load voltage U'_t , is determined both by the circuit's surge impedance as well as by the interrupter's chopping level I_0 . This is a good example of how both circuit and interrupter (thus the arc) determine essential switching phenomena like overvoltage generation that the user of switching material is directly aware of. Current chopping has raised great concern in the past, because in the early days of vacuum interrupters, the interrupter contacts were made of pure copper. This material can produce fairly high chopping levels (order 20 A). Nowadays, the mostly used copper chrome $CuCr30$ contacts produce chopping current values in the order of 3 A. Specially designed "low surge" materials further reduce these value down to 1 A or less .It must be realized, however, that the chopping current has a strongly statistical nature, so that in applications with high switching frequency (notably contactors) the incidental occurrence of much higher chopping currents than the 'nominal' ones is likely.

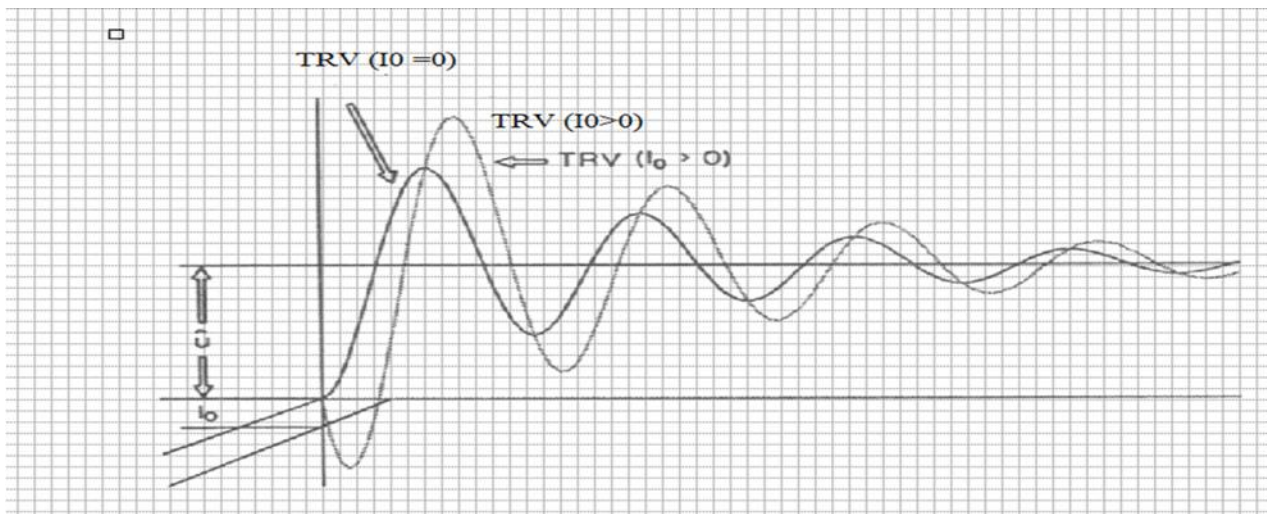


Fig. 1.14 Transient over voltage for inductive load[IEEE tutorial]

Two realistic cases are drawn, the dotted TRV with a negligible chopping level. Note that due to current chopping, the polarity of the initial voltage that arises over the vacuum gap just following interruption has the same polarity as the current. The first peak of TRV - with the same polarity as the arc voltage is called "suppression peak" .

From a practical point of view, current chopping is relevant at the interruption of small inductive current such as:

- ❖ Magnetizing current of transformers (approx.. 0.2 % of the rated current). through chopping might occur at maximum current, problems normally do not occur. The unlikely event of interrupting a transformer inrush current may be hazardous.
- ❖ Inductively loaded transformers. This is a special case where shunt reactors are connected to the tertiary windings of HV transformers.
- ❖ starting current of motors. In this case, current is interrupted during the starting of a motor, when the current is inductive. In some cases (see further) this case needs special attention.

“Detailed information on these switching duties can be obtained from a series of extensive reports of Study Committee of CIGRE , though a large part of the study is on high-voltage circuit breakers Under normal operation, with a high power factor, current chopping also occurs, but the chopping overvoltage is not added to the maximum source voltage (at current zero, source voltage UAN is also small), and creates no difficulty at all”.

In the low current range (few tens of amperes) near AC current zero when current chopping is relevant, the vacuum arc consists of single cathode spot carrying all the current. The anode merely functions as a charge collector, while the interelectrode zone is essentially free of net charge. The cathode spot moves erratically over the cathode surface, thereby creating small (order 10 μm) craters in its path. Experiments clearly show that the formation time of craters is

in the ns region and in a very rapid succession. These craters have to produce the metal vapor, essential to the arc's existence.

Because only one single cathode spot has to maintain the arc by producing sufficient "arcing medium", the efficiency of producing the successive series of emission craters is crucial for the survival of the arc as a whole. Lack of being able to create craters at a sufficient rate causes instability of the arc, manifesting through steep (few $\text{kV}/\mu\text{s}$) and high (order several 100 V) voltage spikes in the arc voltage (few tens of V in stable condition) due to space charges in the plasma .Observation of the arc voltage during such a period of low current shows a large number of such voltage spikes, the frequency of occurrence of which drastically increases as current is reduced further . It is assumed that these voltage spikes are manifestations of the cathode spot's inability to create emission craters at a sufficient rate . The occurrence, amplitude and rise time of these spikes

are depending on the contact material and arc current; the duration depends primarily on the gap length [1][2][3][4][23].

The value of the chopping current is not a constant but depends on the circuit and on the contact material. The addition of capacitance over the interrupter limits the steepness of the arc voltage spikes. Since these spikes may probably be considered as a restoring mechanism after instability in the process of crater formation and renewal capacitance over the arc increases the chopping level, which is confirmed experimentally [5]. On the other hand, added capacitance reduces the circuit's surge impedance, thus reducing the overvoltage generating effect of current chopping.

Series inductance has an opposite effect: it allows a steeper rise of voltage at discontinuity of the arc current. A tendency of the arc to chop is reacted upon by the circuit by a higher voltage ($L \cdot \frac{di}{dt}$), that may help to overcome arc instability or may even reignite the arc. From the material point of view, CuCr30 has been very successful in reducing the chopping level to acceptable values for normal applications. The precise effect of this material on chopping current is not clarified yet in a satisfactory way. At present, CuCr30 is an excellent compromise between the requirements of high current interruption capability, low chopping level and low contact welding tendency (after energizing capacitor banks).

For special purposes low-surge vacuum interrupters have been developed that have been optimized to an extremely low chopping current ($< 1A$). In such class of interrupters, contact material is used that is able to keep the low-current arc's thermal energy concentrated in a small area. This is done by using compound materials in which highly conducting material (like silver Ag) is embedded in poorly conducting frame (like Copper CU). By this, less thermal energy is lost through heat conduction, since the poorly conducting material acts as a heat barrier around the electrically active zone where the (last) cathode spot is active. At increasing content of the poor-thermal conductive component, the chopping current is reduced further. The disadvantage of these special materials is the (much) lower recovery voltage characteristic.

But what is the main characteristics regarding of three phase current chopping:
In such conditions, usually following a very short arcing time, the transient over voltage (TORV) that stresses the gap immediately after interruption exceeds the momentary breakdown voltage of the opening gap[13].

Re ignition follows, causing a high-frequency current (typically several hundreds of kHz) to flow - see (fig.1.11) middle oscillogram. This current arises due to the discharge of the local capacitances (mostly cables) at both sides of the interrupter (C_k and C_g in fig.1.10) over the parasitic inductance (L_p) .

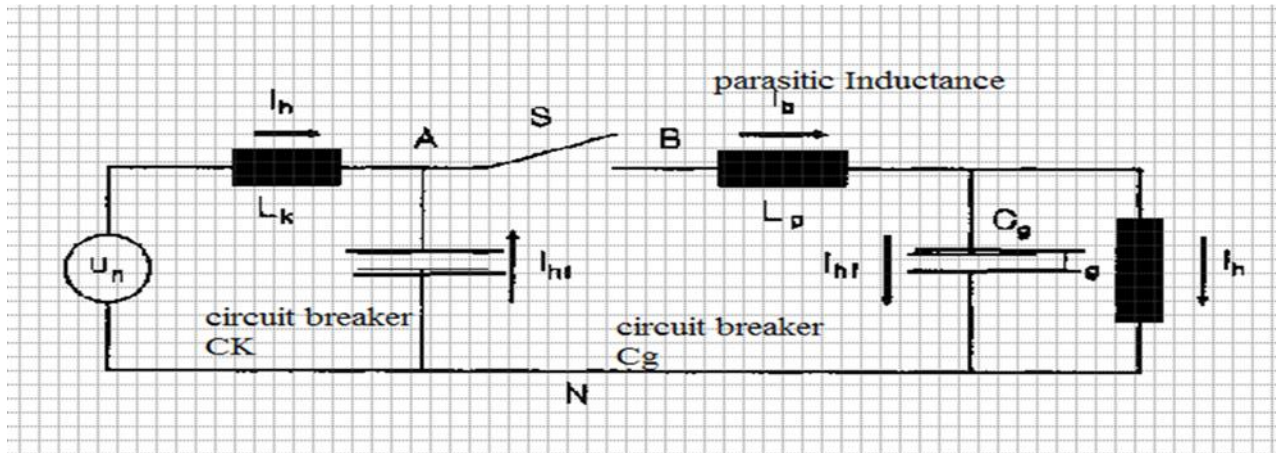


Fig.1.15 Parasitic Inductance experiment [IEEE tutorial]

Due to the excellent interrupting capacity of vacuum interrupters, this current is likely to be interrupted (already at the first current zero in the case of the first two reignitions in fig.1.11 middle), causing a higher and steeper TRV to appear. This steadily increasing voltage is called "voltage escalation". By this mechanism, a higher voltage than without reignition can be built up [1][2][8].

1.5 Transition rates – Experiment test one

A mathematical model which analyzes events during the commutation period of vacuum switching and the transient recovery voltage period afterwards has been proposed for proved that the discharging times only depends on the transient rate of di/dt whereas the voltage transition process would be constant du/dt according to the switching experiment test.

However, the behavior of the interrupter immediately after current zero was not completely modeled. Specifically, the mathematical formulations show the transient recovery voltage rising immediately after current zero [16][17][18][28].

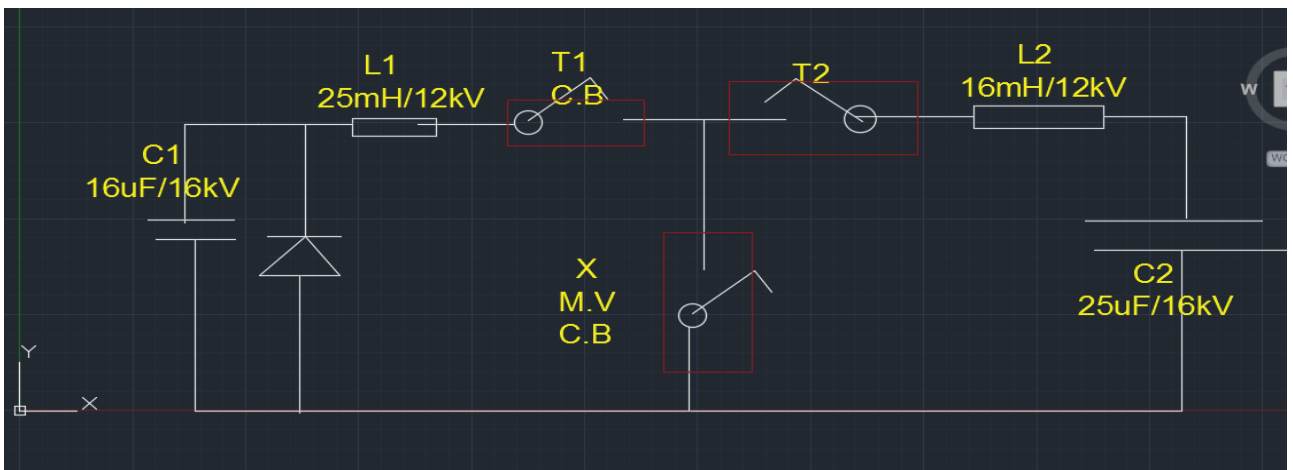


Fig.1.16 Experimental circuit for calculating di/dt

I_{SS} the steady state current being commutated

t_r the ramp down time in microsecond

di/dt the average rate of current decline during current

du/dt the average rate of rise of recovery voltage

V_2 charging voltage on the commutating capacitors C1 and C2.

My analysis for the above experiment tests were repeated by MATLAB /Simulink for verifying the datasheets – Excel datasheets .

Table 1- transition rate of di /dt at 1kA

Number _Tests	I_{SS_KA}	$t_r_{\mu s}$	di/dt	V_2_KV	du/dt
1	1	7.8 μs	128	2	1E+10
2	1	6.9 μs	145	2	1E+10
3	1	6.13 μs	163	2	1E+10
4	1	5.06 μs	197	2	1E+10
5	1	4.32 μs	323	2	1E+10
6	1	3.77 μs	266	2	1E+10
7	1	3.34 μs	299	2	1E+10
8	1	3.0 μs	295	2	1E+10
9	1	3.0 μs	295	2	1E+10
10	1	3.0 μs	295	2	1E+10

Table 2 - transition rate of di /dt at 2kA

	A	B	C	D	E	F	G	H	I
1	post arc current and TRV with commutation of vacuum arcs - discharging times								
2									
3	I _{ss} _KA	tr_us	di/dt	V ₂ _KV	du/dt				
4	2	10,9	183	3	1,05E+10				
5	2	9,1	211	3	1,05E+10				
6	2	7,8	256	3	1,05E+10				
7	2	6,9	291	3	1,05E+10				
8	2	6,13	326	3	1,05E+10				
9	2	5,55	361	3	1,05E+10				
10									
11									
12		di/dt = I _{ss} /tr = 150/3E-3 = 50A/us							
13		di/dt = I _{ss} /tr = 2/10,9E-6 = 183/us							
14									
15									

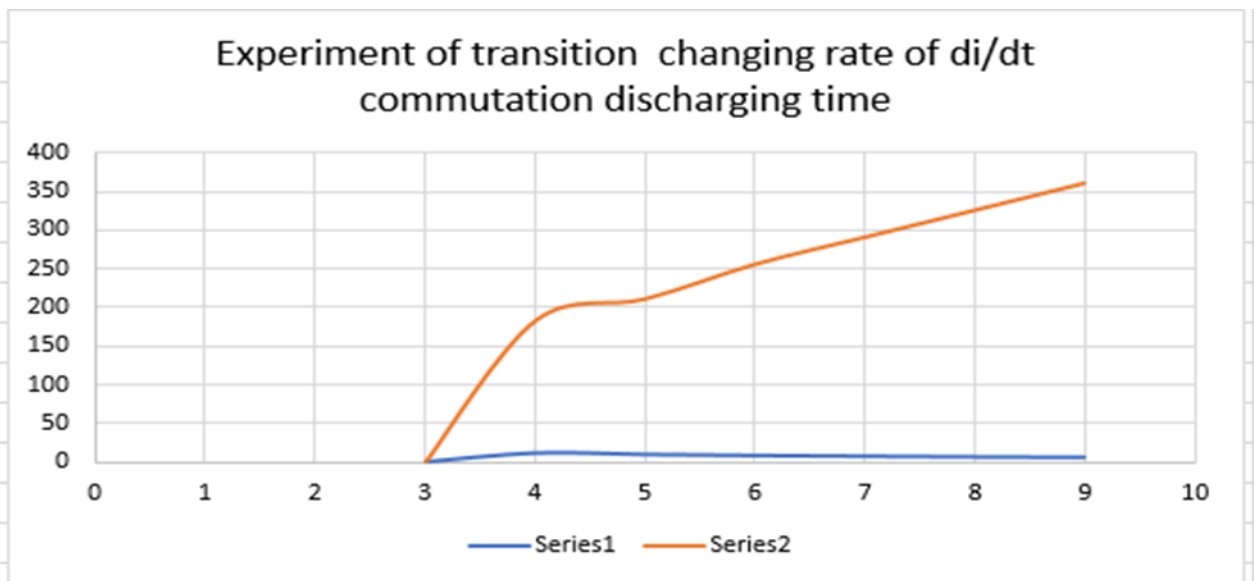


Fig. 1.17 Curve for calculating of di/dt in vacuum interrupter

1.6 Formation of Radial Magnetic Field – Experiment test

The vacuum laboratory experiment was conducted as demountable vacuum tube with a contact gap (40mm) [27][56].

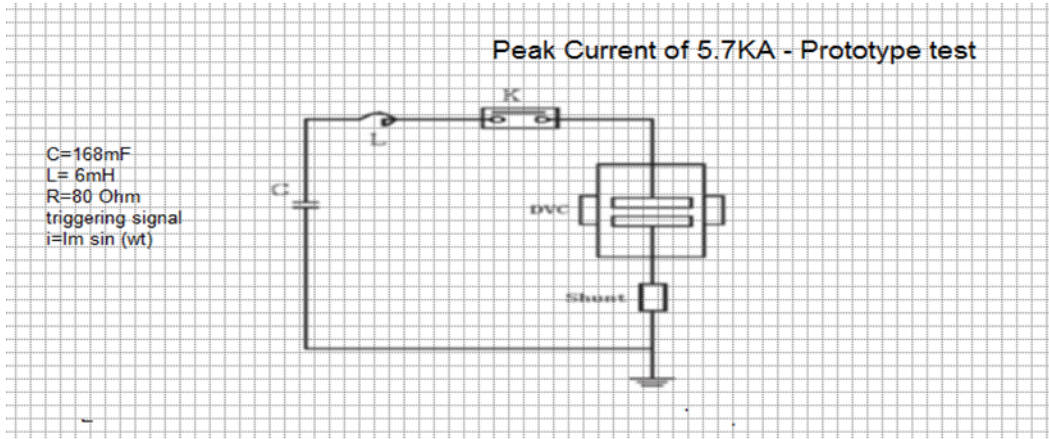


Fig. 1.18 Prototype experiment for formation magnetic field

This experiment was used to observe vacuum current arcing behavior, with vacuum tube through vacuum pumping as $2 \cdot 10^3$ Pa (pascal) for two electroplates of (cucr30) copper chromium as standards of H.V Testing system.

As shown in Fig.1.18,the experimental current was provided by a single frequency L–C oscillating circuit.

- The contacts were always opened and the main switch K was always closed during tests.
- When capacitor bank C (0.0168 F) was discharged, a high dc voltage was added to the vacuum gap between contacts in this sample. While a triggered signal was generated, an L–C discharging current was injected to the vacuum gap and passed the shunt resistor R (80 Ω).
- The inductance L is 0.603 mH. Thus, for the L–C discharging current, the frequency f is 50 Hz, and phase angle ϕ is 0. Therefore, current can be expressed as $i=I_m \sin(\omega t)$. Also, the instantaneous current value can be easily known by the time t if the peak current value I_m has been known.
- Arc current was measured using an 80- $\mu\Omega$ shunt resistance, and arc voltage was measured using a high-voltage probe. The arc voltage and arc current signals were recorded using an oscilloscope.

For the visual investigation of vacuum arcs in side tube to see what were happened , a high speed video camera was used ; *specification this camera was 4000 frames/s .The exposure time of high speed was $3\mu s$.In addition a simulation software (FEM) a commercial 3-D finite element method FEM was used to study the behavior of AMF for each instantaneous of μs (contact gap 40mm – contact diameter100mm of cuucr30).*

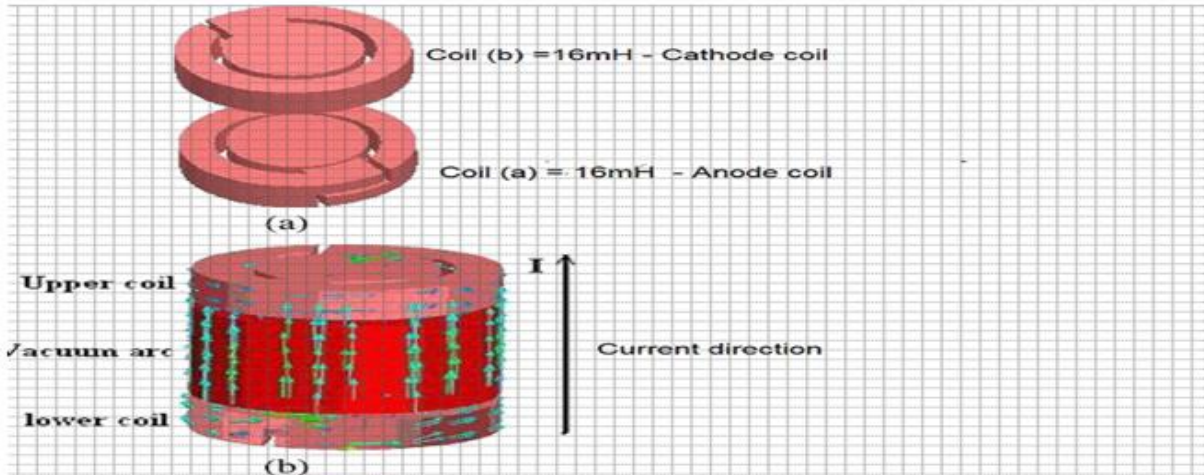


Fig. 1.19 Configuration and current path of the single coil-type AMF contact.
 Configuration of the single coil-type AMF contact. Current path of the single coil-type AMF contact[27] .

My analysis for the above experiment tests were repeated by MATLAB /Simulink for verifying the datasheets – Excel datasheets .

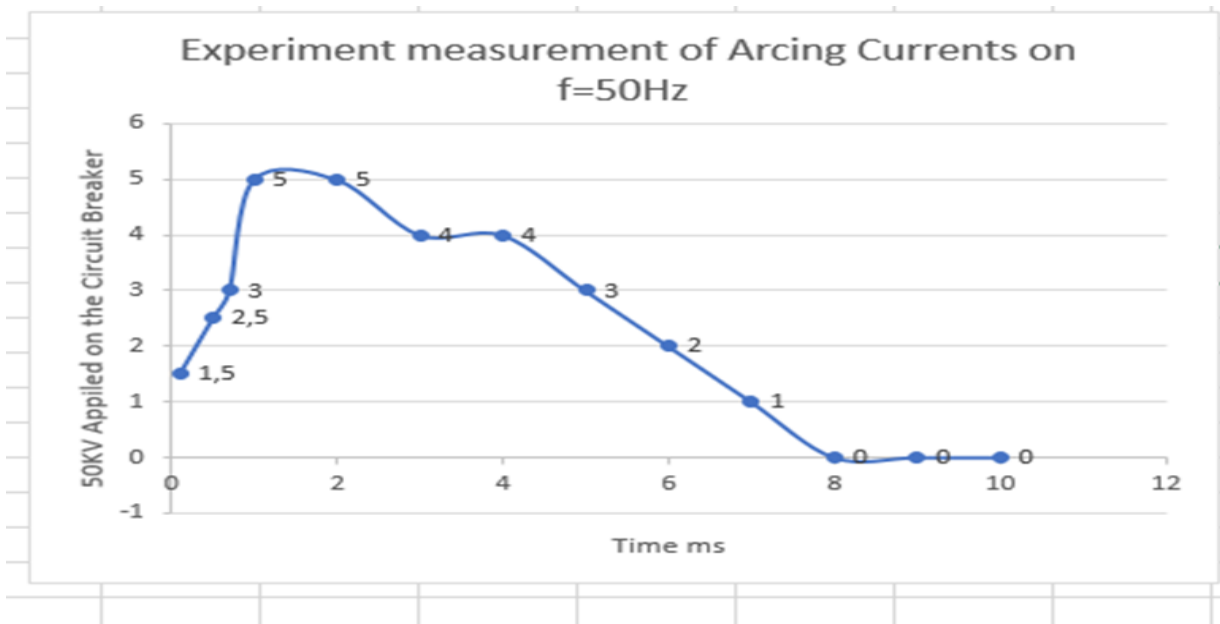


Fig. 1.20 Maximum arcing currents when rotating magnetic field as radial shape

Table 3 Data sheet for calculating of maximum peak value of arcing currents

	A	B	C	D	E	F
1						
2						
3						
4						
5						
6	IK	Ud_KV	Peak_KA			
7	0	0	0			
8	2,5	10	0			
9	5	20	22,7			
10	7,5	25	22,7			
11	10	30	22,7			
12	12,5	35	22,7			
13	15	40	22,7			
14	17,5	45	22,7			
15	20	50	22,7			
16	22,5	55	22,7			
17	25	60	22,7			
18	27,5	65	22,7			
19	30	70	22,7			
20						
21						

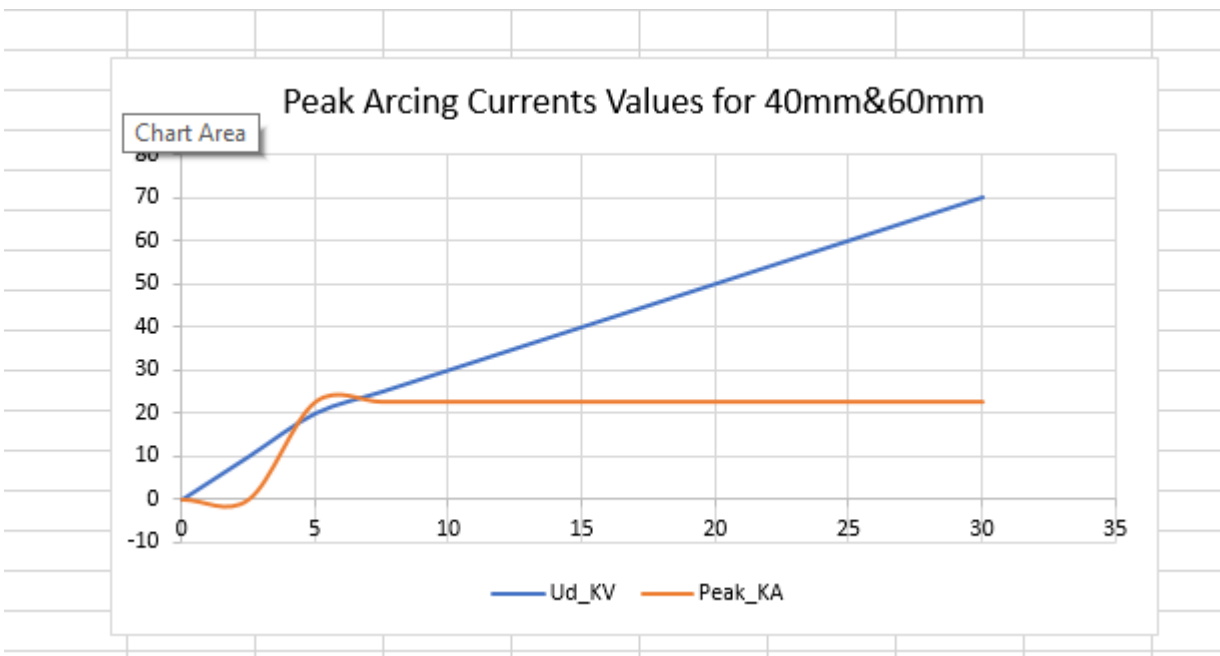


Fig. 1.21 Curves for calculating of maximum peak value of arcing currents
My analysis for evaluating maximum arcing current values

1.6 Conclusions

- 1.** The result is taken that the commutation process depends on the transition rate of di/dt only.
- 2.** The commutation experiment tests were done by scholars Susan .E. Childs & Allan Greenwood & Mietek Glinkowski ,for purpose proving of the transition rates of material that able for commutation .
- 3.** I was repeated the above experiment by MATLAB/ Simulink.
- 4.** My investment these tests for create a similarity sample of LTT damping technique.
- 5.** We can make fabricating of the axial magnetic field between anode and cathode contacts by using of installation two coils for treatment of arcing currents & chopping currents.
- 6.** I was repeated the test of axial magnetic field by analysis of Petersen coils -ABB Laboratory2016.

II. CONTACTING MATERIALS OF M.V SWITCHING

2.1 Analysis of technical materials inside vacuum interrupter

One scholar was made analysis for the verifying of vacuum concepts and his concluded that. Since the arcing current in vacuum is one of the key elements for designing of the circuit breaker as interrupter parts in medium voltage switches or switching system, some knowledge both of its structure and behavior are essential for understanding the operation of vacuum interrupter.

“The name vacuum arc is really incorrect, indeed “if there is a vacuum there is no arc” and “if there is an arc there is no vacuum”[29].

A correct name is metal oxide vapor. Since the arc current which forms when two contacts, or separate interrupter in vacuum that burns the metal oxide vapor between two electroplates “This is a physical phenomenon” “Electroplates Switching Interrupter” .

Nowadays the name of vacuum is more pervasive, and we have uniformly should be accepted this phrase. So, the correct physical description of technical specification is ,vapor metal oxidation and arcing currents as oscillating caused due to medium voltage environment which have been created very strong current disturbances before the current -zero occurrences inside two electroplates in vacuum tubes in M.V switching system.

Vacuum interrupters are very sophisticated switches. Simple in that their geometry and appearance is simple, they have few parts; sophisticated in that much scientific and technical knowledge about how goes into the preparation and assembly of those parts. In principle , all that is required a pair of contacts, a vacuum –tight envelope to enclose and provide for their support, insulation to isolate the contacts from one another when in the open position , and a shield to maintain the integrity of the insulation by protecting it from the products of the arc condensing metal vapor when the switch opens. In as much as the pair-contacts must be separable, the penetration to the moving contact must permit the required movement. This is almost always obtained by a metallic bellows.

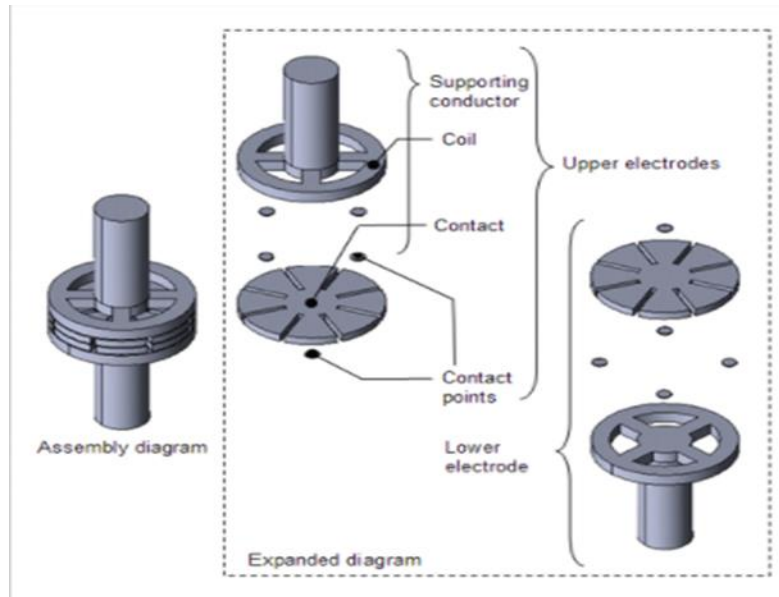
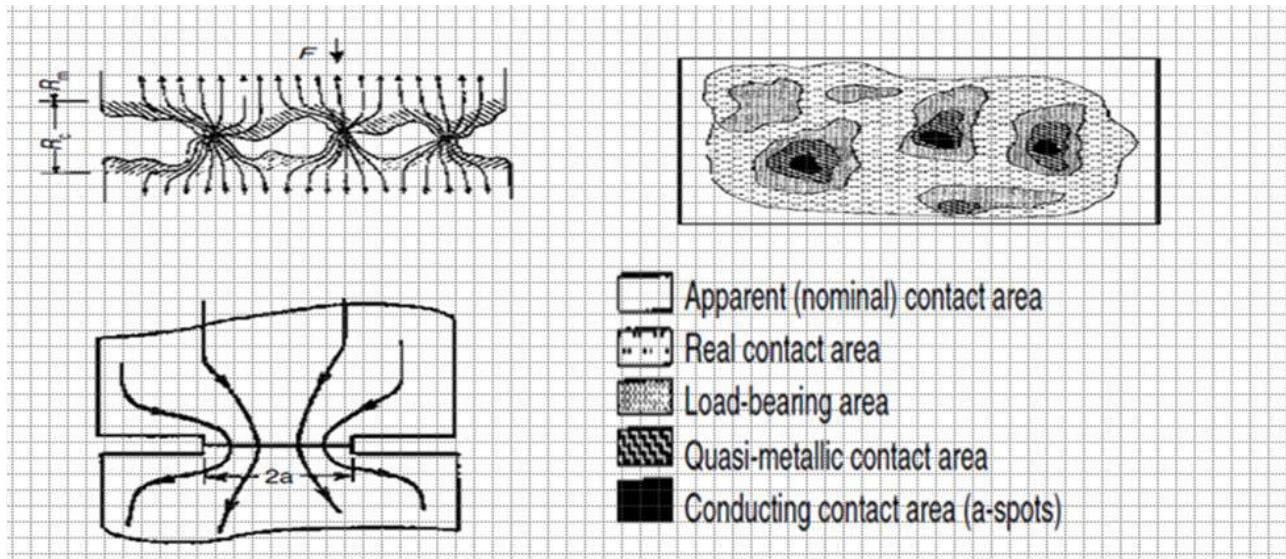


Fig. 2.1 Structure of Anode and Cathode of Interrupter

It has been established that real surfaces in all of medium voltage switches are not flatted even if many processing under technical formation industrial on surfaces have been done but are still some comprise many asperities (hardness, non-uniform molecules) [30][31][32][33][34].

Therefore , when (*electroplates contact interrupters inside medium voltage synchronous fields*) are made between two metals surfaces asperities , hardness of contacting members will penetrate the natural surfaces of materials and other surfaces and creating contaminate films establishing localized metallic contacts, thus contacting paths.[33] As the force increases , the number and the area of these small-metal- or metal contact spots will increase as a result of the rupturing of the surface film and extrusion phenomena of metal through the ruptures in microseconds [30].

These spots, termed a- spots are made cold welds providing the only conducting paths for the transfer of electrical currents. Generally speaking, as a researcher that, the successful interruption of a vacuum arc depends on the dispersal of the arc products, and how do they disperse. We recognize a number of harmful components: metal vapor, metal ions, electrons, gas molecules, metal droplets and/or some particles [35] --[41].



R_m conductor resistance

R_c constriction resistance

a -diameter of a-spot

Fig. 2.2 Schematic of current constriction and real contact area between medium voltage electroplates

2.2 Types of vacuum arcs

Any vacuum circuit interrupter in medium voltage is designed and constructed to close and open states, an electrical circuit breaker to change of the paths both of a synchronous current and electromagnetic fields according to Maxwell theorem of power generation (voltage , current and magnetic fields instantaneously). This change are related to change of the energy in the circuit components, mainly a two electroplates and effects to the dielectric properties which in turns produces a transient manifest by changes in voltages, surging high scale currents or both or creates lightning impulse over-voltages, and switching impulse over-voltages [33]-[47].

Vacuum arcs, we mean current arcs inside of a vacuum tube which have two modes;

1) Diffuse mode

2) Constricted mode

The diffuse mode is characterized by more exceeding bright spots on the cathode electrode These cathode spots are in constant motion over the contact surface and appear to repel each other sometimes during multi interrupter switching times. They have a finite, though variable life time; new ones are created, often by the splitting of the existing spots, as other spots extinguish. The number of spots is determined by the magnitude of the current; for example each spot on copper plate carries of the order 100A . Thus, a copper of 1000A will have approximately 10 cathode spots In a AC half cycle, the number of spots increases progressively to the peak current and decrease until, current zero. The current per spot varies from one cathode material to another [42].

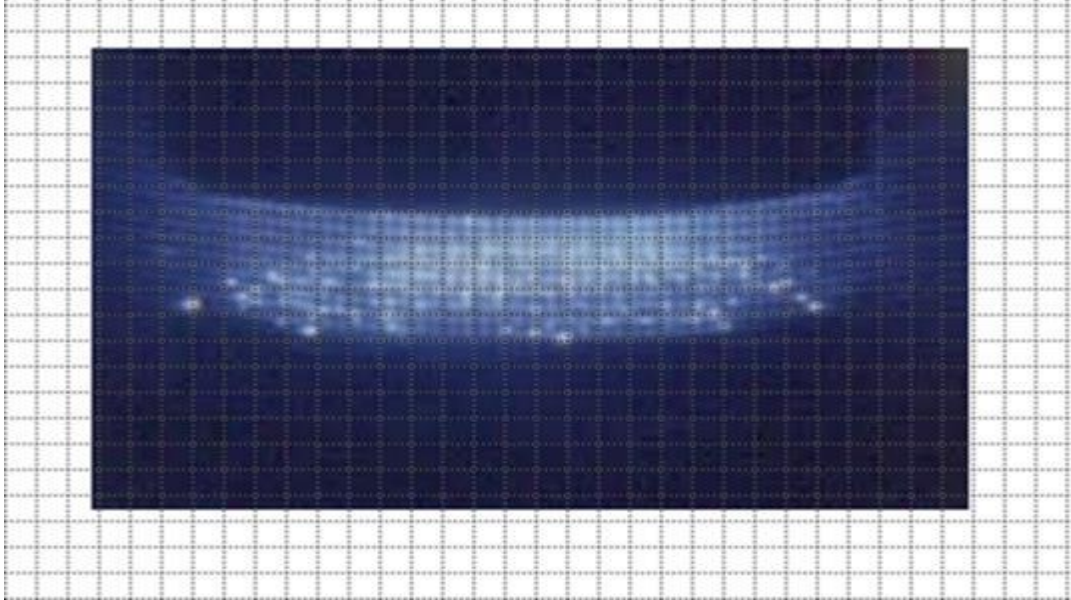


Fig 2.3 Vacuum arcs in the diffuse mode (Courtesy of G.R. Mitchell)

highest for refractory materials and lowest for low boiling point metals This reminder of the diffuse arcing discharge contrast sharply with the cathode spots in that it has a much paler luminosity . The name diffuse is apt for most of the interrupter is filled glowing luminous plumes of conical shape with the apex of each pointing towards its cathode spot; the anode contact is bathed in this glow. The entire assemblage looks like, a number of independent, parallel arcs. The luminous plasma expands until it fills almost the entire volume of the tube (see image below) . It gives an overall impression of a diffuse arc. This figure was provided by Mitchell, who has given a comprehensive description of the vacuum arcs. [46] [51][52][54].

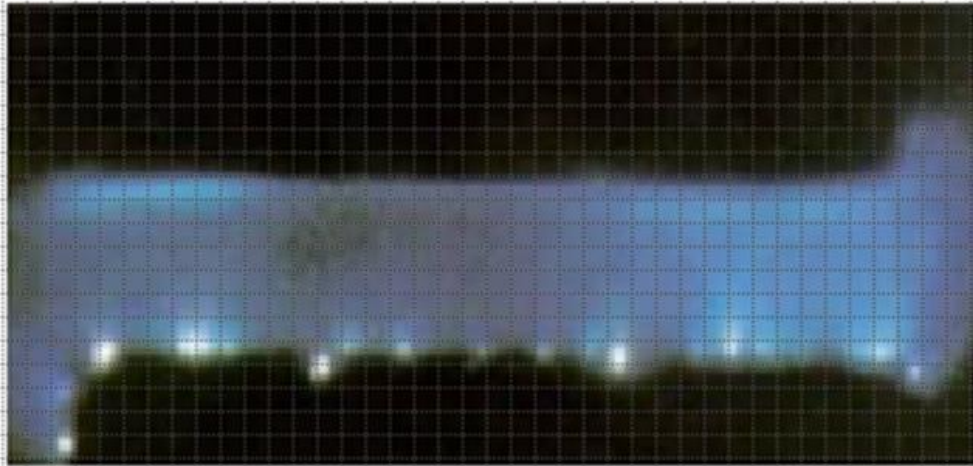


Fig. 2.4 Vacuum arcs in constricted mode indicates the vaporizing metal oxide due to electroplating

Harris and Robinson, graphically describes such remains as “*like the track of a herd of cattle a long a muddy trail*” fig 2.5. It is evident that the surface in such areas has been turbulently molten, the surface of the anode electrode or contact has a matt appearance following diffuse arcing. Metal vaporized at the cathode spots travels radially away to strike and condense on cathode. Since the anode usually subtends a large angle for most of the cathode, the majority of this material condenses on the cathode. Some vapor escapes from between contacts and freezes on the shield. In switches which have glass envelopes (glass shields), this material is clearly evident as a ring of deposited metal encompassing the shield directly across from the contact gap.

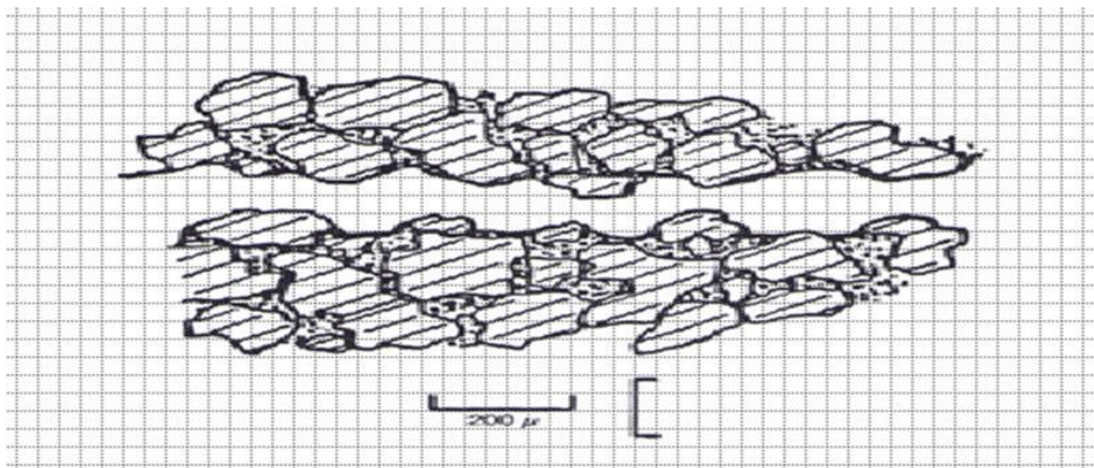


Fig.2.5 Microstructure of chromium copper contact material [Robinson-patent]

Robinson's British patent "Vacuum type electric circuit interrupting devices" British Patent number (1194674,1970) , provides a considerable amount of information regarding (Cu-Cr) at least as originally conceived . The chromium powder comprising particles up to 250µm , is made into a solid block first compressing it with considerable force and then sintering the fragile green material under high vacuum to produce a mechanically stable chromium sponge . The sintered compact is then impregnated with molten copper, again under high vacuum and high temperature. The procedure, at least as originally performed, was to place a disc copper on a disc of the sintered compact like a pat of butter on a crumpet. When the copper melted it flowed into the interstices of the higher melting point chromium. The result on cooling was a compact mass.

An examination of the surface of the cathode after it has supported arc reveals faint tracks over surface. A closer examination with higher magnification shows these tracks to be a criss -cross of carter and other debris see figures below.

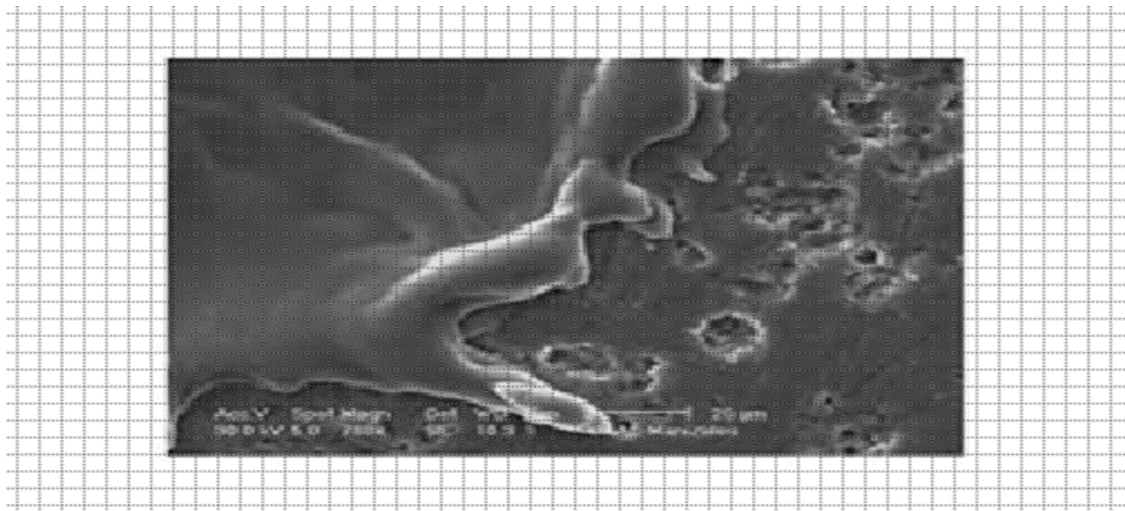


Fig 2.6 Microscope scanning electron micrographs of cathode tracks from vacuum arc on copper

Scanning electron micrographs of cathode tracks from vacuum arc on copper cathode at magnifications: (c) X5000 (Courtesy of L.P Harris 1978 USA).

[Harris] (a mathematical model of cathode spot operation) shows some excellent photographs of such craters taken by scanning electron microscopic:

There is no universal agreement that spots are homogenous Stability of metallic arcs in vacuum believes ,and some others are inclined to agree with him that each little area comprises a number of subcomponents or cell, perhaps ten or more which are the basic elements. Given the dimension just cited and the observed value of approximately 100A per cathode spot, it is evident that the current density is of the order of $10^{-11}10^{-12}$ A/m² . Such a high current density combined with the resistivity of the contact causes considerable joule heating within the contact, behind the spot: this alone will

raise the local temperature. The cathode surface in the spot area is also being bombarded by positive ions, which adds greatly to the local energy input. As a consequence, the cathode is boiling, a stream of metal vapor is issuing from the surface. There is a quite intense electric field in this region caused by positive ion space charge.

The combination of high temperature and strong field create conditions for a considerable flux of electrons to be emitted from the electrode surface at the cathode spot. The subject of electron emission from metals is a profound one. It has been cause of exhaustive inquiry over many years and the source of hundreds, if not thousands. Helpful discussion of the subject will be found in Reference [19][33][35][36][37].

The topic is of sufficient importance to the understanding of vacuum arcs to make a diversion here for a brief summary. According to the band theory of metals, electrons in great numbers

(about $8.5 \times 10^{22}/\text{cm}^3$ for copper) in the conduction band of the metal move freely through the crystal lattice. They endow the metal with its high electrical conductivity in as much as a considerable current can be caused to flow by application of very small electric field. However, for electrons to escape from the metal, even the most energetic of the population at the top of the conduction band, i.e. at the fermi level, they must be overcome a barrier of several volts (~3.8 eV for copper), known as the work function. Essentially, no electrons have this kind of energy at room temperature, so electrons do not escape from metals unaided (except to other conductors) at room temperature.

N:B These electrons emission between electroplates proves that there is not benefits of vacuum theory in medium voltage switching system.

2.3 Calculating of Joule heating in vacuum interrupter

When a metal is heated (Joule heating), on the other hand, the average energy of the conduction band electrons increases in proportion to the temperature rise. The distribution of energies is Gaussian about the most likely energy. Thus with increasing temperature, some fraction will acquire sufficient energy to overcome the work function and escape to the surrounding space. This process, which is referred to as thermionic emission, was first reported at length by Richardson [‘Emission of electricity from hot bodies’ [33] and generally quantified by [Dushman] who gave the following relationship between current density, $J(\text{A}/\text{m}^2)$ and temperature, $T(\text{K})$: Joule Heating.

$$J = AT^2 \exp(-\phi_e/KT) \dots\dots\dots 2.1$$

(2.1) Dushman, where Φ is the thermionic work function, k is Boltzmann’s constant (1.37×10^{-23} joules/K) and e is the electronic charge. The constant A is approximately 6×10^5 for most metals. It is apparent that for $\phi_0 = 3.8 \text{ eV}$ and

T= 3.000K.

$$J=2X 10^6 A/m^2 \text{ basic formula}$$

Which is exceedingly small on the scale discussed for cathode spots. It is evident from this rough calculation that only refractory metals, such as tungsten and molybdenum can produce high thermionic emissions. Metal like copper and silver would melt and boil before reaching a high enough temperature.

It was stated that the cathode surface at the location of a cathode spot is both very hot and under the influence of a strong electric field F . One would expect therefore , that one would enhance the other as far as electron emission is concerned . [Shottky] was the first to consider the combined effect of (temperature T and Field F); his paper appeared in 1923. It was not until many years later that Murphy and Good [34] put the subject into a rigorous framework and described quantitatively what is known as T-F emission (T for temperature and F for field).

With the foregoing background on electron emission from metals , discussion of a model for cathode spot can be resumed . [Lee and Greenwood in 1961] were the first to invoke T-F emission as the active emission mechanism in the cathode spot of a vacuum arc . In a paper described by Ecker vacuum arcs –theory and application[40] the first attempt at a comprehensive treatment of the vacuum current arc spot , the first step forward in the understanding of the vacuum arc , they proceeded to set down basic equations relating to the dependent variable in the cathode region ,Once for example, was concerned with energy balance at the cathode surface , another was the space charge equation . With the aid of these equations. certain critical limiting conditions (there would be no more ions produced than neutrals evaporated) and the physical properties thermal conductivity, evaporation constants works function, etc., of the cathode, they were able to predict current arc behavior, particularly with respect to current chopping. The state of knowledge has increased greatly since that time and so has the rigor of theoretical analysis. For these reasons, Harris model [33][44] is used to improve understanding of cathode spots. A briefly summary of this works is presented but hopefully sufficient to understand the critical processes involved and their dependence on the material properties of the cathode.

2.4 Synthesis of mathematical model

In order for verifying of MATLAB/Simulink our sample precisely, its necessary create one mathematical model for this pupose of research . In any field of sciences every research is based on one or two aspects (to explore to confirmity) [3] , from which all the reserch methods are divided in :

- A) Exploratory
- B) Confirmatory

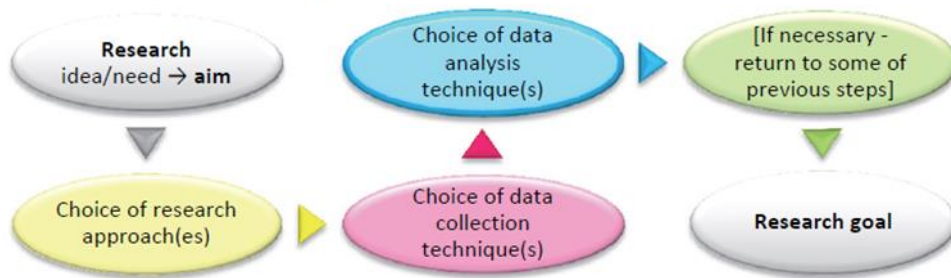


Fig .2.7 Research process

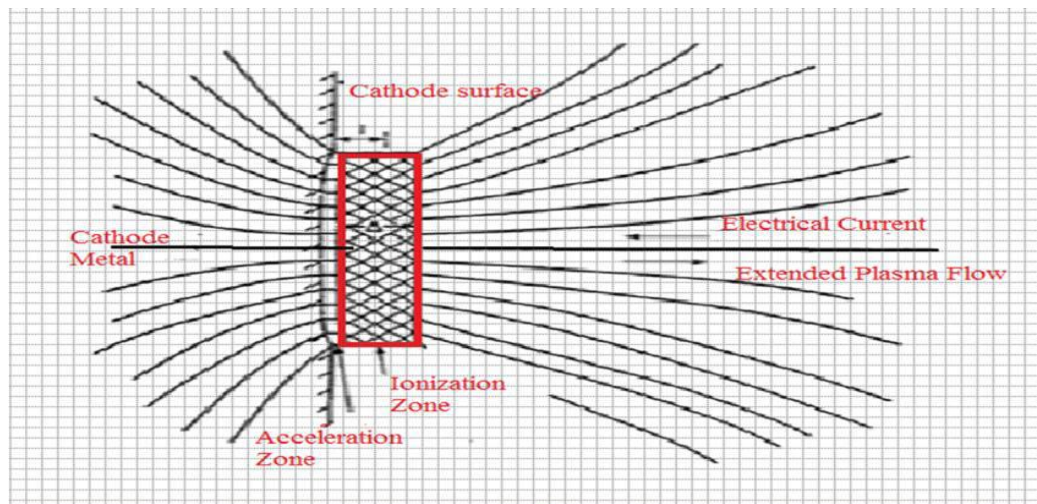


Fig.2.8 Cathode cell geometry and potential distribution in [Harris model]

The cathode spot model is shown in Harris model see Harris model figure above. On the left is the cathode itself, on the right the anode, In the middle is the ionization zone, shown crosshatched. Axial symmetry is assumed, so that the cathode spot is circular, as is the ionization region. It is vitally to understand the scale of this diagram. As indicated earlier, the cathode spot

diameter on copper is $20\mu\text{m}$. The distance L to the center of the ionization zone is mean free path (MFP) for ionization of the copper vapor. Because the local pressure is very high the MFP (mean Free path) is very short, of the order of $1-10 \times 10^{-8} \mu\text{m}$. So, the synthesis mathematical mode basically on Harris who calculated the switching processing times ; Ionization of Ions and electrons, acceleration, arcing currents, transition rates du/dt & di/dt , chopping currents and finally transient over voltage switching time by $600\mu\text{s}$ [2][3][4][5][12]. N:B detailed explanations in chapter III.

2.5 Electrode effects and break- down

The insulation of high voltages in a vacuum is an important task(dielectric properties) because each single interrupter creates a high level of impulse switches over-voltage which effects the quality of insulation and break-downs could be happened , if we did not consider which level will be designed for manufacturing medium voltage switch gear loads .

IF we separate the contacts of vacuum interrupter to establish a gap of a few millimeters and then apply an increasing voltage (AC or DC) to the gap , we find that the breakdown insulation occurs and that the first breakdown may quite low stress, at $10\text{KV}/\text{mm}$ for medium voltage switching level .

Since in this situation, the mean free bath is much greater than any dimension of the vacuum vessel at the rate of 11KV for Power generation unit. thoroughly switching interrupter in which electrons can be emitted metals. These are thermionic and discharging emissions from the surface of a cathode plate including very high temperature (a process restricted to refractory materials),field emission where a powerful electric field is present at the cathode surface and T-F emission ,a combination of temperature and field, as occurs in the cathode spot of vacuum arcs on copper, silver or *Copper-chrome alloy CUCR30* or similar metals under testing in H.V laboratory . It is not clear how these sources of emission apply to the experiment just described where breakdown is initiated by modest voltage impressed a cross the open gap of vacuum interrupter.

There is no high temperature and apparently no powerful filed. Moreover , if electrons are emitted there is nothing in the gap for them to ionize. Some clues begin to emerge if the experiment is continued, i. e.if one reapplies voltage after breakdown has occurred



2.9 Successive breakdowns of contact gap of a vacuum interrupted -experiment by Greenwood

We have conducted tests of this kind many times and what one finds is that breakdowns continue to occur, but at steadily increasing voltage. Some typical data are displayed in fig. 2.11. There is a certain amount of scatter in the points and they appear to be approaching some asymptotic limit. This is because the surge impedance of the test circuit was only 8Ω , thus a breakdown at 100KV could deliver 63KA at 50HZ. The scatter is less if such an experiment is conducted by placing high resistance, 500K5 ($M\Omega$), in series with the high voltage sources, so that breakdowns when they occur conduct only a small current, much of it coming from discharge of local stray capacitance. The procedure just described is referred to as conditioning, or sometimes spark cleaning. If a much lower resistance is used, so that breakdown creates an arc, a certain amount of 'deconditioning' occurs, i.e. when voltage is reapplied, breakdown occurs at relatively low value again. Deconditioning will also occur if the contacts are mechanically closed and then opened again.

These observations suggest that contact surface conditions affect breakdown in these circumstances. The belief is that on typical contacts, even new ones, there are many asperities and occlusions, the last-mentioned may be metallic or not conducting, and that these are the source of greatly enhanced electron emission. Scanning electron microscopic images confirm the presence of such excrescences. Grain boundaries also appear to be important emission sites. Fowler-Nordheim plots on the lines described the field emission is the source of electrons under these conditions, however the results imply that field enhancement factor β is very high, or the work function at emitting sites is unusually low. It would also seem from these calculations that the emitting sites themselves are very small.

There are two theories with respect to the mechanism of breakdown. The first proposes joule heating of a sharp asperity on the cathode which causes it to vaporize and then be ionized by the electrons. The second theory invokes anode involvement. It proposes that an electron beam,

emanating from a site on the cathode, focuses on a spot on the anode and imparts to it a heat flux to cause local anode vaporization. It is likely that both of these mechanisms are operative, the first prevailing in short gaps and the second in longer gaps. Both theories accord with the phenomenon of conditioning, since both have the effect of removing asperities from the contacts. With repeated breakdowns a higher field is required to obtain breakdown conditions with the remaining surface irregularities. Closing the contact or creating an arc between them, creates a new set of debris from weld residue or crater remains.

Miller and Farrall [49] describe an ingenious experiment that clearly demonstrates the dominance of the cathode in the conditioning process. They utilized three electrodes, but used them in pair, any one could be an anode or cathode. Having conditioned one pair, the third was used to replace the anode; the result was inconsequential. When the experiment was repeated and the third electrode was used to replace the conditioned cathode, breakdown voltage was greatly reduced and a fresh sequence of conditioning had to be undertaken to restore the high breakdown voltage integrity.

Much evidence over a wide range of voltage and gap length suggests that breakdown voltage in vacuum varies as the square root of the gap length [41] postulated his clump theory to account for this relationship, 'Clump' refers to a loosely adhering particle on the surface of one or other of the electrodes. The presence of a field in the gap implies surface charge of opposing polarities on the electrodes, some of which charge is shared by the clump. If the clump should break loose, it would accelerate across the gap and deliver an impact to the opposite electrode. The amount of energy delivered will depend on the mass of the clump and square root of the gap voltage.

It was Granberg's proposal that when this energy exceeds some critical value, breakdown would result. The mechanism for the breakdown, whether it is vaporization of a part of the impacting bodies [49] have proposed a consequence of a discharge the clump and the opposing electrode just before impact, was not disclosed. There is no question that free particles, metallic and nonmetallic, exist within the envelopes of vacuum interrupters and that these are a cause of breakdown. Much of what is discussed in breakdown leads one to expect that contact material will have a significant effect on vacuum breakdown since different metals have quite different work functions, vapor pressure curves, hardness, brittleness, Young's modulus, electrical and thermal conductivities, etc., all of which appear to be influencing factors in one way or another. Experiments by Rozanova and Grantburg Bouchard [45] and McCoy et al [46], have confirmed this, yet the information is not necessarily very helpful from a practical point of view as far as vacuum switchgear is concerned. This is because breakdown is but one of several important considerations in selecting contact materials. Other requirements may be in direct conflict.

There are, of course, other stressed gaps in a vacuum interrupter besides the one between the contacts. Specifically, note shield-to-shield and shield-to-endplate gaps.

Here there may be more latitude in selecting material. Nickel and stainless steel, for example, have proved good for shields. Besides spark over of gaps, one must also consider flashover of

insulating surfaces. It is well known from the work [47], that placing an insulator in parallel with a vacuum gap greatly reduces the insulating strength of the gap. In the first place, there is a concentration stress at the triple point where the electrode, insulator and vacuum meet. Also, the field is often distorted by surface charges on the insulation [48] found that the breakdown voltage was independent of degree of vacuum over a considerable range, but observed that the breakdown voltage increased with the surface resistivity of the insulator. So we can make correct distinguished for the above two switching states; Ionization between ions and electrons, acceleration and arcing current generate an electrical arcing phenomena for a complete transition process of du/dt or di/dt state.

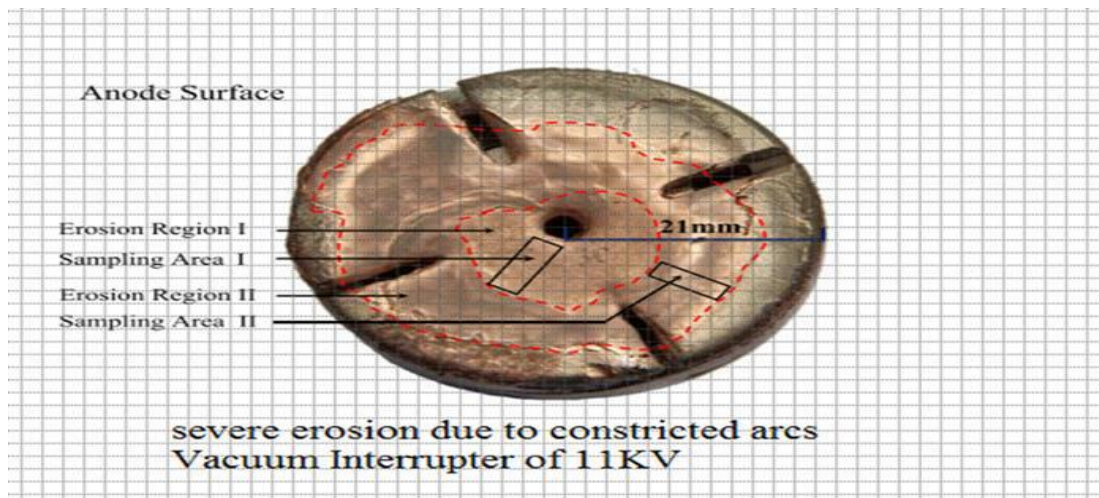


Fig. 2.10 Severe erosion – constricted arcs for interrupter 11KV/630A/40KA

2.6 Transient over voltages formula

The vast majority of power switching devices spend almost all their life in the closed position for conducting current to a load. An arc current is drawn when this device is switching off and a transient recovery voltage creates during this time of interrupting. The time formula is according to circuit diagram shown;

$$TOV = T = \frac{1}{2\pi\sqrt{LC}} \dots \dots (2.2)$$

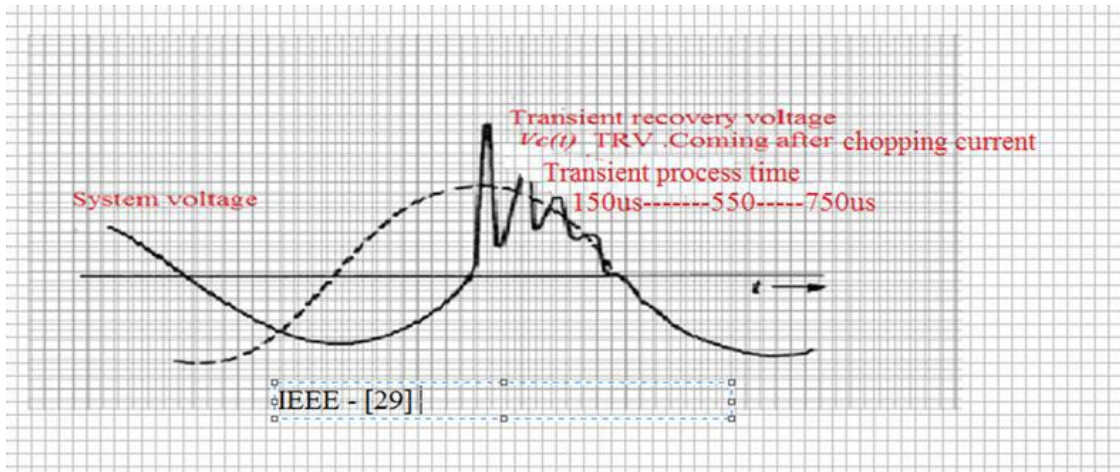


Fig.2.11 High transient over voltages and time sequences

It is assumed that a load (not shown) is being fed through the circuit breaker and that short circuit has just occurred now , isolating the load from the source . L is all the inductance limiting the current to the point of fault, while C is the natural capacitance of the circuit adjacent to the circuit breaker. It comprises capacitance –to –ground bushing, current transformers, and so forth, and perhaps the capacitance of a local transformer, as well as capacitance across the breaker contacts. Resistance and any other form of loss has been neglected. The fault current, being inductive, lags the voltage by 90° , thus when circuit breaker is arcing , the voltage across its contacts is the arc voltage , which for vacuum is very low . This constraint is removed once arcing ceases allowing current from the source to flow into C to bring to source potential. Being a resonant current, the voltage of C, and therefore across the switch, overshoots; in short an oscillation occurs at the natural frequency of the circuit, the period being $T= 12\pi\sqrt{LC}$ This is the TRV referred to previously.

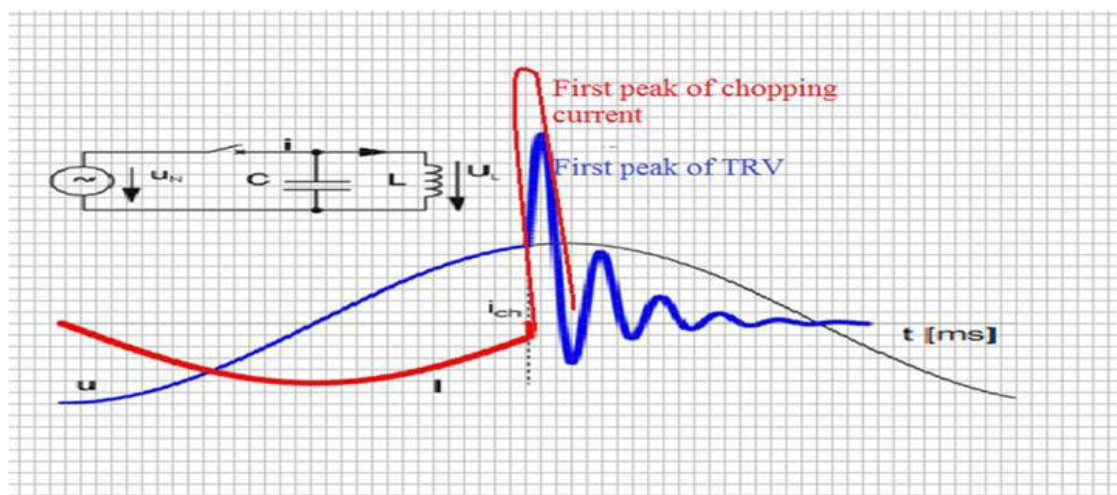


Fig.2.12 Chopping current graph and phasing transient voltage

This peak of transient recovery voltage would be attained in 255 μ s for normal operating mode .

N:B .Some researching papers indicate of the transient recovery voltage for medium circuit breaker of 11KV (200 , 220, 250, 350 and 400 μ s)

$$\zeta = [di/dt][du/dt] \dots \dots \dots (2.3)$$

$[di/dt]$ is the rate of decline of current immediately prior to current zero , $[du/dt]$ is the rate of rise of voltage across the open contacts immediately after current interruption The higher the value of this product, the better the interrupting device . In this regard , vacuum interrupters are far superior other types, also I was described two modes of vacuum arc, the diffuse and constricted modes, for this reasons that will become clear, the constricted arc recover much more slowly than the diffuse arc , implying that the $[du/dt]$ capability is much lower in that mode. Consider these two modes separately , starting first with the diffuse mode. If successful interruption of vacuum arc depends on the dispersal of the arc products, it behoves us to consider what arc those arc products and how do they disperse. We recognize a number of components: metal vapor , metal ions , electrons , gas molecules , metal droplets and partial discharge due to transient recovery voltage or /and switching impulse over voltages .

The model of the arc has continuously generated and being continuously dispersed . Electrons and metal vapor issue from the cathode surface at the cathode spots. The vast majority of vapor is ionized in the ionization region (see figure above) and the metal ions so produced flow to cathode and anode as described , where they recombine with electrons and become metal atom once again , because electromagnetic effectiveness . A small fraction escape to the shields where they are similarly removed from circulation.

The cathode spots move, so they leave behind the trails on the contact surface which continue to emit metal vapor until they cool. Cooling is fairly rapid , depending on the thermal diffusivity of the contact material , and of course, evaporation itself is a powerful cooling process in that each atom evaporated takes with it its latent heat of vaporization Vapor is similarly produced from the region immediately surrounding the active cathode spots, where the temperature is high enough for vapor production , but where conditions of temperature and electric field are inadequate to cause electron emission . Vapor from whatever source disperses because of high particle gradients. Unlike the ions it is not directly influenced by the electric field although it may exchange energy and momentum with ions when collisions occur. Like the ions, the vapor condenses on cool surfaces it encounters and is thereby removed from the gap. In the context of interruption, one is particularly concerned with the population in the contact gap and other electrically stressed regions of the interrupter at current zero and immediately afterwards. This requires that one knows what rates of the different particles and how long they stay in the gap, for these are the factors that

determine their density or concentration. Production of both vapor and ions is dependent on erosion rate from the cathode.

Many scholars of scientists have measured this determined that for a diffuse arc on copper it is range 50-100 $\mu\text{g}/\text{C}$. Some of this is in form of droplets. High vapor pressure materials have greater erosion, but I concentrate on copper since it is a major constituent in most power interrupter contacts. A number of investigators, Tanberg [49], Reece [50], Easton et al [51] and Plyutto [52], have measured the velocity of jet of copper vapor emitted from the cathode spot. They used essentially the same method which was to insert a vane into the vapor and measure the force on the vane or the reaction force on the cathode. This allows one to calculate the momentum exchange and knowing the mass of vapor deposited, the mean velocity can be determined. For copper the figure was found to be approximately 10^4 m/s .

This means that on the average, vapor particle remains in a 1 cm contact gap for about $1\mu\text{s}$ from which one can infer that at the time of arc extinction the gap has very little memory of prior events

This observation clearly has important implications for current interruption at power frequency (50 or 60Hz), where the decline of current zero, $[dI/dt]$ in equation, extremely slow on the time scale of vapor dispersal. As Farrall [52] puts it, 'a vacuum interrupter will begin to recover while the arc is still burning just after the sinusoidal peak'. How different this is from a gas blast interrupter. In vacuum the power frequency arc has difficulty maintaining itself as current zero approached. It usually becomes unstable and is interrupted prematurely. This phenomenon was discussed. Knowing the vapor velocity and the erosion rate, and assuming a velocity distribution (usually Maxwellian) it is possible to compute the vapor density in the gap at any instant during the decline of current. We are particularly interested, in condition at current zero, when dielectric recovery proper begins.

The basic premise is that early in the recovery period, the inter-electrode volume contains a high density of metal vapor which, when high voltage is applied, breaks down through collision effects in the manner discussed before. As the decay of vapor proceeds, the density of neutrals ultimately approaches a level for which the electron mean free path in that vapor is of the order of the gap length. This condition is taken to be a critical one since at that time, break down is assumed to have become independent of the presence of decaying vapor. As implicit assumption has been made in the foregoing, namely that when vapor particles reach a solid surface they condense and are removed from consideration in the gas phase. This is frequently the case. However, if the surface is hot, the accommodation coefficient is less than unity, that is to say some fraction of the particles rebound from the hot surface, causing the vapor density to be higher than computed. Zalucki and Kutzner [59] ("streams of neutral particles reflected from anode in vacuum arc" have investigated the consequences of this. The effect is more important for prolonged

arcing since the flux of vapor itself heats the condensing surface. It is particularly important with a constricted arc. Now turn attention to the ions in the arc as the current declines and see what effect, if any, they may have on recovery. The model used is that described by Childs and Greenwood and later by Childs, Greenwood and Sullivan [45]. As the current commences to decline there are typically a number of cathode spots pouring plasma into the inter-electrode gap. As the current falls, these will extinguish one by one until only one remains. Most of the current is carried by electrons but some fraction is carried by ions; for copper this fraction is approximately 8% [55] it was suggested that the electrons and ions were like two trains on parallel tracks with the electrons train going $(2-s)/(1-s)$ times faster than the ion train

$$\frac{-V}{+V} = \frac{-J}{+J} = \frac{(2-s)}{(1-s)} \dots \dots \dots (2.4) \text{ Joule heating}$$

$(1-s)$ ion current while $(2-s)$ electron current. As the current in the last cathode spot continues its decline following the dictate of the external circuit the electron train must decelerate so that, at current zero, it is travelling at the same speed as the ion train. The gap remains bridge by low impedance plasma, so current continues to flow. The ions have considerable inertia and therefore maintain their progress towards the anode. The electrons on the other hand, continue to decelerate, or in terms of the train analogy, the electron train goes slower than the ion train and the net current is negative. What we are observing is post-arc current. In a very short time the electron train comes to halt and maintain the dI/dt it reverses. However, in doing so, it creates a region adjacent to the anode which is depleted of electrons. It is at this instant when the electrons reverse and the positive ion sheath forms, that the TRV commences to build up and concentrate across the ion sheath.

Conclusion: The movement among ions and electrons travels parallel speed together, but for the collisions between them due to the charging and discharging phenomena.

2.7 Mathematical Fourier transformation model

The behavior of the synchronous fields which have voltage, current and magnetic fields rotate according to the Euler's Formulas as a complex process of transmission between a generator side thoroughly each circuit breaker.

We can construct a mathematical switching intervene:

$$e^{i2\pi\theta} = \cos(2\pi\theta) + i \sin(2\pi\theta) \dots (2.5)$$

This is relationship between the trigonometric functions and the complex exponential functions. Euler's formula states that, for any real number x :

Such as sine and cosine synchronous fields inside vacuum interrupter involve with "Fourier Series Transform" because a chopping currents and transient over voltages comes together for an intervene functions which are represented by these series.

$$f(x) = a_0 + \sum_{n=1}^{\infty} (a_n \cos nx + b_n \sin nx) \dots (2.6) \text{ general Formula}$$

Given such a function $f(x)$, we want to determine the coefficient a_0 , a_n and b_n . We first determine a_0 . Integrating on both side (2) from $-\pi$ to π , we have

$$\int_{-\pi}^{\pi} f(x) dx = \int_{-\pi}^{\pi} a_0 + \sum_{n=1}^{\infty} (a_n \cos nx + b_n \sin nx) dx \dots$$

If term-by-term integration of the series is allowed that we can obtain

$$\int_{-\pi}^{\pi} f(x) dx = a_0 \int_{-\pi}^{\pi} dx + \sum_{n=1}^{\infty} \left(\int_{-\pi}^{\pi} a_n \cos nx dx + b_n \int_{-\pi}^{\pi} \sin nx dx \right)$$

The first term on the right equals $2\pi a_0$, while the other integrals are zero, as you can readily see by performing the integrations. Hence our first result is

$$a_0 = \frac{1}{2\pi} \int_{-\pi}^{\pi} f(x) dx \dots (2.7)$$

We now determine a_1, a_2, \dots by a similar procedure. We multiply (2) by $\cos mx$ Where m is any fixed positive integer, and then integrate from $-\pi$ to π finding By term-by-term integration the right side-hand side becomes

$$f(x) = a_0 \int_{-\pi}^{\pi} \cos mx dx + \sum_{n=1}^{\infty} \left(a_n \int_{-\pi}^{\pi} \cos nx \cos mx dx + b_n \int_{-\pi}^{\pi} \sin nx \cos mx dx \right) (2.8)$$

The first integral is zero, and so is the last integral, because its integrated is an odd function. So we can simplifying the above equation – Fourier Series;

$$\int_{-\pi}^{\pi} \cos nx \cos mx dx = \frac{1}{2} \int_{-\pi}^{\pi} \cos(n+m)x dx + \frac{1}{2} \int_{-\pi}^{\pi} \cos(n-m)x dx \dots$$

In this formula the first integral on the right is 0 for all m and n under consideration ; the last integral is zero when $n \neq m$ and is π when $n=m$. Hence the right hand side (4) equals $a_m \pi$ and our second result is

$$a_m = \frac{1}{\pi} \int_{-\pi}^{\pi} f(x) \cos mx \, dx, \text{ where } m = 1, 2, \dots \text{ (2.9)}$$

$\sin mx$, where m is any fixed positive integer, and then integrate from $-\pi$ to π , we have

$$\int_{-\pi}^{\pi} f(x) \sin mx \, dx = \int_{-\pi}^{\pi} \left[a_0 + \sum_{n=1}^{\infty} (a_n \cos nx + b_n \sin nx) \right] \sin mx \, dx \dots \dots \text{ (2.10)}$$

fields for all value of x . Throughout calculus, angles are measured in radians so that both functions have the period 2π . $f(-x) = f(x)$ for all x is called an even function. $f(-x) = -f(x)$ for all x , then $f(x)$ is called an odd function. These concepts are quite important concepts. Since

$$\sin(-x) = -\sin(x), \quad \cos(-x) = \cos x$$

Sine x is odd while cosine x is even.

The functions sine x and cosine x are related by identity $\sin^2 x + \cos^2 x = 1$ we can obtain:

$$\sin(x + y) = \sin x \cos y + \cos x \sin y$$

$$\sin(x - y) = \sin x \cos y - \cos x \sin y$$

In particular, $\sin 2x = 2 \sin x \cos x$. The additional formulas of cosine function are

$$\cos(x + y) = \cos x \cos y - \sin x \sin y$$

$$\cos(x - y) = \cos x \cos y + \sin x \sin y$$

$$\sin x \sin y = \frac{1}{2} [-\cos(x + y) + \cos(x - y)]$$

$$\cos x \cos y = \frac{1}{2} [\cos(x + y) + \cos(x - y)]$$

The two formulas are very important for clarifying Fourier transform

$$\int_{-\pi}^{\pi} \cos nx \cos mx \, dx = \frac{1}{2} \int_{-\pi}^{\pi} \cos(n + m)x \, dx + \frac{1}{2} \int_{-\pi}^{\pi} \cos(n - m)x \, dx$$

In this formula the first integral on the right is 0 for all m and n under consideration; the last integral is zero when $n \neq m$ and π when $n=m$. Hence the right hand side (4) equals $a_m \pi$, and our second result is

$$a_0 = \frac{1}{2\pi} \int_{-\pi}^{\pi} f(x) dx \dots \dots \dots (2.11)$$

$$a_n = \frac{1}{\pi} \int_{-\pi}^{\pi} f(x) \cos nx \, dx \dots \dots (2.12)$$

$$b_n = \frac{1}{\pi} \int_{-\pi}^{\pi} f(x) \sin nx \, dx \dots \dots \dots (2.13)$$

For $n=1,2,3,\dots$ For each periodic function $f(x)$ for Fourier coefficients of $F(x)$ being given inside interrupter for switching process with period 2π so, we may compute the

$$a_0 + a_1 \cos x + b_1 \sin x + \dots \dots a_n \cos nx + b_n \sin nx + \dots$$

It's obvious that the Fourier series describes also a heat which generates inside vacuum plates that we can applied the same technique for both mathematical and physical problems and especially those involving linear differential equations for the transition rates of du/dt or di/dt thoroughly switching processes together by using time domain [25][26][28].

2.8 Experiment test for calculating of chopping currents

Calculating of the first peak value of oscillating currents and evaluate the transient over voltages on Petersen Reactor Coil Automatic Tuning, $Z_0=3000\Omega$.

$$U_T = I_{ch} * Z_{Load} \dots \dots (2.14)$$

U_T – voltage of the first peak value.

I_{ch} – current chopping.

Z_{Load} - Load Impedance .

In order to verifying the statistical approach of the correctly calculation of first peak values for each circuit breaker: $U_T = 0.9 \times 3000 = 2700 \text{ V}$ first peak transient voltage.

$U_{MAX} = 2.7\text{KV} + 10 \text{ KV} = 12.7\text{KV}$ reasonable transient over- voltage. Thus, the first table .1 indicates the data sheet regarding my calculation permissible for full operation loads:

Table 4 - calculating chopping currents and transient over voltages

No	IC_A	UT_KV	U_KV	<u>Umax_KV</u>	<u>Ud_KV</u>	Results
1	0.1	0.3	10	10.3	28	Acceptable
2	0.2	0.6	10	10.6	28	Acceptable
3	0.3	0.9	10	10.9	28	Acceptable
4	0.5	1.5	10	11.5	28	Acceptable
5	0.9	1.7	10	12.7	28	Acceptable
6	1	3	10	13	28	Acceptable
7	2	6	10	16	28	Acceptable
8	3	9	10	19	28	Acceptable
9	4	12	10	22	28	Acceptable
10	5	15	10	25	28	Critical
11	6	18	10	28	28	Critical
12	7	21	10	31	28	Disruptive
13	8	24	10	34	28	Disruptive
14	9	27	10	37	28	Disruptive
15	10	30	10	40	28	Disruptive



Fig.2.13 Measurement Instrument of chopping currents- ABB Norway

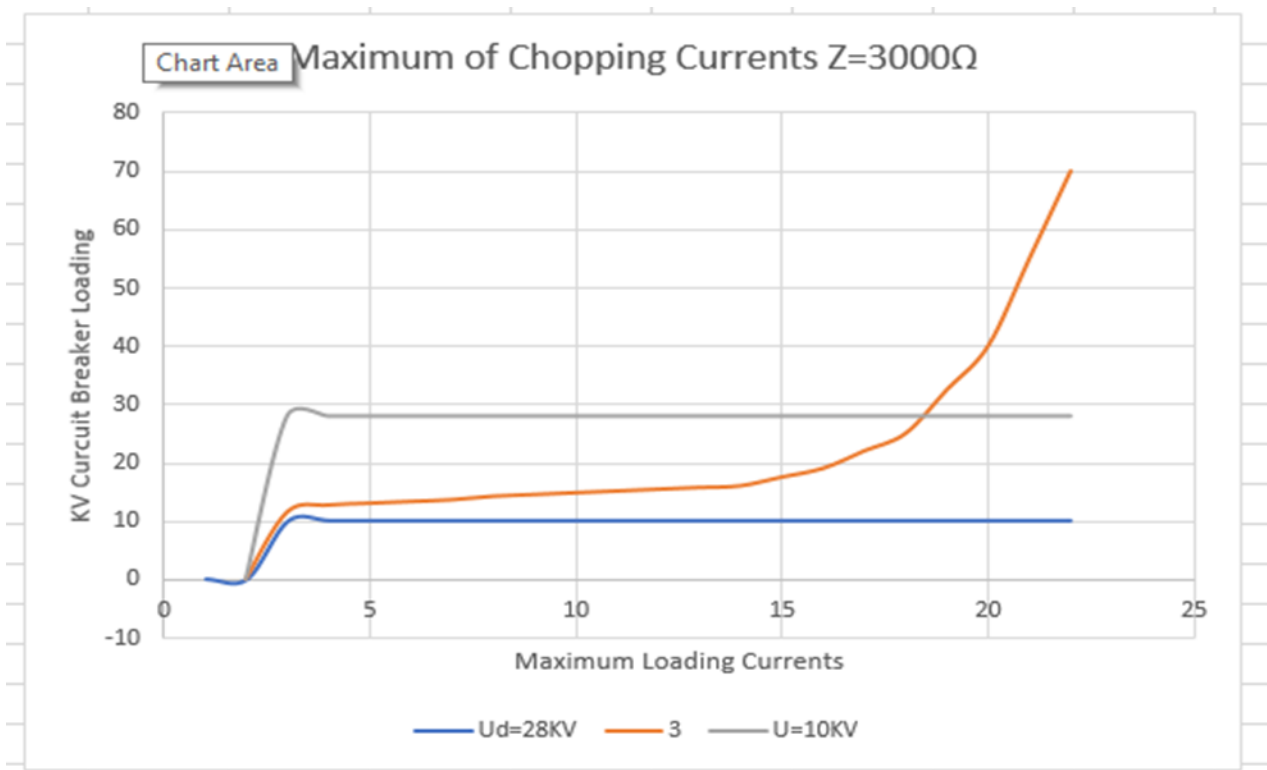


Fig.2.14 Calculation of first peak value of chopping current

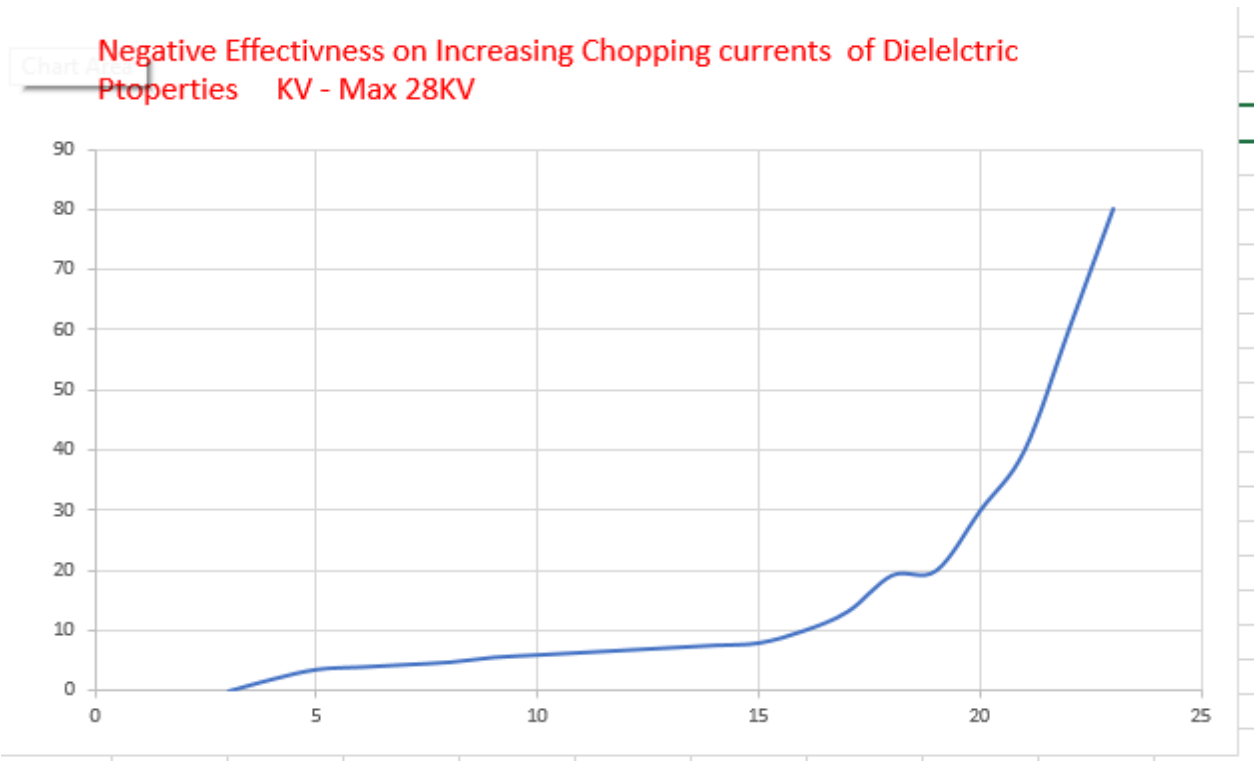


Fig. 2.15 Negative Effectiveness of chopping currents on insulation

Table 5- calculating table of data sheet for negative effectiveness on dielectric properties

No	IC_A	UT_KV	U_KV	<u>Umax_KV</u>	<u>Ud_KV</u>	Results
1	0.1	0.55	10	10.55	28	Acceptable
2	0.2	1.1	10	11.1	28	Acceptable
3	0.3	1.65	10	12.65	28	Acceptable
4	0.5	2.2	10	13.2	28	Acceptable
5	1	5.5	10	16.5	28	Acceptable
6	2	11	10	21	28	Acceptable
7	3	16.5	10	26.5	28	Critical
8	4	22	10	32	28	Disruptive
9	5	27.5	10	37.5	28	Disruptive
10	7	38.5	10	48.5	28	Disruptive
11	10	55	10	65	28	Disruptive



Fig. 2.16 Petersen Reactor Coil Transformer in ABB Norway

2.9 Calculating of NSD discharging times – Experiment Test

There is another negative effectiveness comes from outside of vacuum interrupter. In order to get more quantitative information results on the discharged occurrence many tests of experiments performed at Eindhoven University of Technology [9][23]. The experiment was implemented for testing of three capacitors parallel with vacuum circuit breaker VCB. The parameters of each capacitor of: (1.1MHz) (430KHz) and (72KHz) connecting with power transformer 12KV as we seen in the figure below:

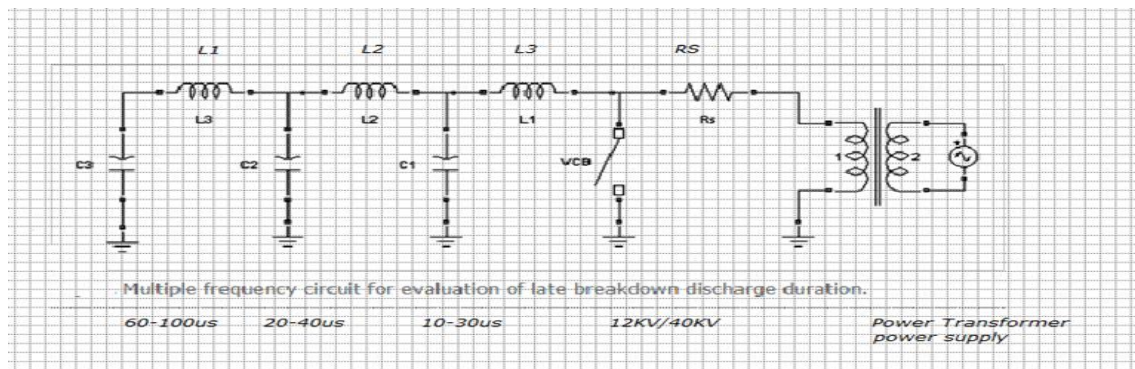


Fig2.1 Circuit for calculating of discharge switching times for three capacitors

Each capacitor will (start to) discharge upon breakdown of the test-breaker. The discharge frequencies are chosen such as to simulate the various circuit parts that will contribute

to a high-frequency (HF) discharge upon breakdown. Of an interrupter in a real circuit; various stray capacitances and inductances will contribute to a multi frequency oscillation through the arc.

In the experimental approach described here, the three inductance-capacitance (LC) circuits are meant to represent circuit parts that are in the immediate vicinity of the gap (L1C1: 1.1 MHz), at some distance (meters) away from the gap (L2C2: 430 kHz), and relatively remote (tens of meters) from the gap (L3C3: 72 kHz).

It turned out that the frequency of occurrence of late breakdown differed greatly from breaker to breaker, and in order to obtain a sufficiently high number of results for both breakers, the approach was chosen to monitor the first prestrike that occurs upon closing of the contacts.

Comparison of the discharge characteristics (oscillogram, breakdown voltage, duration of discharge, HF current interruption mode) of the prestrike discharge with the actual late breakdown discharge showed no difference. Thus, it is assumed that the processes that determine the duration of the first prestrike arc are equivalent to those governing the late breakdown arc.

Analysis the results:

In the first series, discharges were monitored in oscillatory circuits of only one single frequency (L1C1, L2C2, or L3C3). A striking and very clear difference in discharge duration is observed. In Fig.3.19 examples of the discharge current [Fig.3.18(a)] and voltage across the interrupter [Fig.3.18 (b)] are given, together with the cumulative fraction of duration of HF current flow for each of the two interrupters (solid and dotted curves, respectively) and for each of the three discharge frequencies.

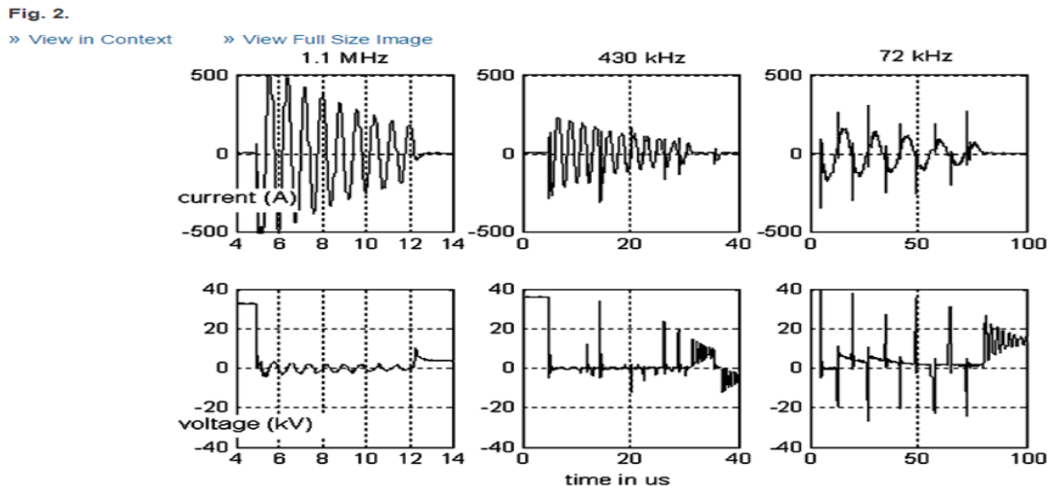


Fig 2.18 Measured discharges in three single frequency circuits. (a) Current through VCB. (b) Voltage across VCB. (c) Cumulative fraction of discharge duration in circuits LC1 (1.1 MHz), LC2 (430 MHz), LC3 (72 kHz). Dashed: VCB A. Drawn: VCB B.

For each of the three frequencies, a different re ignition mechanism can be observed.

1).L1C1 (1.1 MHz, typical discharge duration $10\mu\text{s}$); du/dt . At this frequency, the transient recovery voltage (TRV) following HF current zero is not important. Apparently, of the current is decisive whether or not HF current is interrupted. Once the HF current is interrupted, the feeding capacitor is discharged to a large degree because of the high damping in the L1C1 circuit at this frequency (damping time constant $680\mu\text{s}$).

2).In this mode, thermal processes determine the duration of the HF arcing.

L3C3 (72 kHz, typical discharge duration $60\text{--}100\mu\text{s}$); du/dt . At this frequency, TRV rises after every HF current zero. Apparently, the gap is able to interrupt at every HF current zero, but the TRV thereafter cannot be withstood. Hence, di electrical processes determine fully whether arcing will continue or not. Because of the lower frequency, the driving capacitor C3 can maintain its voltage relatively long (damping time constant is $830\mu\text{s}$).

3).L2C2 (430 kHz, typical discharge duration $200\mu\text{s}$) du/dt . In this intermediate discharge frequency range, a mixture of both of the previous processes (L1C1 and L3C3) is present. Initially, at high, this quantity determines the HF current interruption result. In a later arcing stage, when is reduced due to the damping in the circuit, TROV becomes decisive (damping time constant $210\mu\text{s}$).

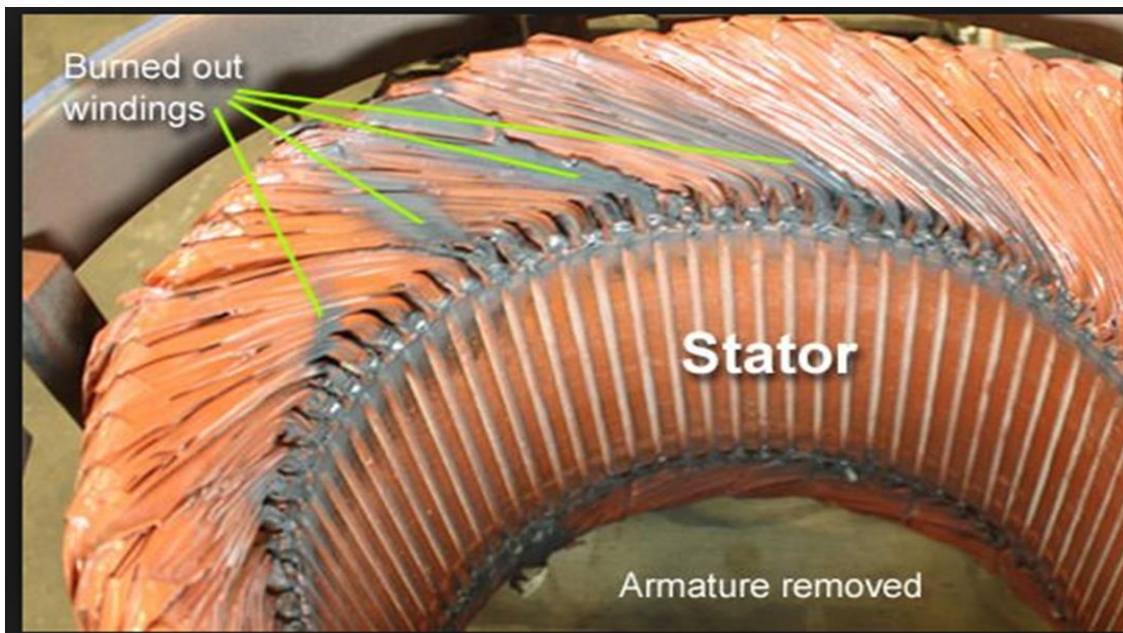


Fig.2.19 Negative effectiveness of primitive switching impulse on 11kV Induction motor

2.10 Conclusions

1. There is a joule heating initiated inside of each vacuum sealing interrupter because there are intervene phenomena due to oscillation of processing switching steps.
2. The intervene among arcing currents, chopping currents and others which involved a Fourier transformation inside vacuum interrupter finally.
3. In MATLAB /Simulink confirmed that the switching negative effectiveness taken $600\mu\text{s}$.
4. The results obtained from chopping currents also confirmed that chopping currents measurement values (3A/5A and 7A) for the first chopping values, this data sheets we obtained from one transformer Petersen reactor coil ABB Factory.
5. There are further electrostatic -grounding capacitors, measuring by Mr. R.P.P. Smeets would be return back when interrupting.

III. DESIGN CIRCUIT & MATHEMATICAL APPLICATIONS

3.1 Hypothesis of static vacuum Interrupter

In order to design vacuum soft starter precisely, the following steps shall be considered

3.1.1 Analysis the designing of the existing Petersen Coil Automatic Tuning

3.1.2 Fabricating of Petersen Coil -Anode & cathode Coils

3.1.3 Inserting of LTT rectifying circuit

3.1.4 Synthesis of mathematical model

3.1.5 Synthesis of MATLAB/Simulink models

3.1.1 Analysis the designing of the existing Petersen Coil Automatic Tuning

Petersen coils are used in faults of 3-phase systems to limit arcing currents during earth faults process. The coil was first developed by William Petersen and still installed in all substations. However, the use of modern power electronics has revolutionized the performance of these classical solutions which called Arc Suppression Coil (ASC) and the modern of power electronics have been offered a new automatic tuning technique. My second invention was fabricated this reactor to be more convenient in each pole of interrupter [1][7][18].

The basic theory of damping currents is zero-sequence-voltage $U_0 = 0$ that means the transition rate of interrupter will be $du/dt = \text{Zero Voltage Switching} = \text{Zero Value}$

$$U_0 = 0 \text{ Zero Sequence Voltage (3.1)}$$

3.1.2 Fabricating of Petersen Coil

For designing of Petersen coil automatic tuning for the function of quenching both of arcing currents and chopping currents, it is customary to assume that the highest allowable current is produced at the arc suppression value. Upon this basis the following formula for the ohmic value. The current limiting coil should be considered of a resistor, an inductor, a capacitor or any combination of these.

$$I = \frac{KVA * 1000}{\sqrt{3} * V1} \dots (3.2)$$

$$Z_p = \frac{V}{\sqrt{3} * I} \dots (3.3)$$

Z_p = Impedance for Anode & Cathode Coils

I = maximum current passing in coil, amperes

V = transformer turned line volts 12kV

KVA = winding of transformer coil, KVA

Co= Coefficient of arcing currents & Chopping currents

So, the designing formula for Anode and cathode coils

$$Z_p = \frac{V^2}{C_o * KVA * 2000} \text{ ohms for single pole of interrupter (3.3)}$$

$$L = \frac{1}{3 * \omega c} \dots \dots \dots (3.4)$$

Sample one $L = 16 \text{ mH}$ for $Z = 62.699 \text{ Ohm}$ Anode & Cathode Coils

$Z_p = 32.00 \text{ } \Omega$ for Anode winding Coil-1.75mm cross section

$Z_p = 32.00 \text{ } \Omega$ for Cathode winding Coil 1.75mm cross section

THY Rating 63A/12kV/ 1200 μ s/A 180KA / LTT type

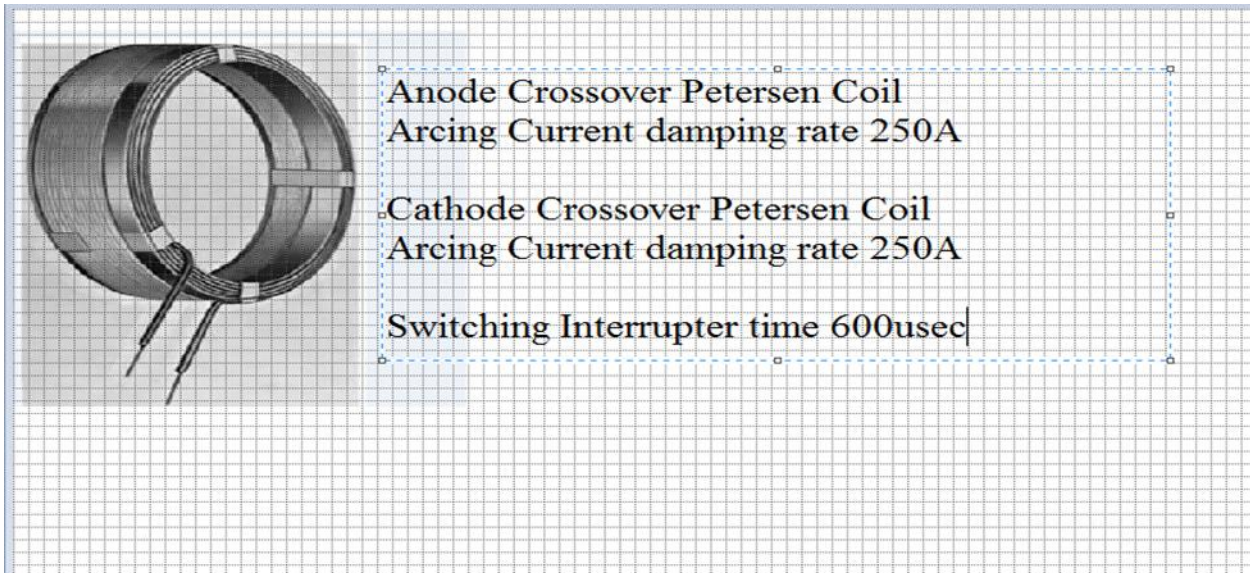


Fig. 3.1 Fabricated Petersen Coil – Designing Stage

Its customary typical, the coil shall be designing a cylindrical winding shaped that to be fitted in the Anode Pole & Cathode Pole.

SION/3AES SIMENS 12kV/630A

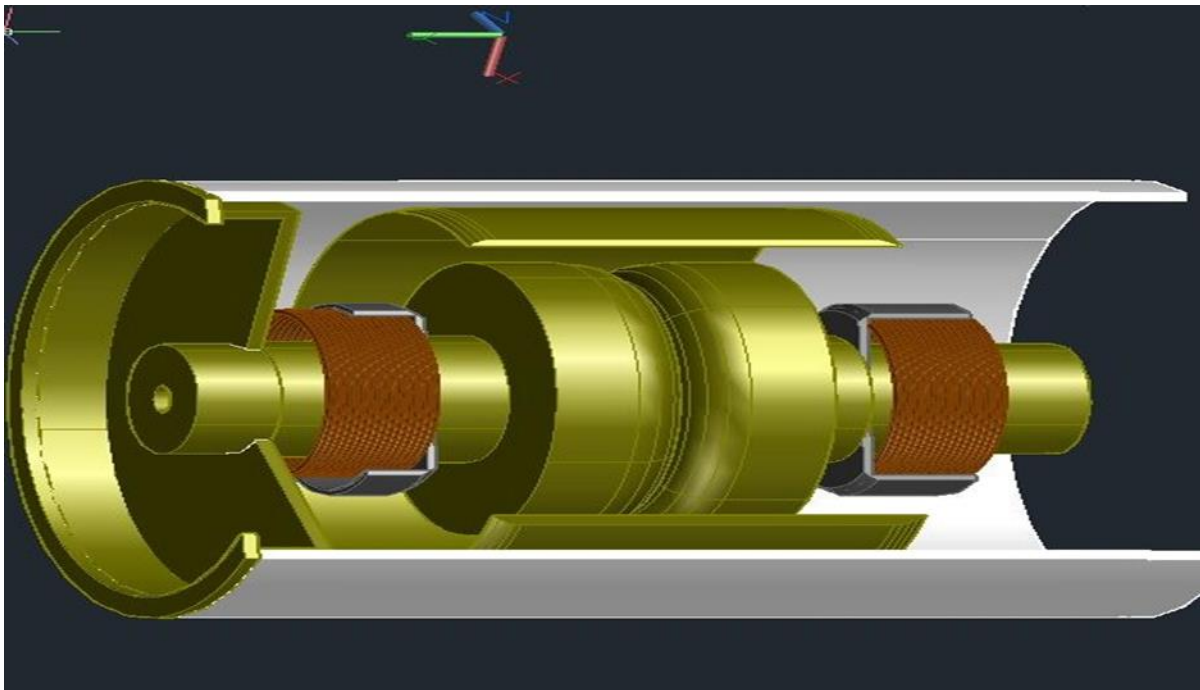


Fig. 3.2 Fabricated Petersen coil – Designing stage-sample one
Brown coils – Anode and Cathode – two coils inserted inside vacuum poles
Dimensions R= 25mm L= 50mm

Sample two $L = 20\text{mH}$ for $Z = 50.24\ \Omega$ Anode & Cathode Coils
 $Z_p = 50\ \Omega$ for Anode winding Coil- 1.55mm cross section
 $Z_p = 50\ \Omega$ for Cathode winding Coil-1.55mm cross section
THY Rating 125A/12kV/ 1200 μs /A 180KA / LTT

SION/3AES SIMENS 12kV

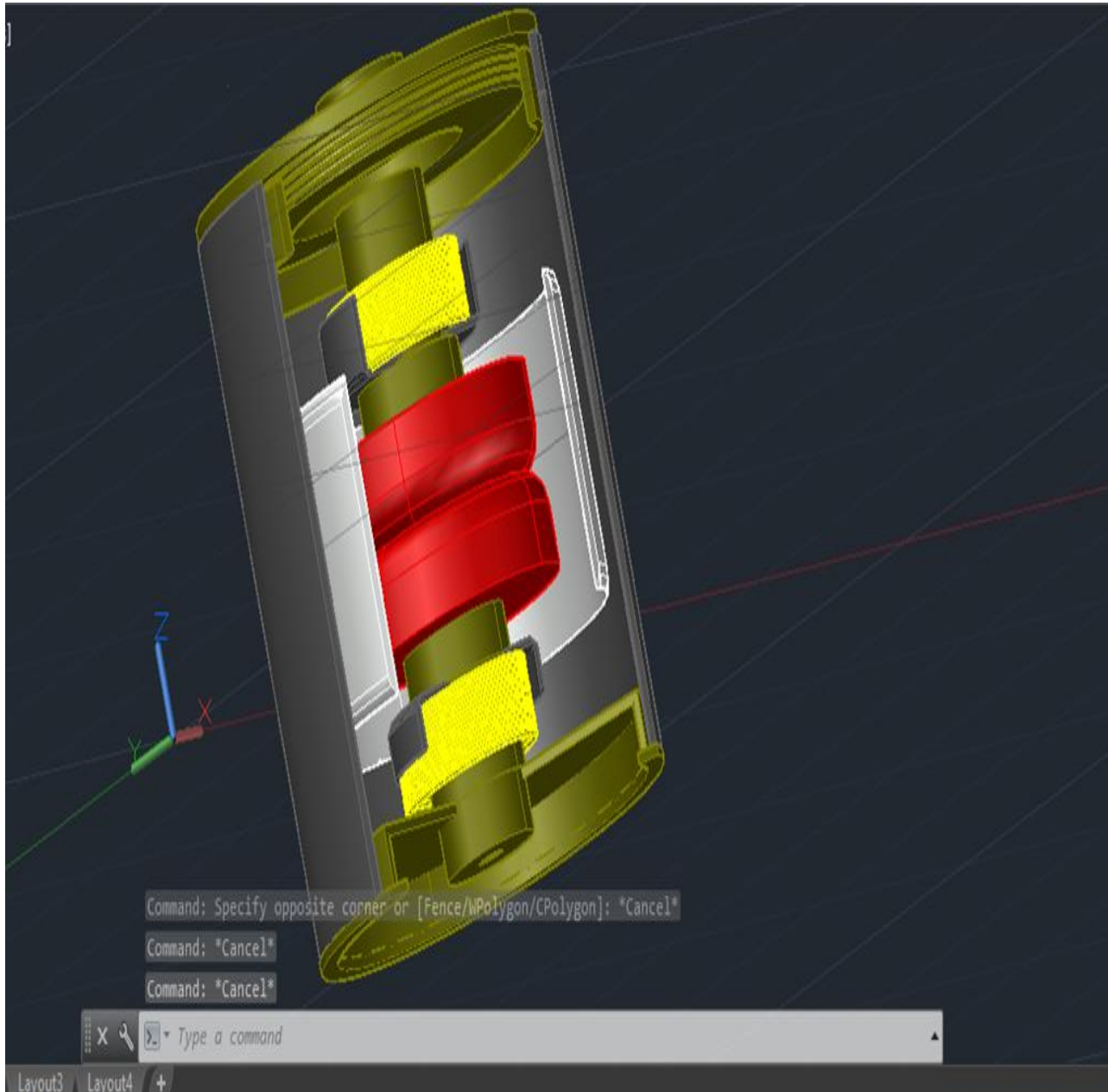


Fig. 3.3 Fabricated Petersen Coil –sample two

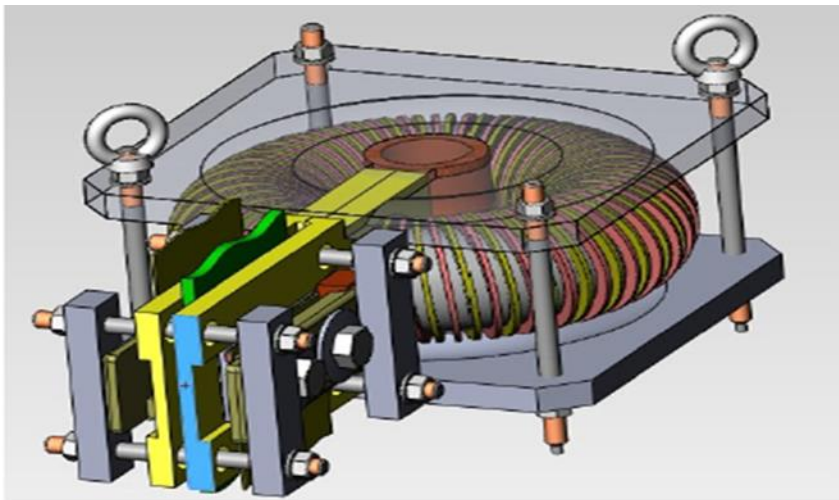


Fig. 3.4 Modification sample of Anode & Cathode Poles - St Petersburg Institute

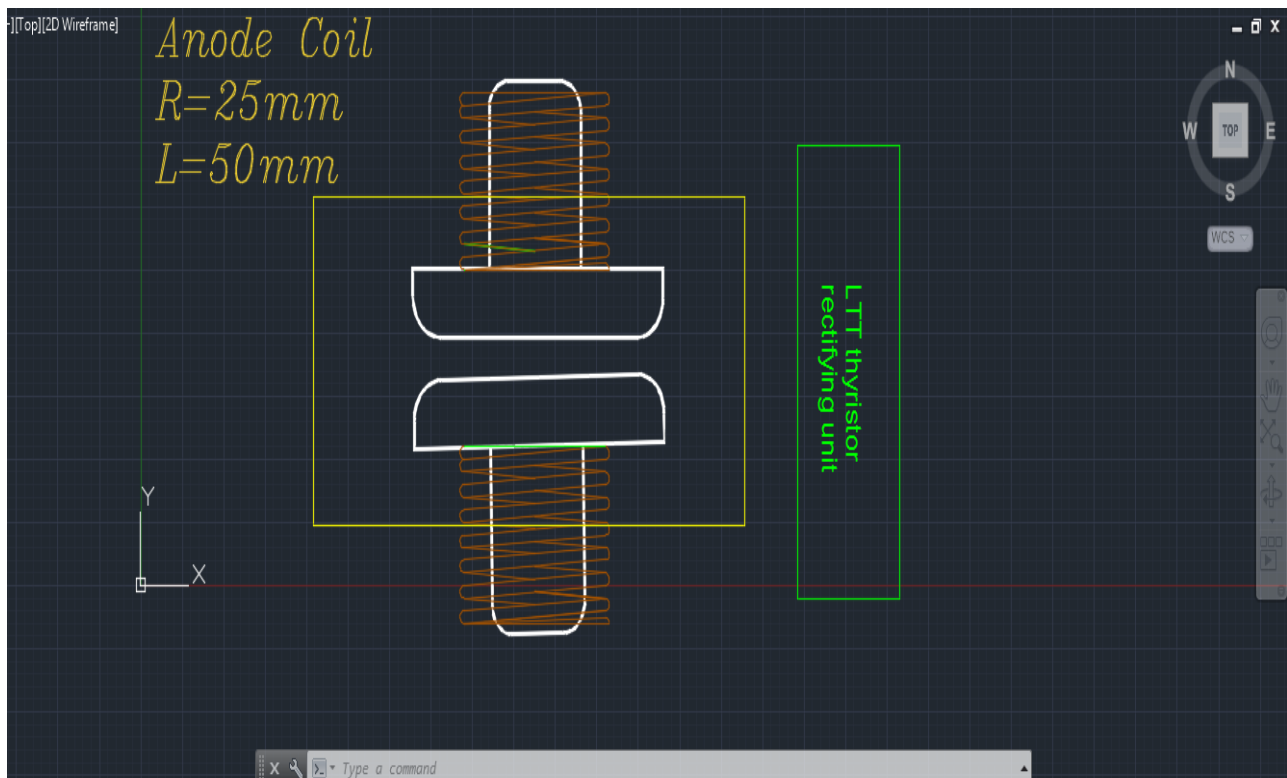


Fig. 3.5 Modification of Anode & Cathode Poles -experiment test

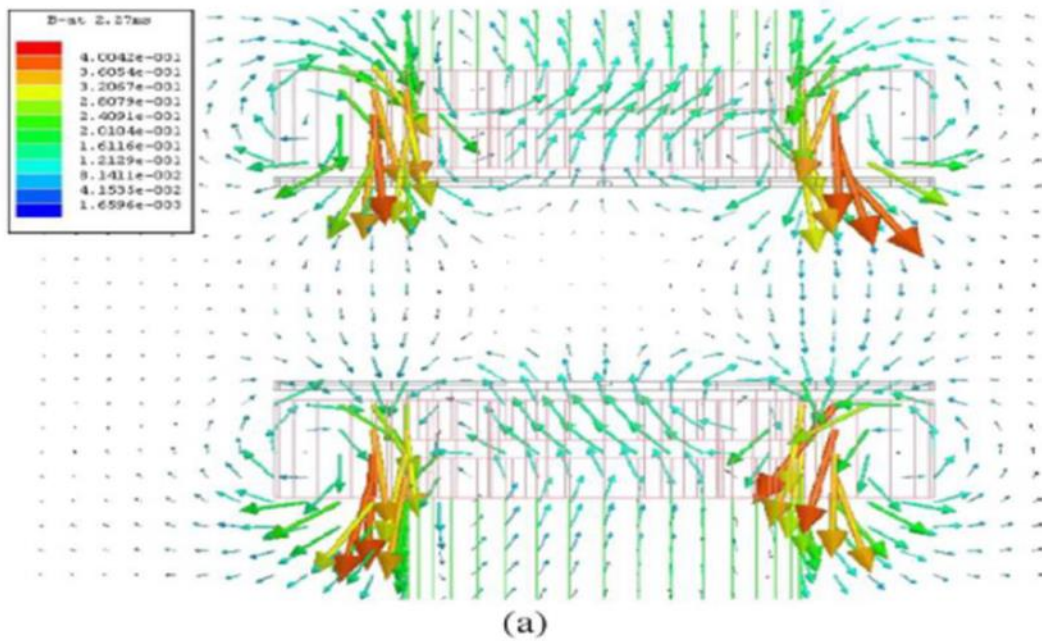


Fig. 3.6 AMF rotates between anode and cathode Petersen coils

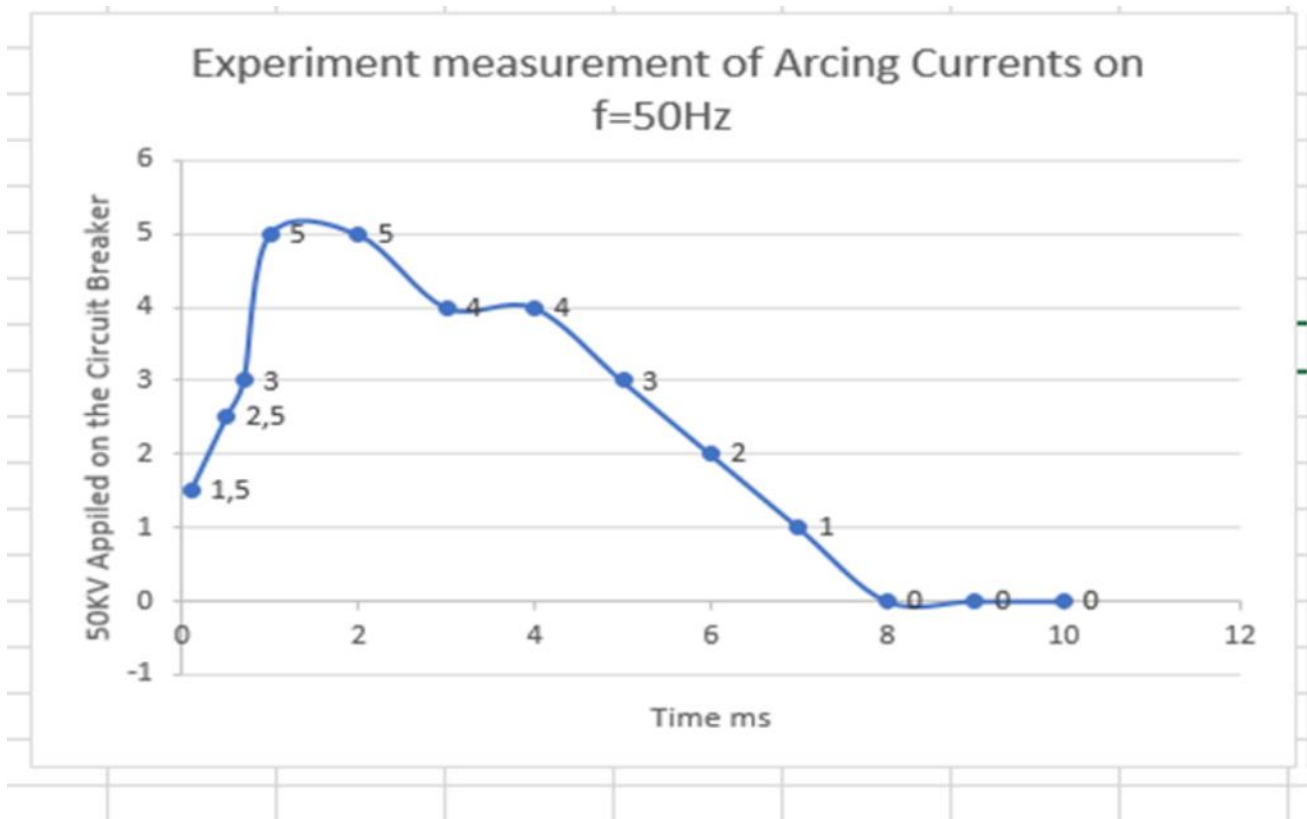


Fig. 3.7 Maximum arcing currents – experiment MATLAB test

Sample three $L = 40\text{mH}$ for Anode & Cathode Coils
 $Z_p = 63.00$ for Anode winding Coil -1.1mm cross section
 $Z_p = 63.00 \Omega$ for Cathode winding Coil -1.1mm cross section
THY Rating 250 A/12kV/ 1200 $\mu\text{s/A}$ 180KA / LTT

SION/3AE1 SIMENS 12kV/630A

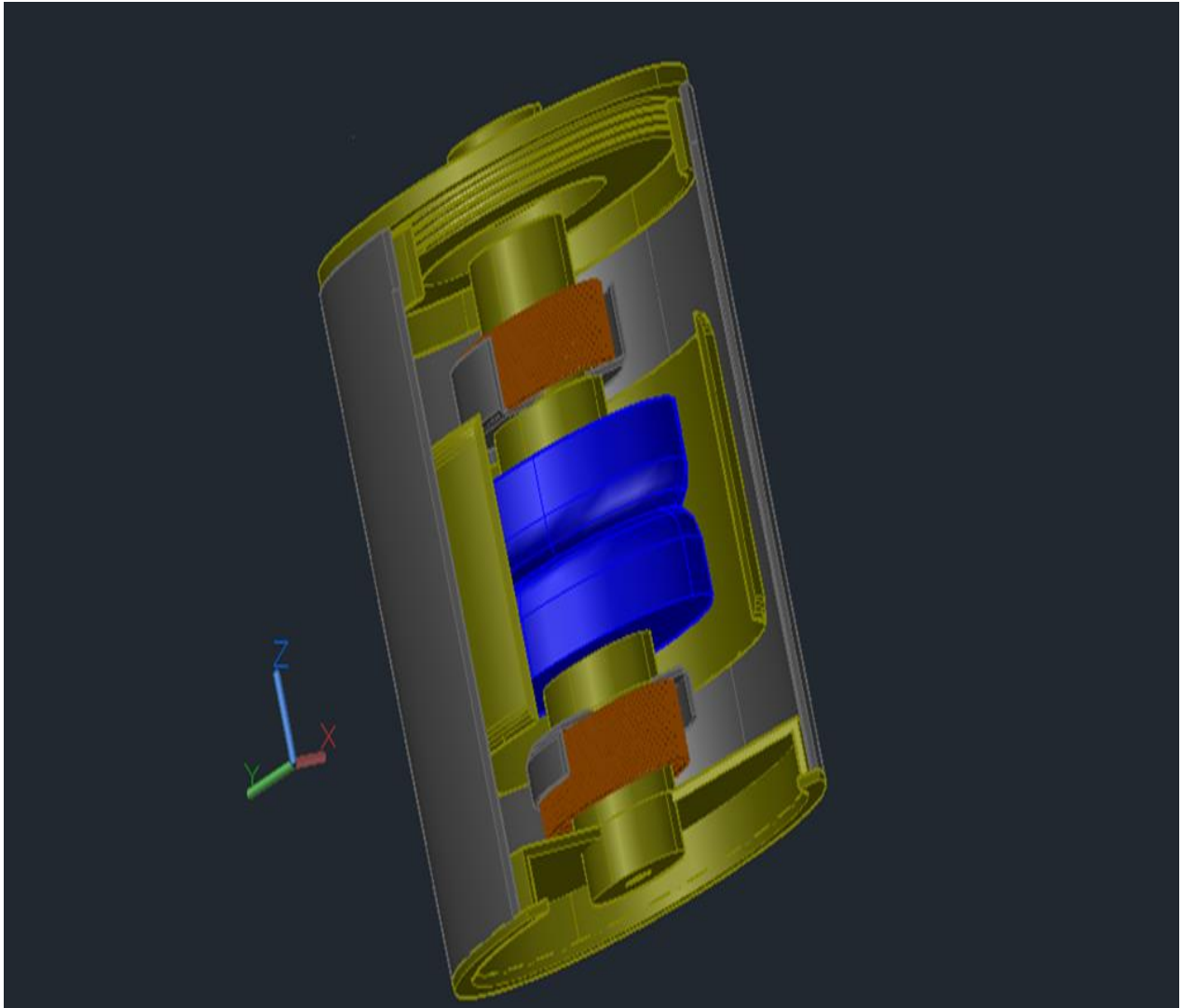


Fig. 3.8 Designing of Petersen Reactor Coil Automatic Tuning Anode & cathode- sample three

3.1.3 Inserting of LTT rectifying circuit

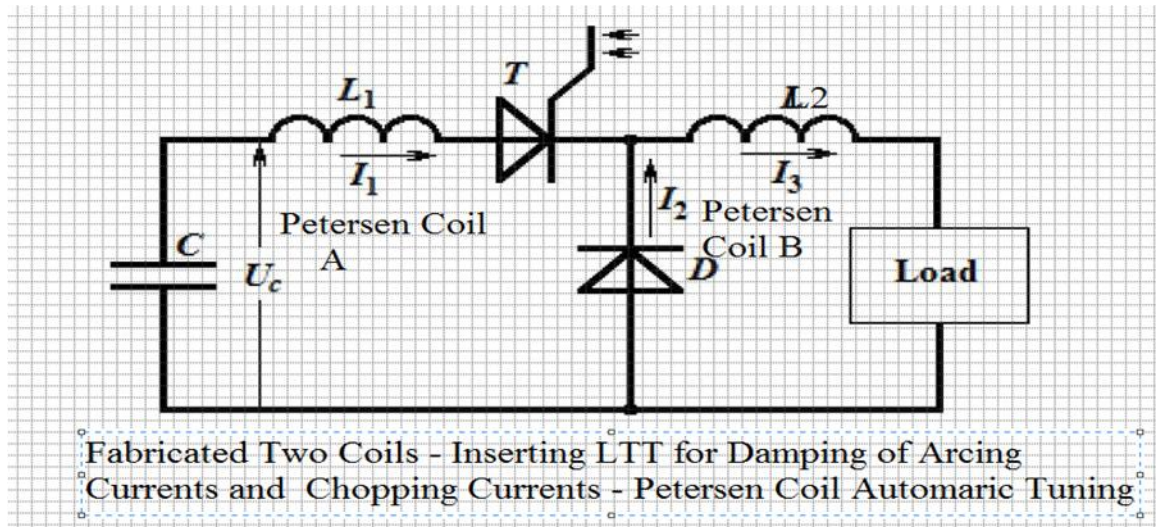


Fig. 3.9 Theory of damping application by inserting LTT Thyristor

The function of this circuit fig. 3.5 is a similar of my proposed circuit L1 & L2 two elements of reactor coils insets on one LTT thyristor for discharging of the capacitance charges to the load

A) Definition of mathematical concepts

In order to create mathematical formula which is being more facility for damping application of two coils (Anode Coil A & Cathode Coil B) in parallel operation technique including one thyristor set for soft interrupter, we shall design basic module of inductive reactance value of 25 mH for my thesis of proposal circuit.

B) Basic module of Inductive reactance with inserting LTT rectifying circuit

3.1.4 Synthesis of mathematical model

If we have $f(t)$ mathematical function contains all positive values of t . When multiply $f(t)$ by e^{-st} and integrate with respect to t from zero to infinity. The result integral exists, it is a function of S , say $F(S)$:

$$F(s) = \int_0^{\infty} e^{-st} f(t) dt \quad (3.5)$$

This is general Laplace transform which describes a linear operation. That is for any function “ I am referring here in MATLAB /Simulink” “ Symbol Operator” as followings

$$\begin{aligned} L\{af(t) + bg(t)\} &= aL(f) + bL(g) \\ &= a \int_0^{\infty} e^{-st} [af(t) + bg(t)] dt \\ &= a \int_0^{\infty} e^{-st} f(t) + b \int_0^{\infty} e^{-st} g(t) dt \dots \dots \dots (3.6) \end{aligned}$$

$$L(t^a) = \int_0^{\infty} e^{-st} t^a dt$$

These two equations will be simplified that the damping mathematical application shall be involved

$$e^{at} t^n = \frac{n!}{(s-a)^{n+1}} \dots \dots (3.8)$$

General formula of damping application

$$e^{at} \cos(\omega t) = \frac{(s-a)}{(s-a)^2 + \omega^2} \quad (3.9)$$

Real Part of damping application

$$e^{at} \sin(\omega t) = \frac{\omega}{(s-a)^2 + \omega^2} \quad (3.10)$$

Imaginary part of damping application

In this case of rectifying both of arcing currents and chopping currents $I_p = I_{arc} + I_{ch}$

$$I_p = \sqrt{\frac{1}{2\pi} \int_0^\pi I^2 d(\omega t)}$$

$$= \sqrt{\frac{I_m^2}{2\pi} \int_0^\pi \sin^2 \omega t d(\omega t)}$$

$= \frac{I_m}{2}$ rectifying values of arcing currents and chopping currents

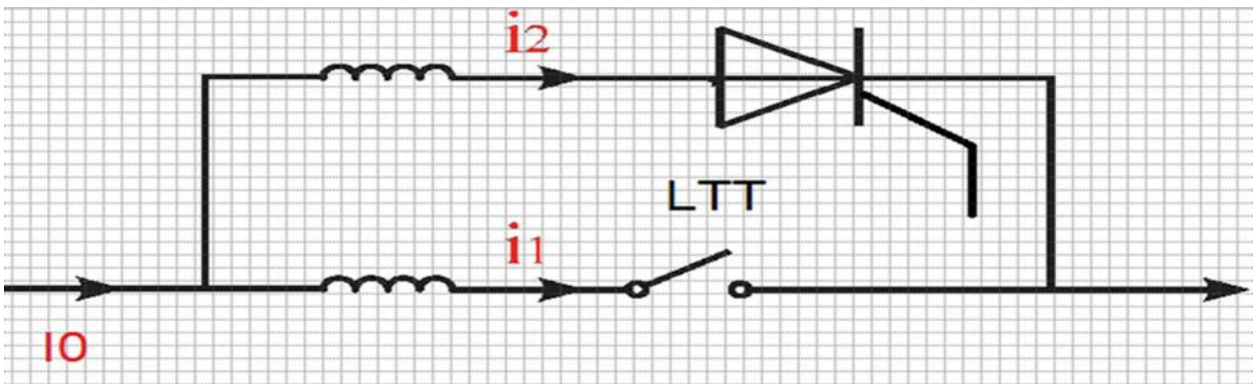


Fig.3.10 Synthesis mathematical model

$$I_0 = i_1 + i_2 \dots (3.11)$$

$$V_1 + L_1 \frac{di_1}{dt} = V_2 + L_2 \frac{di_2}{dt} \dots (3.12)$$

Commutation can be done by either a mechanical vacuum switching or a semiconductor switching here my designing uses LTT . The commutation begins at $t=0$ and ends at $t=T$, the total current remains I_0 as shown in fig. A4.5 and fig. A4.5 :

During the process, a voltage is established by the commutating switch represented by a constant voltage source as V_1 in figure to overcome V_2 which is the voltage drop of the main breaker .The currents in both branches satisfy the following equations

$$T = \frac{L_1 + L_2}{V_1 - V_2} * I_0 \dots (3.13)$$

$$E = \frac{(L1 + L2)}{2} * 10^2 \quad (3.14)$$

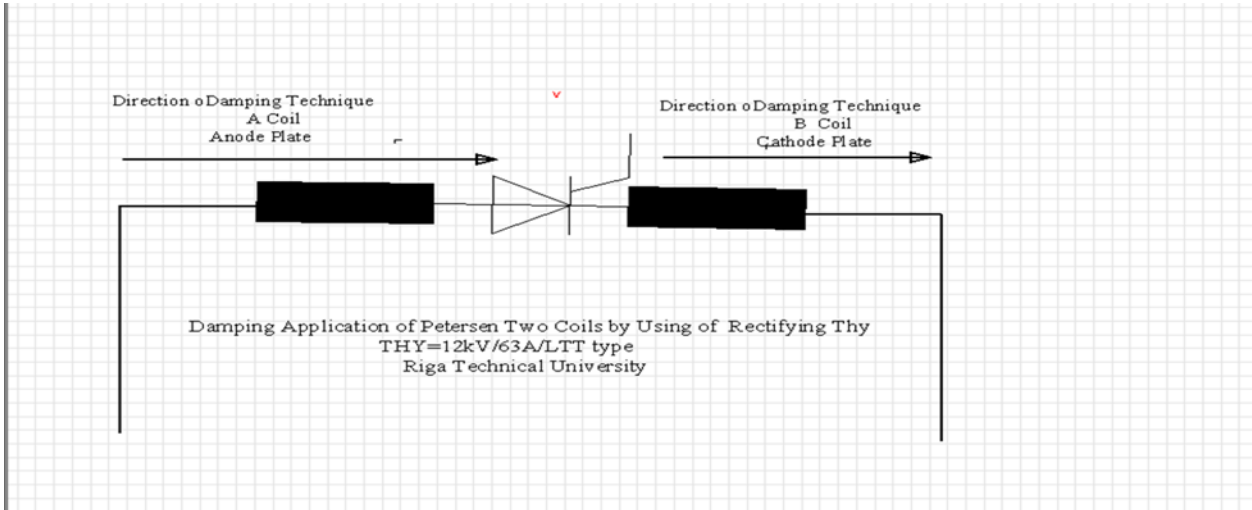


Fig. 3.11 Basic module circuit for damping application (novelty)

3.1.5 Synthesis of MATLAB/Simulink models

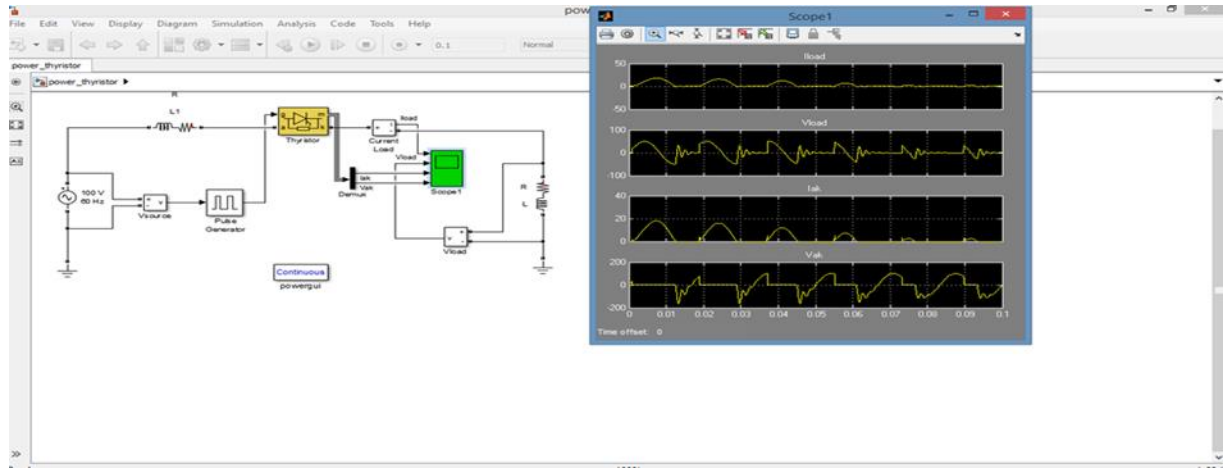


Fig. 3.12 Mathematical Matlab Model

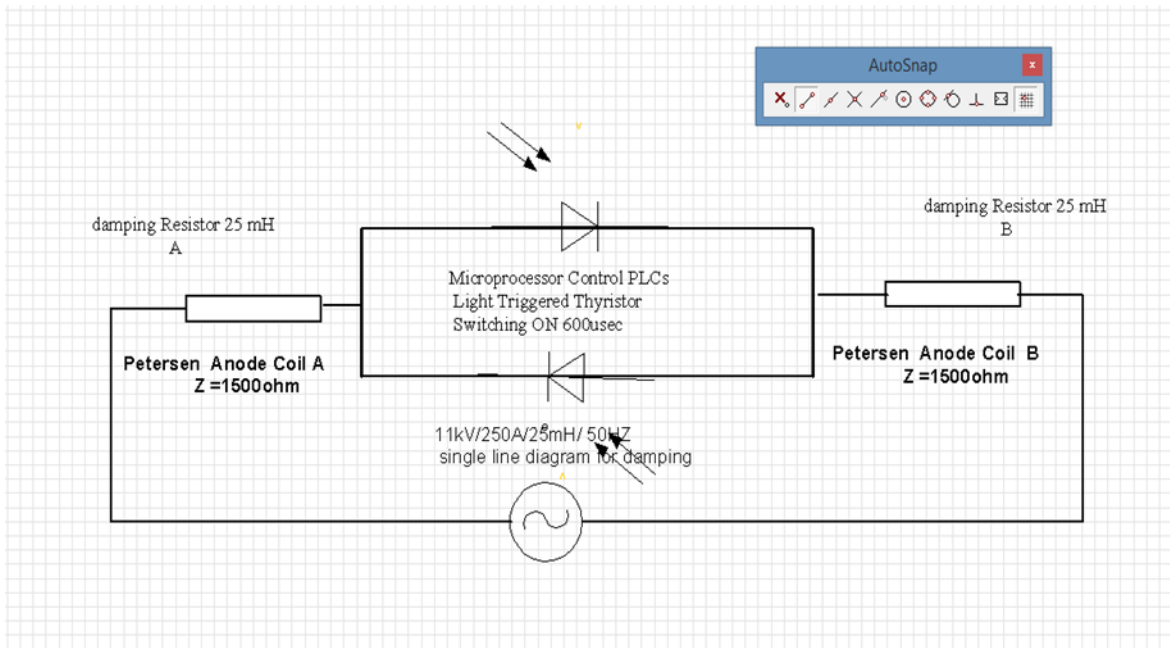


Fig. 3.13 Synthesis mathematical model

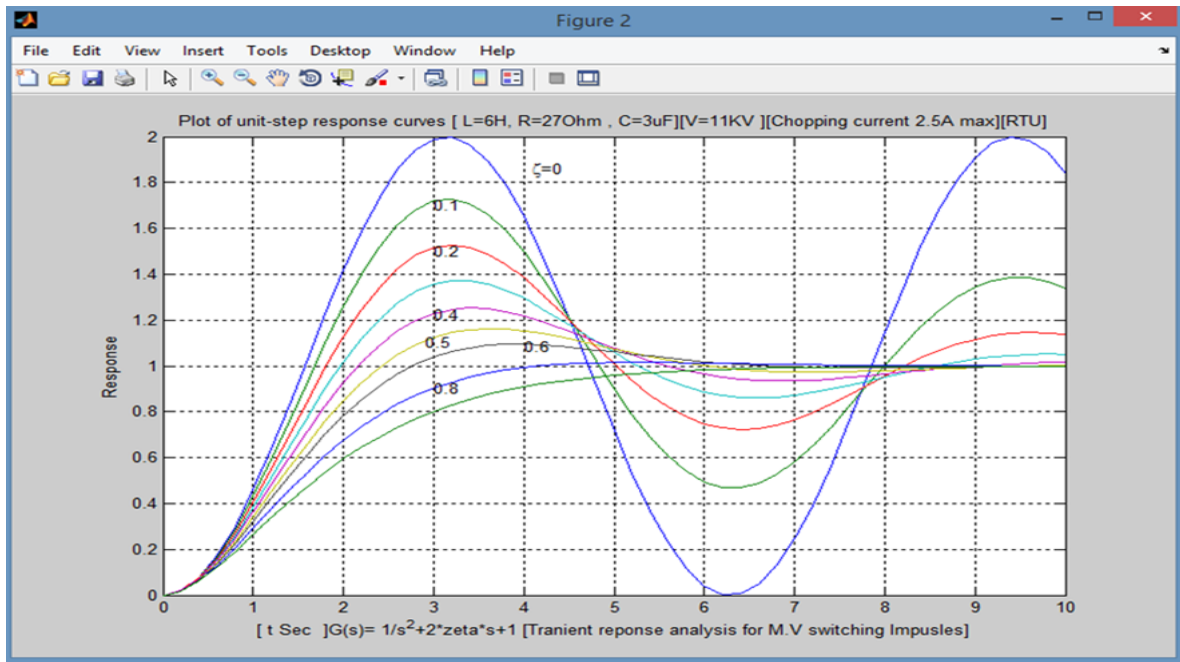


Fig.3.14 Generalized plot of Laplace transformation - damping circuit- MATLAB

Main Conclusions

The analysis of the all experiment scientific samples on interrupter technology, the following scientific information could be obtained:

1. There are the intervene process when the transition rates of du/dt and di/dt were happened which the chopping currents come with the transient over voltages together.
2. We need another sophisticated instrument for prove of the frequency changing in the original synchronous power system which changed to; 150Hz & 400Hz fir L1 & L3 .
3. The LTT thyristor application was offered very advanced in the rectifying technology of soft starting interrupter.
4. The facility of splitting of vacuum arcs (Arcing currents) by semiconductor power electronics was verified last 2015 for one experiment sample [67].
5. The basic principle of Petersen transformer theory is strongly applied for both of arcing currents and chopping currents with transient over voltages together because the application of Plcs offered very facilities for precisely operation process on $600\mu s$.

Damping Mathematical Application

1. The first set of experiment

The first attempted for creating of damping application on 15kV interrupter physically as real sample that by two scholars; Allan Greenwood and T.H .Lee That sample was funded from general electric. Some tips that we can concluded from this vital researching project [65]. In this circuit, the three components R-L-C are all in series with the voltage source. The governing differential equation can be found by substituting into Kirchhoff's voltage law (KVL) the constitutive equation for each of the three elements. From the KVL;

$$V_R + V_L + V_C = V(t) \dots \dots \dots (A1.1)$$

$$RI(t) + L \frac{dI}{dt} + \frac{1}{C} \int_{-\infty}^t I(t)dt = V(t) \dots (A1.2)$$

$$\frac{d^2}{dt^2} + \frac{R}{L} \frac{d}{dt} I(t) + \frac{1}{LC} = 0 \dots \dots \dots (A1.3)$$

$$\frac{d^2}{d^2} I(t) + 2\alpha \frac{d}{dt} I(t) + \omega_0^2 I(t) = 0 \dots \dots (A1. 4)$$

The RLC filters are described as a second-order circuit, meaning that any voltage or current in the circuit can be described by a second-order differential equation in circuit analysis. The oscillating of the medium voltage switching processes involve two elementary configurations will be considered. In the first, components R, L and C are arranged in parallel whereas in the second, they are joined in series. The networks involved in a very large number of practical transient problems in power switching systems can be safely reduced to one or other of these elementary circuits for the purpose of analysis. In many other instances, the circuit can be reduced to a number of these simple circuits, which are so loosely coupled, that on being treated independently, they yield results of acceptable engineering accuracy.

Damping is caused by the resistance in the circuit. It determines whether or not the circuit will resonate naturally (that is, without a driving source). Circuits which will resonate in this way are described as underdamped and those that will not are overdamped. Damping attenuation (symbol α) is measured in nepers per second. However, the unit less damping factor (symbol ζ , zeta) is often a more useful measure, which is related to α by;[65]

$$\zeta = \frac{\alpha}{\omega_0} \quad (\text{symbol } \zeta, \text{ zeta})$$

α and ω_0 are both in units of angular frequency. α is called the neper frequency, or attenuation, and is a measure of how fast the transient response of the circuit will die away after the stimulus has been removed. Neper occurs in the name because the units can also be considered to be nepers per second, neper being a unit of attenuation. ω_0 is the angular resonance frequency. The analysis shows that the effect of damping in an oscillatory circuit can be described in terms of a single parameter, designated η , or its reciprocal λ , which is the ratio of the resistance to the surge impedance of the circuit, i.e.,

$$n = \frac{R}{Z_0} = \frac{R}{\sqrt{\frac{L}{C}}} = \frac{1}{\lambda} \dots \dots \dots (A1.5)$$

This fact permits the construction of generalized damping curves for different values of η , from which the solutions to any practical problems can be extracted with about the same effort as one would expend in using a table of logarithms.

Such curves are presented in this report. Thus, the analysis is more than a mathematical exercise in circuit aesthetics; it is a useful instrument for studying various transient problems in electric medium voltage switching system. For analysis of the basic circuits, the first interesting fact that the characteristic parts of the differential equations describing the behavior of the two circuits; series and parallel;

$$\frac{d^2(i)}{dt^2} = \frac{1}{RC} \frac{di}{dt} + \frac{i}{LC} = 0 \dots \dots \dots (A1.6)$$

For the series circuit of RLC, the equation;

$$\frac{d^2 V}{dt^2} + \frac{R}{L} \frac{dV}{dt} + \frac{V}{LC} = 0 \dots \dots \dots (A1.7)$$

Where the V is the voltage across any component or the current through the circuit. We note that the only difference between above equations (1.6) and (1.7) is the coefficients of the second terms. These coefficients are themselves interesting. To satisfy equations (1.6) and (1.7) they must have the dimension T^{-1} ; accordingly we designate them as following :

$$\text{Parallel circuit time constant} = RC = T_p \dots \dots \dots (A1.8a)$$

$$\text{Series circuit time constant} = \frac{L}{R} = T_s \dots \dots \dots (A1.8b)$$

Observe that the product of these time constants is square of the angular period of the undamped circuit ,i.e.,

$$T_p T_s = T^2 \dots \dots \dots (A1.9)$$

$$\frac{T_p}{T_s} = \frac{R^2}{Z_0^2} \dots \dots \dots (A1.10)$$

The relationships lead to a very beautiful duality in the analysis of the series and parallel circuits. To determine any specific current or voltage in equation (1.16) or equation (1.17), the equation must be solved and the initial conditions for specific current or voltage must be entered into the solution when evaluating the constants integration. Consider the solution for the current in the inductor in the parallel circuit. Let this current be I_L . The differential equation describing this current is ;

$$\frac{d^2 I_L}{dt^2} + \frac{1}{T_p} \frac{dI_L}{dt} + \frac{I_L}{T^2} = 0 \dots \dots \dots (A1.11)$$

Which is to be solved for the initial condition of a voltage, $V(0)$, on the capacitor .

In the symbols of the Laplace transform the solution to equation (1.11) may be written:

$$iL_{(s)} = \frac{V(0)}{L} * \frac{1}{\left[S^2 + \frac{S}{T_p} + \frac{1}{T^2} \right]} \dots \dots \dots (A1.12)$$

Equation (1.12) contains the basic transform of the parallel R, L, C circuit. It, or variations of it, will always appear in operational solutions when such as a circuit is stimulated. The inverse transform depends upon the degree of damping, and therefore, upon the relative value of certain parameters, as follows:

$$\begin{aligned} & \text{If } T/T_p < 2 \\ L^{-1} * \frac{1}{\left[S^2 + \frac{S}{T_p} + \frac{1}{T^2} \right]} &= \frac{2T_p e^{-\frac{t}{2T_p}} \sin(4\eta^2 - 1)^{1/2} \frac{t}{2T_p}}{(4\eta^2 - 1)^{1/2}} \dots \dots \dots (A1.13) \end{aligned}$$

$$\text{If } \frac{T}{T_p} > 2$$

$$L^{-1} * \frac{1}{\left[S^2 + \frac{S}{T_p} + \frac{1}{T^2}\right]} = \frac{2T}{(1 - 4\eta^2)^{1/2}} e^{-\frac{t}{2T_p}} \sinh\left(1 - 4\eta^2\right)^{1/2} \frac{t}{2T_p} \dots \dots \dots (A1.14)$$

Or if $\frac{T}{T_p} = 2$

$$L^{-1} * \frac{1}{\left[S^2 + \frac{S}{T_p} + \frac{1}{T^2}\right]} = te^{-\frac{T}{T_p^2}} \dots \dots \dots (A1.15)$$

Equation (1.15) represents the oscillatory mode, which according to the condition cited occurs when

$\eta > 0.5$, or $T/T_p < 2$. When $\eta < 0.5$, which is the next condition, the current is overdamped and does not oscillate. The special case of critical damping, equation (1.21), occurs when $\eta = 0.5$.

Consider the solution for the oscillatory condition. From equations (1.12) and (1.13) this can be stated:

$$I_L = \frac{V(0)}{Z(0)} * \frac{2\eta}{(4\eta^2 - 1)^{1/2}} * e^{-\frac{t}{T_p}} * \sin(4\eta^2 - 1)^{1/2} t / 2T_p \dots \dots (A1.16)$$

As R is progressively increased, damping diminishes, until, when R is infinite, the current is completely underdamped and we have the simple parallel LC circuit for which $\eta = \infty$. This limit can be obtained from equation (1.16)[70][71]:

$$I_{L \text{ undamped}} = \frac{V(0)}{Z(0)} \sin \frac{t}{T} = \frac{V(0)}{Z(0)} \sin \omega_0 t \dots \dots (A1.17)$$

Where $\omega_0 = \frac{1}{T}$ is the angular natural frequency of the circuit. The peak amplitude of this current $V(0)/Z(0)$, will be used as a standard for comparison and will be designated I_L . We specify a per-unit current for any damped condition by:

$$\text{per unit } I_L = \frac{I_L}{I_L} \dots \dots \dots (A1.18)$$

So, that for the inductor current we may write from equations (A1.15) and (A1.17)

$$\text{per unit } I_L = \frac{2\eta}{(2\eta^2-1)^{1/2}} * e^{\frac{-t}{2Tp}} * \sin(4\eta^2 - 1)^{1/2}t/2 \quad \dots\dots(A1.18)$$

We now let $t' = t/T = \omega_0 t$ (A1.19)

Then $t/2Tp = t'/2\eta$ and equation (1.19) simplifies to per unit

$$\text{per unit } I_L = \frac{2\eta}{(4\eta^2 - 1)^{1/2}} * e^{\frac{-t'}{2\eta}} * \sin(4\eta^2 - 1)^{1/2}t'/2\eta \quad \dots\dots(A1.20)$$

Equation (1.17) expresses in dimensionless form the current in the inductor of any parallel RLC circuit, with any degree of damping. We note that the only parameter involved is η , so that a family of generalized curves can be drawn from equation (1.19) for different values of η , with the dimensionless quantity, t' , as abscissa. This has been done in Fig. . Where $\eta = 0.5$, the sine function changes from a circular to a hyperbolic function. We might have developed the curves for this condition independently, following the same argument, but starting from equation (1.10). As such we shall shortly see that the curves of Fig. are by no means restricted to calculating the inductor current in a parallel RLC circuit under conditions of a subsidence transient, but have a far wider application. However, to gain familiarity with these curves, consider a specific example where the inductor current is required in a circuit in which the components have the following values : $R=105$ ohms, $L=5$ henrys, $C=0.002$ uf(microfarad). (These values are typical of an unloaded transformer, where R represents the equivalent loss resistance [65].

$$\text{Suppose } V(0) = 13.8\sqrt{2} \text{ KV}$$

$$Z_0 = \sqrt{\frac{L}{C}} = \left[\frac{5}{2 \times 10^{-9}} \right] = 5 \times 10^4 \text{ ohm}$$

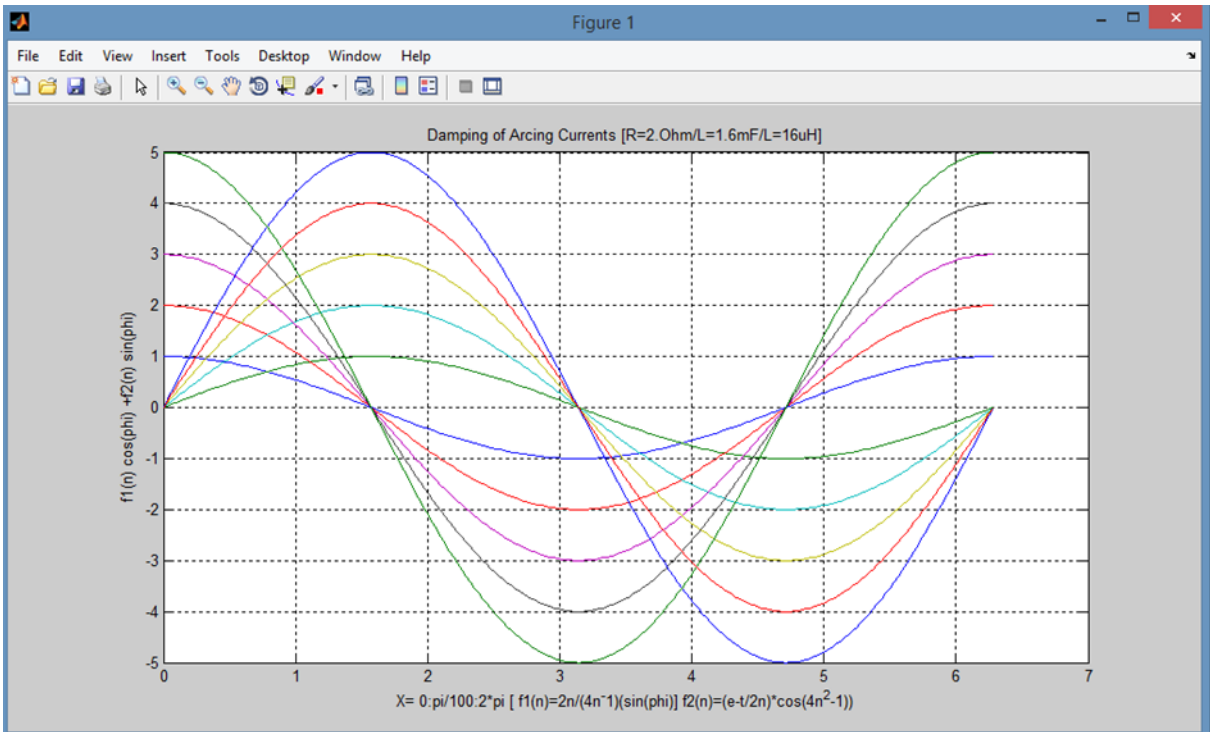


Fig. A1.1 Mathematical model- Generalized plot of inverse transform

2. Analysis the experiment

In general, the damping equations were represented two type of formulas;

$$\sin(\omega t + \theta) \text{ and } \cos(\omega t + \theta)$$

The above curves will be calculating of Zeta by MATLAB

Splitting of Arcing Currents – Power Electronics -Experiment Test – 1

The second attempted was done by group of scholars from Bei hang University, China last 2015, by using of power electronics for splitting of arcing currents, basically this application depends on theory of “ *R.L. Boxman and Wolf . C. Kurrat* ”[69][70] , but this type of application does not damping of arcing currents, chopping currents as mentioned in my proposed theory of damping application by inserting rectifying LTT thyristor technique for soft interrupter [67].

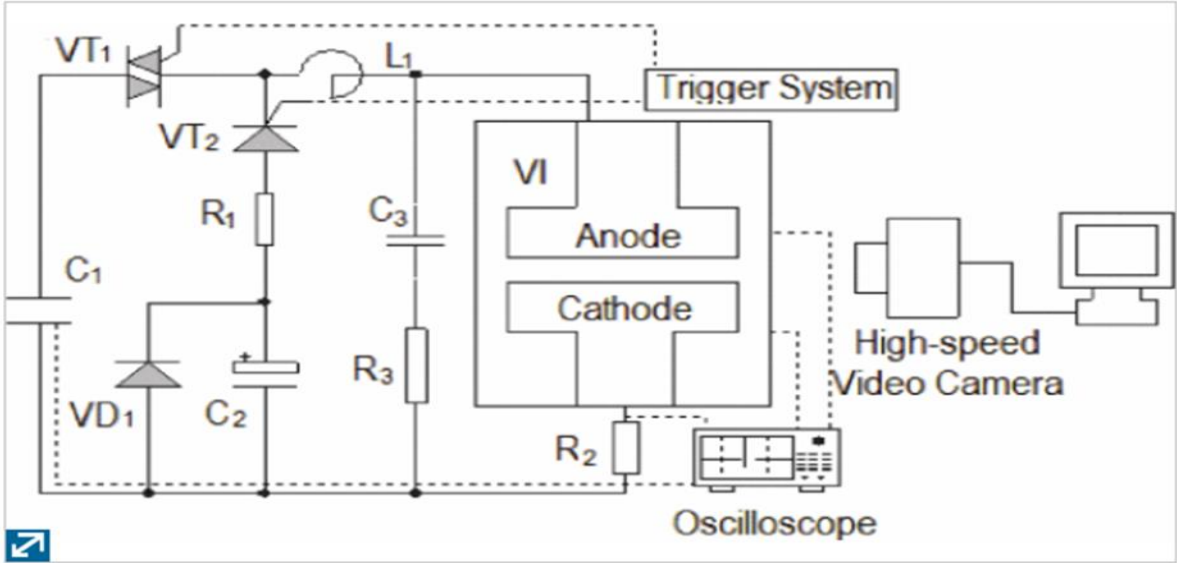


Fig. 1 Schematic diagram of experimental system

Fig.A2.1 Power electronic splitting of arcing currents- China experiment

The arc behavior has a significant impact on the interrupting ability [71]. Boxman and Wolf have dealt with the investigation of the behavior patterns of vacuum arcs with TMF contacts. Boxman [69] investigated split arc at power frequency and proposed that the splitting arc is apparently caused by the electrode geometry, since it occurs both with and without the imposition of the external radial magnetic field. Wolf [70], [71]presented the cup-shaped TMF contacts had reproducible and continuous movements of the arc along the contact rim with low fluctuations of the arc voltage and instantaneous arc velocities up to 100 m/s. Vacuum arc voltage and frequency characteristics were studied with the butt-type contacts at frequency of 150Hz and the impact of noise was also analyzed. In our previous study about the arc appearance and the dynamic volt-ampere characteristics at intermediate-frequency under 66mm TMF contacts, the split arc was not observed [69]–[74] “Harris Model” .

1. Experimental Setup

Experimental system is shown in Fig.A1 - A single-frequency oscillation circuit is used to study the intermediate-frequency vacuum arc. Firstly, charging voltage of capacitor is higher than capacitor. After charging, the vacuum interrupter VI is closed. In this case, we trigger thyristor VT_2 and open the vacuum interrupter to ignite direct-current arc. Then we trigger thyristor VT_1 to inject intermediate-frequency current. Finally, the VT_2 switched off due to negative voltage. VT_1 triggers the signal until the end of experiment. By adjusting the capacitor and inductor, frequency of current can be achieved. Peak value of the first sinusoidal half-cycle current can change from 2kA to 30kA. Capacitor and resistor are used to adjust the rate of rise of recovery voltages (RRRV) parameters. A MotionProX3 high-speed video camera with a speed of 16,400frames/s and an exposure time of records the arc appearance. Experiments were carried out under condition of removed shield cup-type TMF vacuum interrupters with a contact diameter of 40mm and an opening distance of 2mm, as shown in Fig. 2B The material of the contacts is *CuCr50*.



Fig. A2.2 Cup -type vacuum interrupter with TMF contacts

2. Arc currents Splitting

The typical vacuum arc appearance, arc voltage and arc current waveforms were shown in Fig.A2 and (A3) respectively. The current and frequency was 6kA-rms and 400Hz, respectively. As shown in Fig.A3, the arc concentrates at the site of its initiation at t_1 which is defined as main arc column. With the increase of the current, the arc column diameter increases, and the main arc column start to move in Amp direction- direction after t_5 . At t_8 , two separate arc columns which were marked by arrow are formed in the opposite (retrograde) direction, contrary to the Ampere rule. However, the separate arc columns scattered at the perimeter of the contacts, and the other parts remained diffuse. The separate arc columns start to move after its formation. The motion

direction of the splitting arc is agreed to the main arc column. Apparently, the arc velocity and direction is subject to the impact of the separate arc column. The separate arc columns disappeared before the main arc column with current decrease.

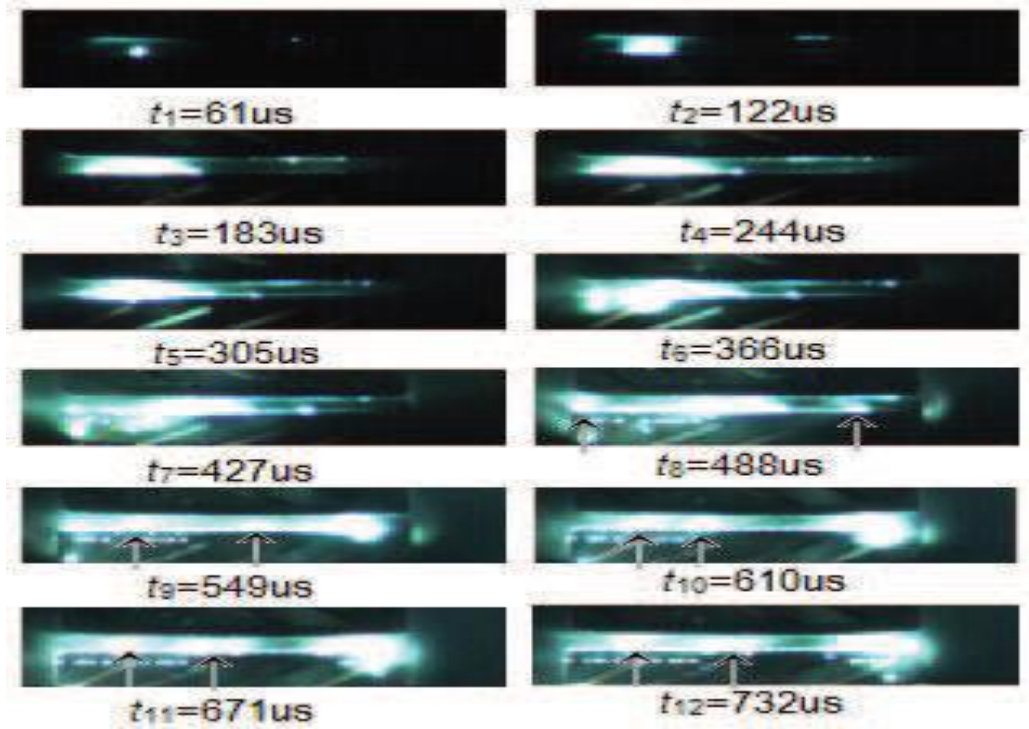


Fig. A2.3 Time of arcing currents

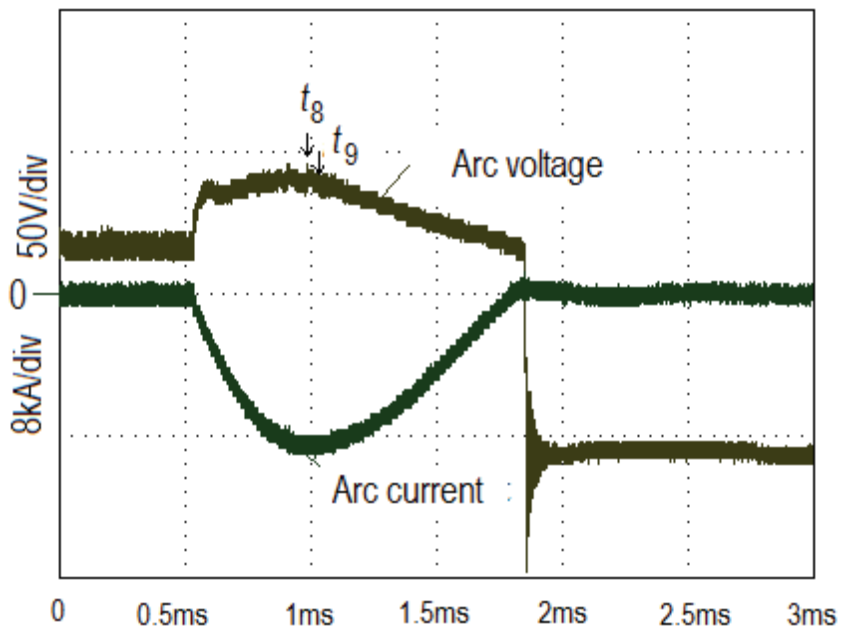


Fig. A2.4 Arc currents

As shown in Fig. 3 (C), arc voltage is reduced at t_8 and t_9 when the split arc phenomenon occurs, and the current is close to the peak value. Instantaneous resistance of arc column equals to the instantaneous voltage divided by the instantaneous current. The arc voltage is mainly composed of

cathode drop, arc column drop, and anode drop. Anode drop is ignored when the arc current is small. The cathode drop about 16V was subtracted by instantaneous voltage. The arc column instantaneous resistance corresponds to the arc voltage. According to Fig.3 (C), the instantaneous resistances of arc columns at t_7 to t_{12} are 3.6 m Ω , 3.7m Ω , 3.6 m Ω , 2.9 m Ω , 3.2m Ω , and 3.4 m Ω , respectively. It can infer that the separate arc columns are the reason for the reduction of the instantaneous resistance.

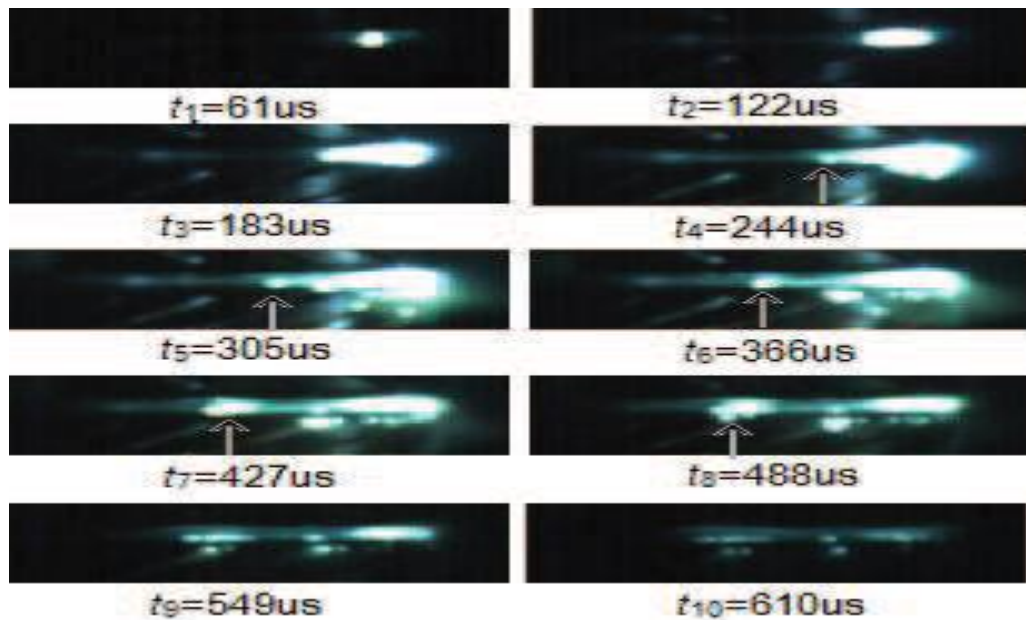


Fig. A2.5 Arc currents appearance

At higher currents and frequencies, the splitting arc also has different characteristic as shown in Fig.A5. A separate arc currents column is formed at t_4 in retrograde direction, and the separate arc column begins to move after its formation. An interesting phenomenon can be observed that the separated arc column diameter increases with the current decrease. The movement direction of the separate arc column is opposite to the main arc column. The separate arc column moves away from the main arc column. The average velocity of separate arc column is about 56m/s from t_4 to t_8 .

Splitting of Arcing Currents – Power Electronics -Experiment Test –2

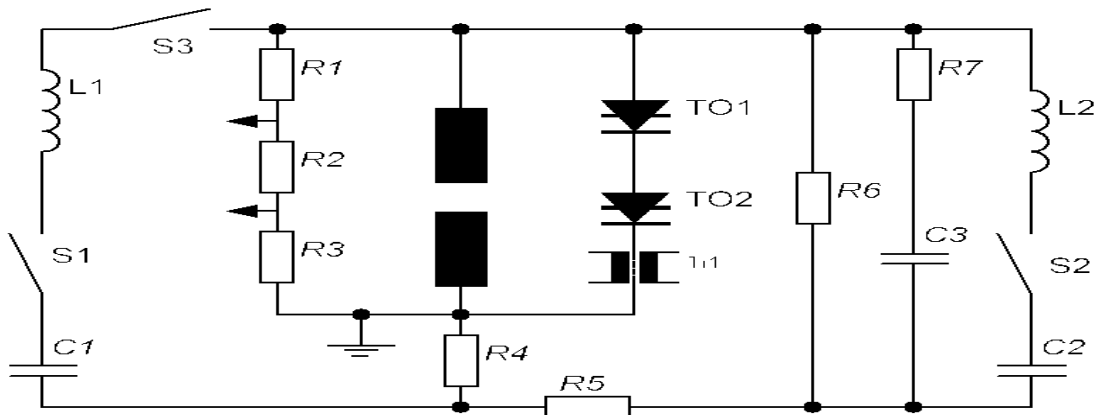


Fig. A2.6 Experiment two

One of the problems of a vacuum circuit breaker (VCB) is that its arcing currents gap can be broken by transient over voltages when the current passes through zero. The breakdown is due to dense plasma and electrode material vapors produced by the arc until the end of the current half-period. We think that the problem can be resolved by parallel connection of a controlled semiconductor switch, e.g., a thyristor, to the vacuum gap.

The use of only thyristors in high-current switching equipment is problematic due to a relatively large (up to several volts) voltage drop across them. However, parallel connection of a VCB and a thyristor greatly reduces the requirements on both devices. In this case, the current flows through the thyristor for a short time, i.e., within a single half-period, and hence, there is no long-term high-current loads. At the same time, the ignition of an arc with a rather high potential fall (20–100 V) on the separation of the VCB contacts creates conditions for partial or full current switching to the semiconductor element. This, as expected, can greatly decrease the current load on the VCB, considerably lengthen the VCB lifetime, and almost eliminate the problem of its breakdowns by transient over voltages. The foregoing approach can reduce the requirements on VCBs.

Research data on arc shunting can be found in some papers. For example, the protection of contact gaps in switching inductive loads of low-voltage low-current circuits was considered elsewhere [114]. Experiments with the so-called H-shaped circuit were performed but the maximum current in the experiments was limited to 2.5 kA [115]. In some studies, the shunting element was a low-ohmic resistor [116], [117], but these studies relate to the interruption of direct current. In the ac networks, a single-sided conductive element must be used, for example, the thyristors.

This paper develops the idea of using a semiconductor switch to shunt VCB interelectrode gaps. In the experiments reported, the maximum current through the VCB and thyristor assembly reached 12 kA.

Experimental Setup and Research Techniques

The schematic of the experimental setup is shown in Fig. A2.6. The setup is based on the Weil–Dobke synthetic circuit [118], which simulates the operation of a VCB in real electric networks. The low-voltage circuit is formed by elements $L1=130\ \mu\text{H}$ and $C1=75\ \mu\text{F}$ with thyristor switch S_1 and produces 10-ms arcs with a peak current of up to 50 kA.

The high-voltage circuit is formed by elements $L2=3.7\ \mu\text{H}$ and $C2=48\ \mu\text{F}$ with switch S_2 based on an air gap and produces a harmonic current pulse with a full width at the base of 1 ms and the amplitude of ~ 5 kA. Once the current passes through zero, this circuit generates a TRV pulse of up to 41 kV. Switch S_3 serves for the separation of the high-voltage and low-voltage circuits.

Experiments were performed in a baked vacuum chamber. The residual pressure in the chamber was kept at less than 10^{-5} Pa by an ion pump. The contact gap was formed by two identical copper–chromium electrodes of 2 cm diameter. The electrodes were separated at the rate of ~ 1 m/s. The thyristor assembly represented two series-connected photo thyristors TO_1 and TO_2 both triggered at a time by a pulse duration of $15\ \mu\text{s}$. The delay of the trigger pulse with respect to the beginning of the current pulse was varied from 0 to 10.3 ms. The voltage across the VCB contacts and the voltage drop across the thyristor assembly were measured with an active divider ($R1/R2/R3$). The electrical signal from the divider was fed to an oscilloscope of model AKTAKOM ACK-3107 with a bandwidth up to 100 MHz per channel. The current was measured with a low-resistance shunt ($R4=0.1\ \text{m}\Omega$). The current in the thyristor circuit was measured using a preliminary calibrated Rogowski coil (Tr_1). The arc current was determined by the difference in current between the shunt and Rogowski coil.

Experiments were also performed with a larger number of semiconductor elements for which a diode assembly, instead of the thyristor assembly, was connected in parallel to the VCB (Fig. 1). The transient characteristics of diodes and thyristors in the ON-state are close, and the instant at which diodes become conducting can be controlled by varying the instant of contact separation in a VCB. In the experiments, we used the sections of five and ten series-connected diodes, such that the number of diodes in the assembly could be 5, 10, 15, and 20. The maximum current through the VCB and thyristor assembly reached 12 kA. The TRV was 10 kV. These parameters were specified by technical characteristics of the thyristors (voltage rating). For the diode assembly, the maximum current was 8 kA. TRV was not applied. The experimental conditions are shown in Table A.I

Type	Number	I_{max} , kA	TRV, kV
Thyristors	2	12	10
Diodes	5, 10, 15, 20	8	0

Results and Discussion

In this section, we use the following notations of the timestamp.

1. t_{cs} is the contact separation.
2. t_{tp} is the thyristor trigger pulse.
3. t_{fs} is the full current switching.
4. t_{cz} is the current zero.
5. t_v is the a sharp growth of voltage.
6. t_{br} is the breakdown.

A. Thyristor Assembly

The current switching from the VCB to the thyristor assembly was studied by triggering the thyristors at different points in time. Fig. A2.7 general -shows the oscillograms illustrating the current switching for the thyristor trigger pulse (time t_{tp}) applied before the instant of contact separation (time t_{cs}). When the contacts are closed, the voltage drop across them is ≤ 1 V, which is insufficient for the thyristors to be ON. Therefore, no current arises in the thyristor circuit until the point of contact separation. Once the contacts are separated, an arc discharge is ignited in the VCB, the voltage drop in the gap reaches 15–20 V, and the current in the thyristor circuit starts increasing. By the point in time t_{fs} , the thyristors are fully ON and the total current is switched to the thyristors. The energy release in the arc begins to decrease in time t_{tp} , and in time t_{fs} , the arc is completely quenched.

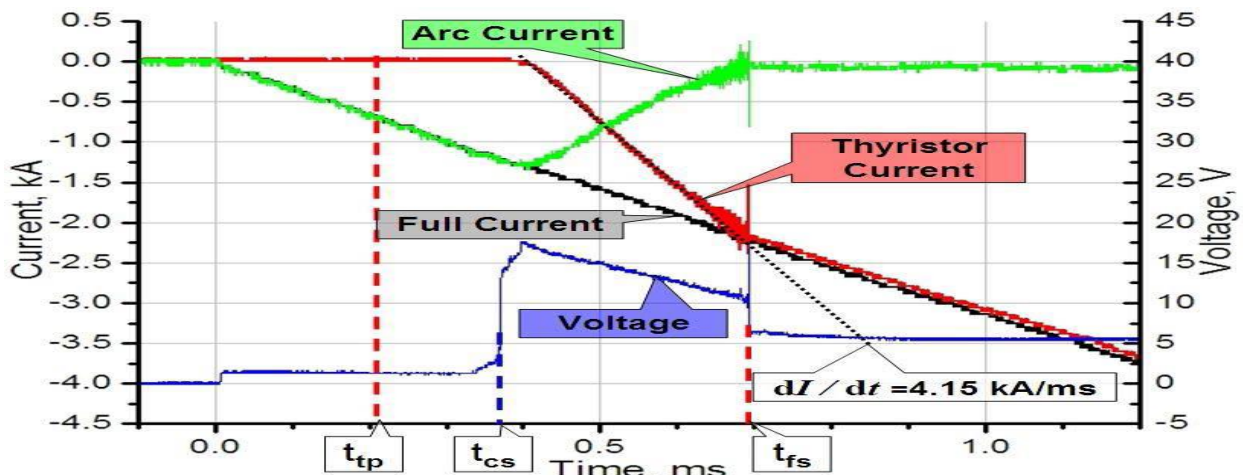


Fig. A2.7 General -arcing currents and function of thyristor

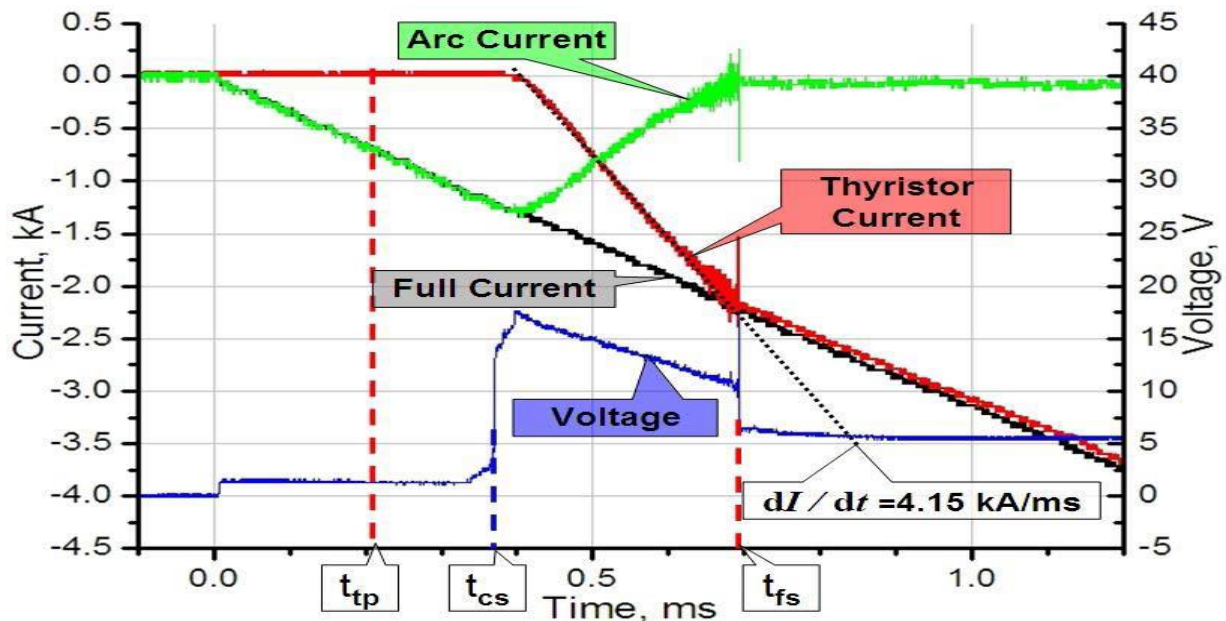


Fig. A2.8 Detailed oscillograms illustrating the current switching from the VCB to the thyristors. Points in time: t_{cs} —instant of VCB contact separation, t_{tp} —thyristor trigger pulse, and t_{fs} —full current switching.

If the thyristor trigger pulse is applied after the instant of contact separation, fig. 2.8 the voltage drop is already sufficient for the thyristors to operate and the current immediately starts flowing through them. The analysis of the experimental results reveals a rather interesting fact. It is known that the minimum voltage required for a vacuum arc to operate at copper electrodes is about 13–16 V [119]–[120][121]. In our case, the minimum voltage is about 15 V and corresponds to the instant of contact separation. However, during the interval t_{tp} – t_{fs} of current switching from the VCB to the thyristors, the voltage decreases to 8–10 V, but the arc continues to operate. In view of the decrease in the arc current, the number of cathode spots is not increased. In this case, it can be supposed that the voltage of 8–10 V is sufficient for the operation of cathode spots. As a result, the arc burns at the voltage close to the ionization potential. Furthermore, the switching time of current from the VCB to the thyristor assembly depending on the switching current was investigated. In this case, the contact separation time t_{cs} was kept constant at 0.5 ms. The time of the thyristor trigger pulse t_{tp} was varied. Thus, when the difference value (t_{tp} – t_{cs}) is increased, the switching current also increases. The time during which the current passes from the VCB to the thyristors (the switching time) is defined as the difference between the times (t_{fs} – t_{tp}). The value of the switching time is determined at the time of t_{tp} . The dependence of the switching time is shown in Fig. A2.9.

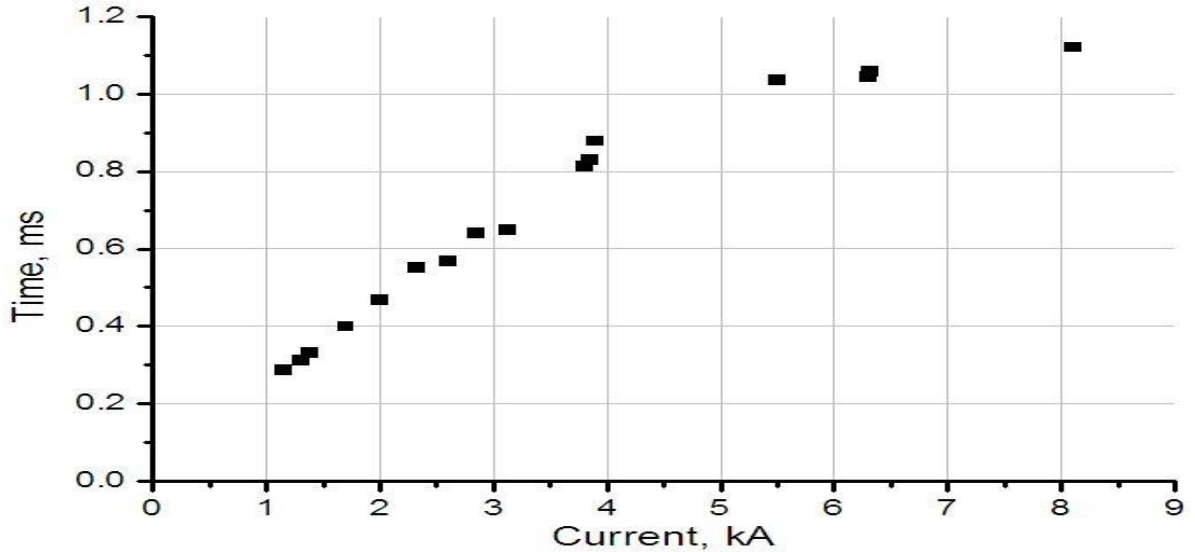


Fig. A2.9 Switching time versus the current from the VCB to the thyristor assembly

On the basis of the received data, it can be concluded that the switching time depends on the value of the switching current and does not depend on the total current flowing through the VCB-thyristor assembly system. The switching time for the case in Fig. A2.8 is about 300 ms ($t_{fs}-t_{cs}$) at the switching current of 1.3 kA (current at the time t_{cs}). Knowing the switching time and switching current, it can determine the rate of current switching from the VCB to the thyristor assembly. For the current from 1 to 8 kA, the rate of current switching ranges from 4 to 7.2 kA/ms.

B. Breaking Capacity of the VCB-Thyristor System

First, we determined the conditions under which the VCB in the absence of thyristors was broken down with a high probability as the current passed through zero with subsequent increase in TRV. For this purpose, we varied the current amplitude and the instant of separation of the VCB contacts. The amplitude of the TRV in all experiments was invariant (10 kV) and so was its pulse shape. It was found that the delay of contact separation t_{cs} did not result in a stable breakdown in response to the applied TRV. At the current amplitude of 8.5 kA, no breakdown was observed up to the point when t_{cs} approached the time of zero current t_{cz} : $(t_{cz}-t_{cs}) \sim 150 \mu s$, i.e., when the interelectrode gap by the time t_{cz} was $\sim 150 \mu m$. At the discharge current amplitude of 10 and 12 kA, the situation was the same. However, the probability of a breakdown at small delays $t_{cs} < 2$ ms was high. At $t_{cs} = 0.5$ ms and 10 kA, the probability of a breakdown was 60%–70%, and at 12 kA, the VCB was broken down repeatedly. These were the so-called late breakdowns occurring at the point in time t_{br} spaced from the point of zero current t_{cz} by several hundred microseconds, which is many factors greater than the rise time of the TRV. Therefore, in

further tests, i.e., with the thyristor assembly connected in parallel to the VCB, the contacts were separated immediately after the beginning of the current pulse ($t_{cs} \sim 0.5$ ms).

In studying the influence of the thyristors connected in parallel to the VCB on its operation, we were to find a critical time delay of thyristor triggering (t_{tp}). If the thyristors become conducting earlier than the critical point (for example, during the initial current phase), the current is switched to the thyristors long before it passes through zero and the VCB comes under the action of high TRV. Conversely, if the thyristors become conducting later than the critical point, the VCB is broken down.

At a current amplitude of 10 kA, breakdowns began to arise when the thyristors were triggered at t_{tp} closer than $500 \mu s$ to the point of zero current ($t_{cz} - t_{tp}) < 500 \mu s$. These were late breakdowns and their character was probabilistic. Fig.2.10 shows the oscillograms for triggering of the thyristors $300 \mu s$ ahead of the TRV pulse when the VCB was broken down in 50% of cases, and the typical breakdown delay time with respect to the rise of the TRV ($t_{br} - t_v$) was $100\text{--}300 \mu s$.

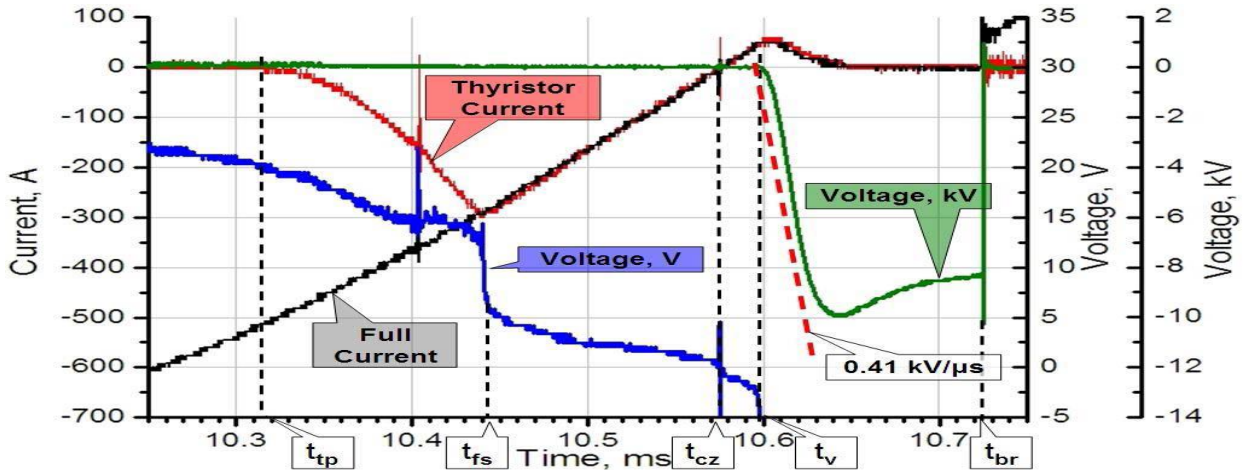


Fig.A 2.10 Oscillograms for parallel connection of the thyristor assembly and VCB with late $t_{cs} = 0.5$ ms

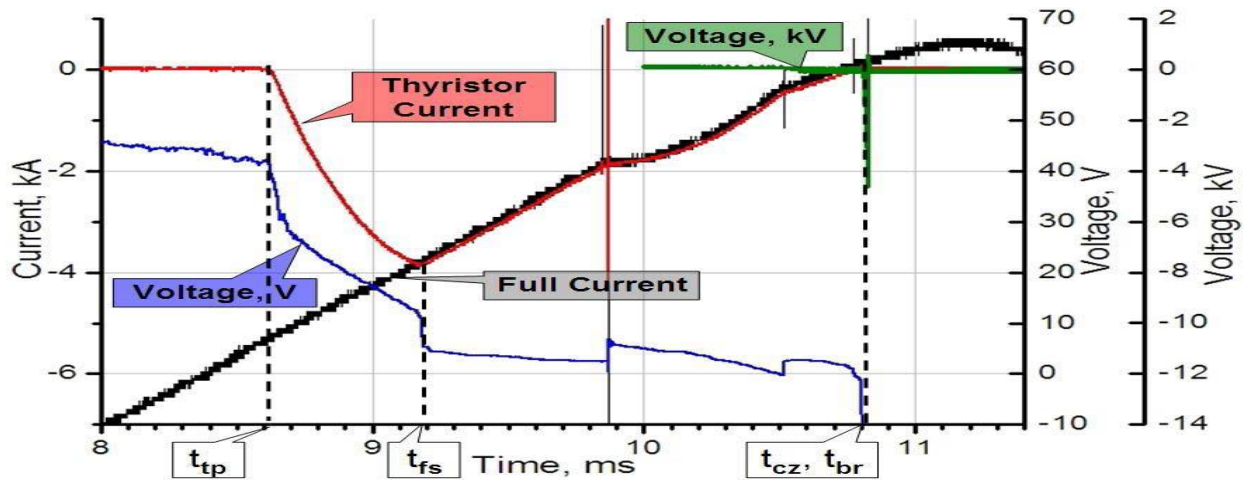


Fig. A2.11 Oscillograms for parallel connection of the thyristor assembly and VCB early gap breakdown. $t_{cs} = 0.5$ ms for both the cases.

At a current amplitude of 10 kA, breakdowns began to arise when the thyristors were triggered at t_{tp} closer than $500 \mu s$ to the point of zero current $(t_{cz} - t_{tp}) < 500 \mu s$. These were late breakdowns and their character was probabilistic. Fig.A2.12 shows the oscillograms for triggering of the thyristors $300 \mu s$ ahead of the TRV pulse when the VCB was broken down in 50% of cases, and the typical breakdown delay time with respect to the rise of the TRV ($t_{br} - t_v$) was $100 - 300 \mu s$.

At an arc current amplitude of 12 kA, the critical time was $t_{tp} = 8 - 8.5$ ms [$(t_{cz} - t_{tp}) \sim 2.2 - 2.7$ ms]. An example of oscillograms is shown in Fig.2.8. At $t_{tp} = 7.5$ ms, no breakdown took place. The first breakdown occurred at $t_{tp} = 8$ ms, and even at $t_{tp} = 8.65$ ms (2.2 ms before the point of zero current), the VCB was broken down repeatedly. Both late and early breakdowns during the voltage rise time were observed [Fig.2.7 and 2.9]. As the time delay of thyristor triggering was further increased (was brought closer to the point of zero current), repeated breakdowns were also observed and their character was the same.

a. Analysis Arc splitting application

1. The experiment one above reflects the hypothesis for using power electronics for splitting of arcing currents (150Hz /400Hz and 800Hz). This vital experiment encourages for using of power electronics for damping of both arcing currents and chopping currents simultaneously.
2. The experiment two indicates the treatment of high scales of currents and we can used this procedures for (50Hz/150Hz/400Hz) when chopping happens inside vacuum tube.

**Pulse Power Equipment by LTT Thyristor
Development and Research of Heavy Pulse Current LTT Switches**

1. Introduction

The advancement of pulse power equipment is related, first of all, to the progress in developing high pulse current switches. Until quite recently, the high-current switching problem was solved by spark gaps characterized by a high overloading ability and relatively simple triggering circuits. However, the operation life of these switches is limited as a result of electrode erosion, in addition to self-triggering, which is typical of them. Semiconductor devices, when used for high-current switching, have a number of advantages over spark gaps, namely, high reliability, no self-triggering, arc-free switching, and environmental safety. The disadvantages of semiconductor switches are low overload ability (in current and voltage), limited slope of current rise, and probable damage by the action of overvoltage at reverse recovery. Among the known types of semiconductor devices, the reverse switching (RSD) are characterized by fast switching and permissible currents amounting to tens and hundreds of kiloamperes [21] [22][61].

However, rather complicated and powerful high-voltage circuits are required to trigger RSDs. Various types of powerful pulse thyristors are also used as high-voltage switches, among which the light triggered thyristors (LTTs) have the most convenient method of triggering [61].

LTTs, like other semiconductor switches for high pulse currents, are made in disk-type packages, which are stacked for high-voltage applications requiring the cascade connection of semiconductor devices (Figs. 1 and 6).

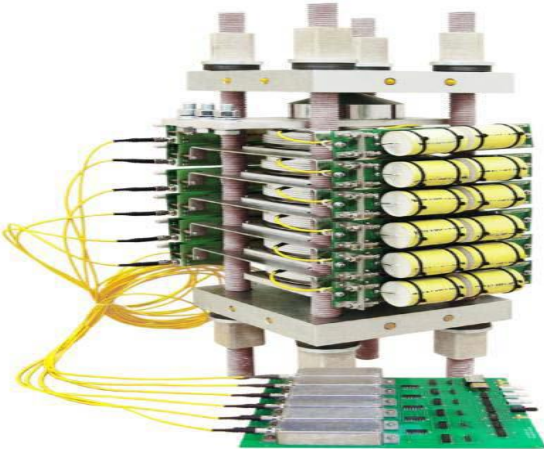


Fig. A.3.1 Semiconductor switch assembled from six LTTs of TL1193-2500-42 type and the driver board with six light pulse emitters (in the foreground).

Low-voltage drivers of LTTs are located at a distance well away from the high-voltage circuits of the facility. The drivers include semiconductor injection lasers, which generate light pulses with a power of 150–300 mW transmitted to LTT through fiber optic cables (Fig. A6).

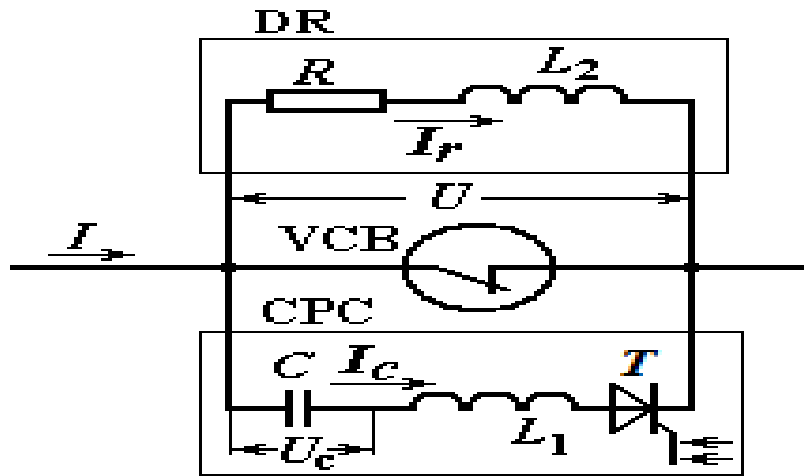


Fig. A.3.2 Discharge circuits of CPC. T — the LTT unit (Fig.A6)

To ensure the reliable operation of switches at high currents and high voltages, it is necessary to provide switching processes taking into account the features of semiconductor devices. In this paper, the LTT operation regimes in pulse facilities are investigated, and the conditions for reliable operation of LTT switches are defined. This paper also presents the experience in applying the LTTs in the discharge circuit of countercurrent capacitor banks (CPC) for the ITER fast discharge unit (FDU) and in the pulse forming network (PFN) with crowbar diodes.

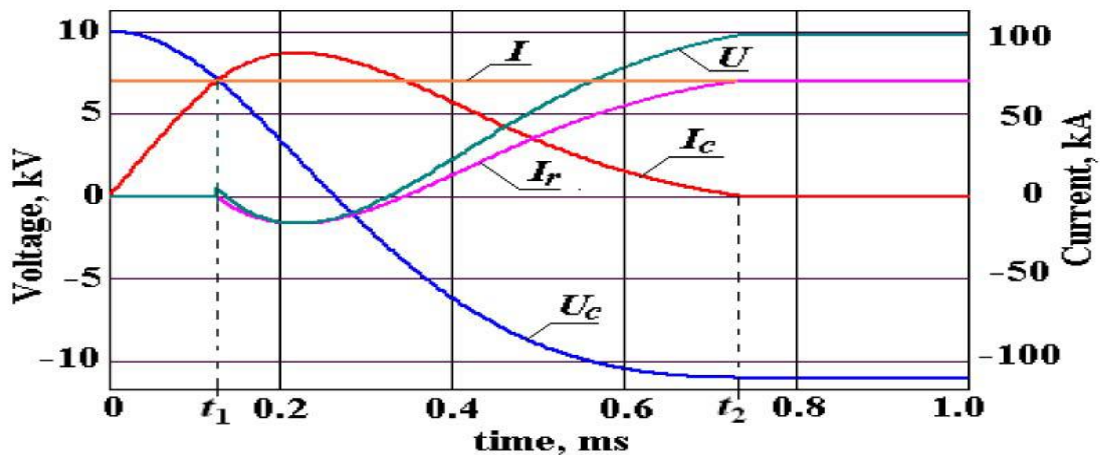


Fig. A.3.3 Currents and voltages in the circuits of Fig. 1 at fast discharge.
 $C = 1.6 \text{ mF}$, $L_1 = 16 \text{ } \mu\text{H}$, $L_2 = 2 \text{ } \mu\text{H}$, $R = 0.14 \text{ } \Omega$, $I = 70 \text{ kA}$, and

$$U_{c,0} = 10 \text{ kV.}$$

LTT in Discharge Circuits of Countercurrent Capacitor Banks for ITER Fast Discharge Units

The CPC is intended for quenching of an arc appearing at the opening of contacts of the vacuum circuit breaker (VCB) in the circuits of ITER superconducting magnet systems. The design and operation regimes of CPC are presented in figure3.4

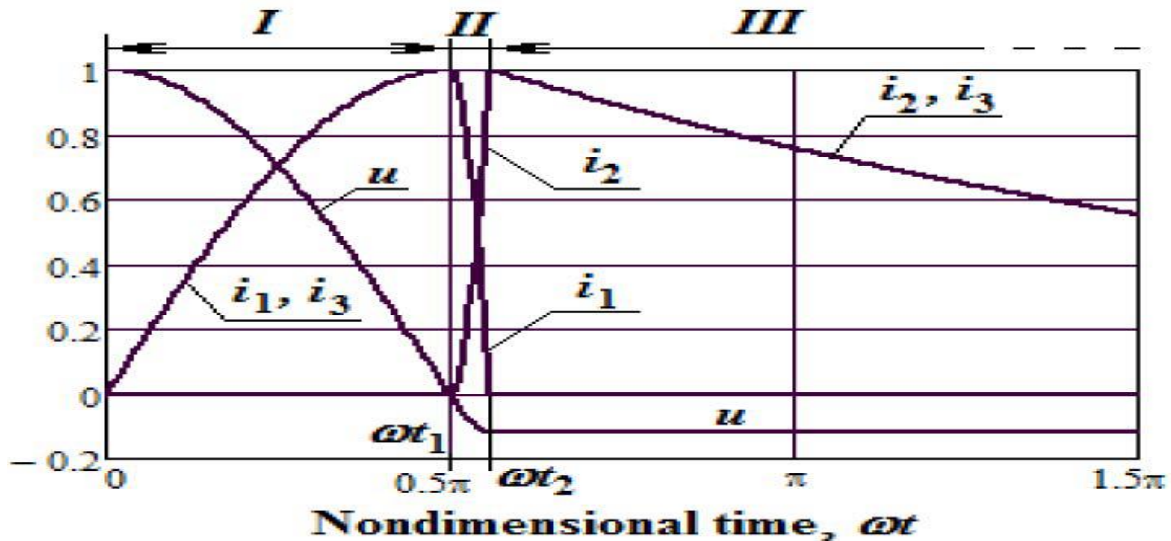


Fig. A.3.4 Discharge of PFN. Dimensionless functions: $u = U_c/U_0$,
 $i_1 = I_1/I_m$, $i_2 = I_2/I_m$, $i_3 = I_3/I_m \cdot (L_1/(L + L_1))^{1/2} = (t_2 - t_1)/$
 $t_1 = 0.12$

During the switching process at the opening of VCB (Fig. A3.2), the external current I flows through the arc between the VCB opening contacts. The charge voltage of the capacitor C is chosen so that the amplitude of the pulse current $I_{c,max} \approx (U_{c,0} C / (L_1 + L))^{1/2}$ exceeds the external current I . At the time instant, when the capacitor discharge current is equal to the external current $I_c(t_1) = I$, the arc is quenched and the current in VCB is interrupted. Then, the current I_c flows into the circuit of the discharge resistor (DR). The current and voltage waveforms shown in Fig. 3 illustrate the transients at fast discharge in the circuits shown in Fig.A7.

At the time t_2 , when the capacitor discharge is completed, the LTT is switched OFF. At this time instant, the voltage equal to the sum of the reverse voltage $U_{rev} = (L_1 + L_2)(di_c/dt)|_{t_2+}$ and the pulse over voltages appearing at reverse recovery of the thyristors are applied to LTT.

The CPC is tested in the short-circuit regime. In this regime, current in LTTs has the form of one sinusoidal half-wave; the current pulse amplitude is somewhat higher than during operation in the FDU. Switch-OFF of LTTs is accompanied by overvoltage, the value of which is close to the capacitor charge voltage plus the voltage spike caused by the reverse recovery of a semiconductor

switch . Thus, the operation conditions of the LTT switch (Fig. 1), when under test, are harder than the operation regimes in FDU.

2. Discharge circuit and Application of LTT

In order to clarifying my theory for the benefits of LTT Thyristor for discharging phenomenon and the application of attenuation in the cathode coil reactor of my samples, its necessary proving in this example [61]. “ The CPC is intended for quenching of an arc appearing at the opening of contacts of the vacuum circuit breaker (VCB)in the circuits of ITER superconducting magnet systems. The design and operation regimes of CPC are presented in [4]. During the switching process at the opening of VCB(Fig.A3.2), the external current I flows through the arc between the VCB opening contacts. The charge voltage of the capacitor C is chosen so that the amplitude of the pulse current

$$[I_{c,max} \approx (U_{c,0} \sqrt{C}/\sqrt{L1})]$$

exceeds the external current I .

At the time instant, when the capacitor discharge current is equal to the external current $I_c(t_1) = I$, the arc is quenched and the current in VCB is interrupted. Then, the current I_c flows into the circuit of the discharge resistor (DR).

The current and voltage waveforms shown in Fig. 3 illustrate the transients at fast discharge in the circuits shown in Fig.A3.2 . At the time t_2 , when the capacitor discharge is completed, the LTT is switched OFF. At this time instant, the voltage equal to the sum of the reverse voltage

$U_{rev} = (L_1 + L_2)(d I_c/dt)|_{t_2+}$ and the pulse over voltages appearing at reverse recovery of the thyristors are applied to LTT. The CPC is tested in the short-circuit regime. In this regime, current in LTTs has the form of one sinusoidal half-wave; the current pulse amplitude is somewhat higher than during operation in the FDU. Switch-OFF of LTTs is accompanied by overvoltage, the value of which is close to the capacitor charge voltage plus the voltage spike caused by the reverse recovery of a semiconductor switch. Thus, the operation conditions of the LTT switch (Fig.3.4) when under test, are harder than the operation regimes in FDU”[61] .

Transition of Switching Rates du/dt & di/dt for Snubber Application

The implementation of direct current (DC) transmission systems in new applications. The reason behind this prediction is that most power electronic systems, today, already implement an intermediate DC stage, which provides an easy access point for similar systems to be coupled to. This enables electrical energy to be exchanged among the respective systems. Such a direct DC coupling reduces the number of power conversion stages and results in a more reliable system with high efficiency. However, fast, reliable and maintenance-free DC switchgear needs to be developed before such a system can be realized.

A large retrofit market for mechanical DC switchgear already exists for present DC applications such as traction for public transport and material handling systems. This also provides an interesting market for new DC switchgear in the future. The interest in using conventional DC switches for the ever-increasing power demands (short circuit power and currents) have subsided dramatically because of their high maintenance.

The maintenance is required to counteract the contact erosion and subsequent damage to the insulated parts, brought about by the extended period of arcing when the switch is forced to open [52]. This has led to an increased interest in hybrid switching techniques and has already resulted in several direct current -hybrid switch (DC-HS) patents for ABB, El pro, GEC-Alstom, Schneider, Siemens and Westinghouse.

Even so, present techniques for constructing hybrid switches (HS) still have many disadvantages although they are being implemented in industry. This contribution first describes the problems encountered when implementing the common techniques of Zero Voltage Switching (ZVS) as well as Zero Current Switching (ZCS) and thereafter defines a new hybrid switch topology which combines both these switching techniques and thereby eliminates several of the disadvantages mentioned above.

Preliminary tests on a prototype of this hybrid switch technology, with a rated current of 7 kA and a line voltage of 3 kV DC, will be discussed. The prototype itself is shown in (Fig.A4.1)

5.1 Hybrid switching

Hybrid switching was already described by Heumann and Koppelman in 1965. A HS combines a mechanical switch with a solid-state semiconductor to profit from the low on-state resistance (mechanical switch) and reduced arcing (semiconductor), respectively. The advantages and disadvantages regarding mechanical and solid-state switching are given by Atmadji and Sloot. The HS is able to turn-off significantly faster than its conventional mechanical counterpart. Hereby, the conducted current is interrupted long before it can reach its prospective fault level, and therefore also at a far lower current value than would be the case for a mechanical switch. This implies that a low current-breaking capacity HS would be able to replace a mechanical switch with far higher current-breaking capacity.

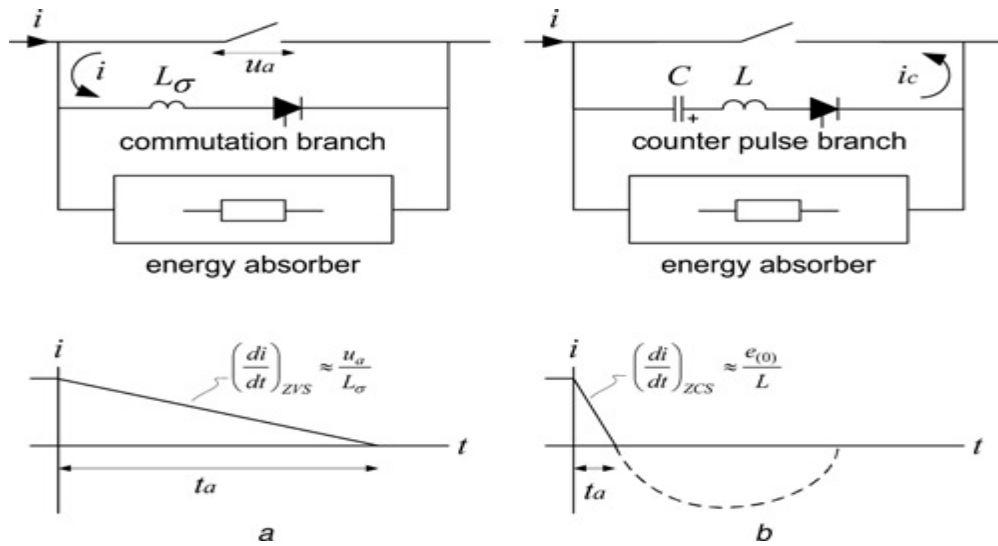


Fig. A4.1 Turn-off technique in a hybrid switch topology
 For ZVS switching the du/dt is determined mainly by parasitic components.
 The energy absorber reduces the voltage caused by the line
 current and the stored grid energy
 a for ZVS = du/dt
 b for ZCS = di/dt

Extensive research is being done on new HS topologies, like the one recently presented by Francis et al., which removes some of the disadvantages mentioned above but only for a specific topology or application. Their results indicate that the contact wear for a HS (*defined as material losses because of arc formation*) is two to three orders of magnitude lower than that for conventional breakers. Another important conclusion from them is that the material wear rapidly increases at arc durations (50–100 ms). Unfortunately, a HS still has a moving contact, making the occurrence of a short arc unavoidable for a successful commutation. The maximum arcing time together with the commutation speed (i.e. di/dt) can be translated to a maximum turn-off current [53] and is used as a design criterion.

In general, two main techniques such as zero voltage switching (ZVS) and zero current switching (ZCS) are used in hybrid switching. These techniques, which are discussed in the next paragraphs, must reduce the arcing time and thereby increase the lifetime of the mechanical switch. The energy provided to an arc during the turn-off transition depends on the voltage across the mechanical switch, the current through the mechanical switch, and the duration of the arc. In general, arc reduction and thereby radiated electro-magnetic interference (EMI) reduction can be realized by introducing a parallel branch to the mechanical switch, as shown in (Fig.A4.1).

5.1.1 Zero voltage switching

During ZVS, the main current is commutated to the parallel branch, which keeps the voltage across the switch close to zero when opening. The commutation process is dominated mainly by the arc voltage and the stray inductance between the mechanical switch and the power electronics. These parasitic components determine the typical ZVS turn-off technique, which is shown in Fig. a. The rate of current rise in the commutation branch can be determined by one mathematical formula ;

$$\left(\frac{di}{dt}\right) = \frac{U_a - U_{Tavg} - (i \cdot r_T)}{L_\sigma} \quad (A4.1)$$

where u_a is the material dependent arc voltage, u_{Tavg} the average on-state semiconductor voltage du/dt and L_σ the stray inductance between the mechanical switch and the commutation branch. The $i \cdot r_T$ component can be neglected if it is small in relation to the $(u_a - u_{Tavg})$ component. If the contact current and voltage are greater than the minimum required values for arc formation, an arc will form [53]. Shortly, after releasing the contacts, when the opening slit is close to $50\mu\text{m}$, the arc voltage steps to the so-called minimum required value that is typically between 11 and 14 V. The non-inductive voltage drop must remain smaller than the arc voltage in order for the current transfer to complete. It is possible to determine the maximum arcing time during the ZVS technique when the turn-off current, the typical rate of current rise, the stray inductance and the semiconductor parameters are known.

$$\begin{aligned} t_a(i) &\cong i * \left(\frac{L_\sigma}{U_a - U_{T0} - \left(\frac{1}{2}\right) r_T * i} \right) + t_d \\ &= i \left(\frac{di}{dt} \right) + t_d \quad (ZVS) = \frac{du}{dt} \dots \dots (A4.2) \end{aligned}$$

where i is the turn-off current, u_{T0} the semiconductor threshold voltage, r_T is the slope resistance and t_d the semiconductor turn-on delay time. This turn-on delay is often larger than that mentioned in most datasheets because of the low forward voltage and the often-reduced gate current at turn-on. Thus, the largest currents can be switched off when a small delay time, a large arc voltage, a small on-state voltage and a small stray inductance is realized complete ZVS commutation is illustrated in Fig. A11.

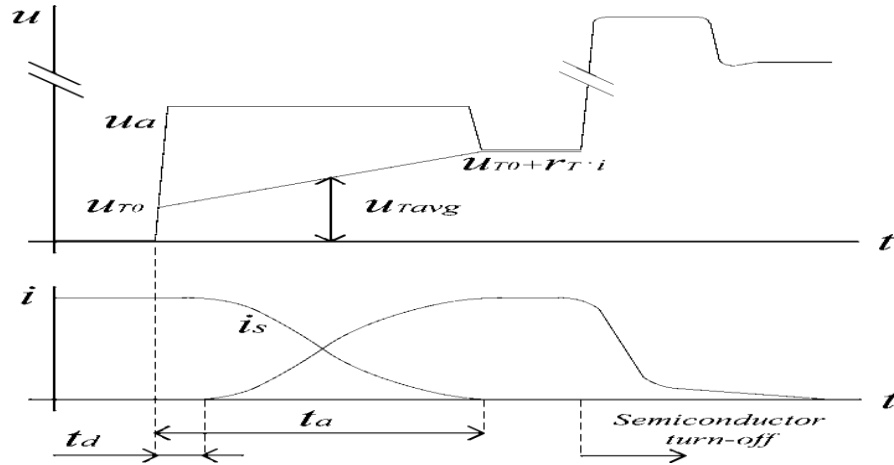


Fig. A4.2 Typical commutation when using the ZVS technique, where u_a is the arcing voltage, u_T the thyristor threshold voltage, i_s is the mechanical switch current, t_d the delay time thyristor t_a and the arcing time mechanical switch

Fig.A12 shows the arcing time against turn-off current for typical di/dt values [52] and a delay time t_d of 10 ms. This, together with the parameters mentioned in Hybrid switching application that is an important design criterion for hybrid ZVS techniques. For example, the parameters $u_a - u_{Tavg} = 4$ V and $L\sigma_{100} = \text{nH}$, resulting in an average di/dt of $40\mu\text{s/A}$, will enable currents up to ≈ 3.7 kA to be interrupted without violating the maximum critical arcing time of 100 μs .

5.1.2 Zero current switching

In the ZCS turn-off technique di/dt , an additional resonant current is realized, which flows in the opposite direction to the mechanical switch to reduce the main current (Fig.A10 b). At the moment, the switch opens the current through the mechanical switch is already close to zero, which reduces the arcing time and thereby the radiated EMI drastically. The counter current is realized with a pre charged capacitor, and the peak value (i_c) must be at least equal to the maximum short circuit current. This results in the first constraint for the determination of L and C in the counter pulse branch, shown in Fig. A10b.

$$e(0) - i_c * \sqrt{\frac{L}{C}} = 0 \dots (A4.3)$$

where $e(0)$ is the capacitor pre-charge value, L the total loop inductance and C the capacitance. Selecting the oscillation frequency is the next step. Its half period should be equal to the time required to open the mechanical switch just far enough that it is able to withstand the full network voltage. This results in the second constraint.

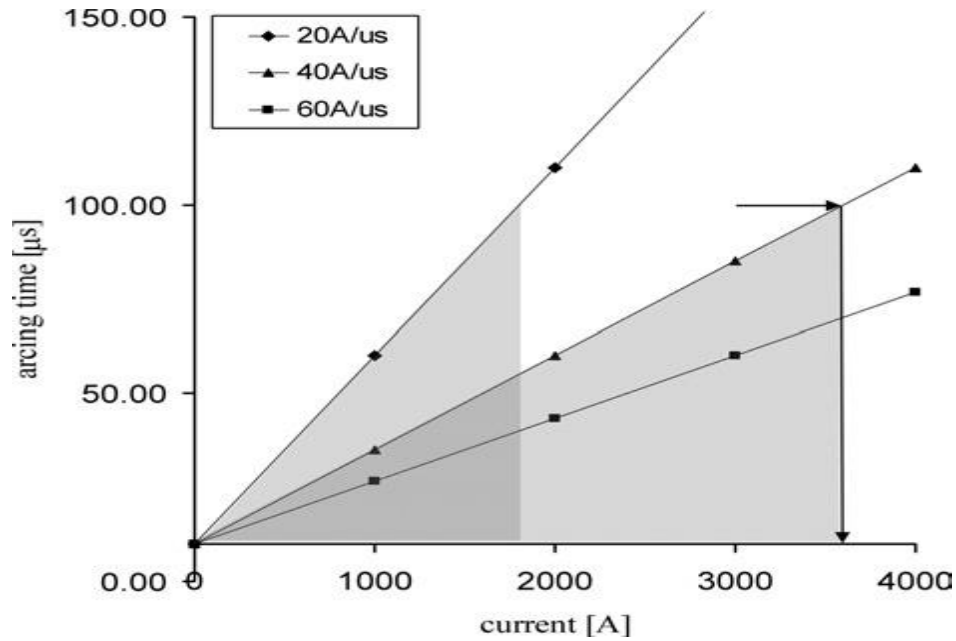


Fig . A4.3 Typical arcing time against turn-off current for three di/dt values

5.2 System set-up and working principle

Figure A13. shows the main components of power electronics which inset the combined HS as well as the DC grid representation that was used. The complete HS assembly is divided into two main cabinets, the ZVS(du/dt) and ZCS (di/dt) cabinet, respectively. The cabinet in the middle contains the ZVS power electronics (here after called main stack), the mechanical switch and its electromagnetic (EM) drive [54].

The main stack has been mounted parallel to the mechanical switch that has two anti parallel branches: a Gate Turn Off thyristor (GTO) branch and diode branch, T6 and D6, respectively. Current reduction during ZCS is performed by a LC counter pulse circuit, realized in a separate cabinet, and is located around T7, L7 and C7. This ZCS cabinet also contains the energy absorber (C7), the chopper (R8 and T8) and the charge reversal electronics (L9 and T9).

All commutation steps have been subdivided into equivalent circuits, which contain only linear components (such as sources R, L and C). To determine the component specifications for both switching techniques, the equivalent circuits have been used to derive analytical (current) waveforms. Table 1 shows the components used for this first prototype.

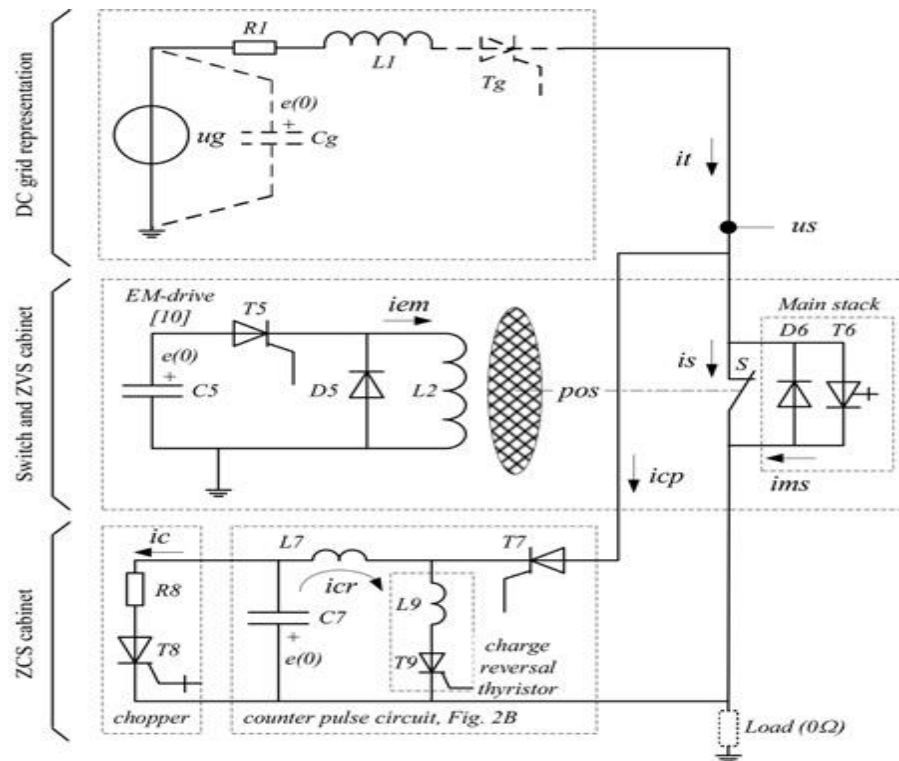


Fig. A4.4 Hybrid switching by inserting power electronics

Table A4.1
Components used for the ZVS and ZCS topologies

Component	Type/value	Remark
C7 series	1170 μ F	Two in
D6 series	4500V 1300A Fast diode	Two in
L7	25 μ H	At 1KHz
L9	40 μ H	At 1KHz
R1	37m Ω	
R8	445m Ω	
T6	4500V/4000A GTO	Two in series
T7	8500V/1200A thyristor	Two in series
T8	4500V/3500 A IGCT	Two in series
		Four parallel
T9	8500V/1200A thyristor	
C5/ T5/	1200 μ F thyristor 2000A/5200V	
D5/	2500A/5500V diode	
L2	8-23 μ H	

4.3 Switching process in power electronics

the loop inductance $L\sigma$, the arc voltage and the turn-on delay of the semiconductor switch. The inductance depends on the loop area. During normal conductive operation, the mechanical switch is closed. After the opening command, thyristor T6 is fired and the EM drive opens the mechanical contact. The arc voltage initiates the commutation, and when the commutation is completed, T6 is turned-off, both is respectively [52]. For all states mentioned equivalent circuits have been determined, which contains linear components (such as sources R, Land C). Analytical current waveforms for a ZVS turn-off sequence, with the same sequence indication was used.

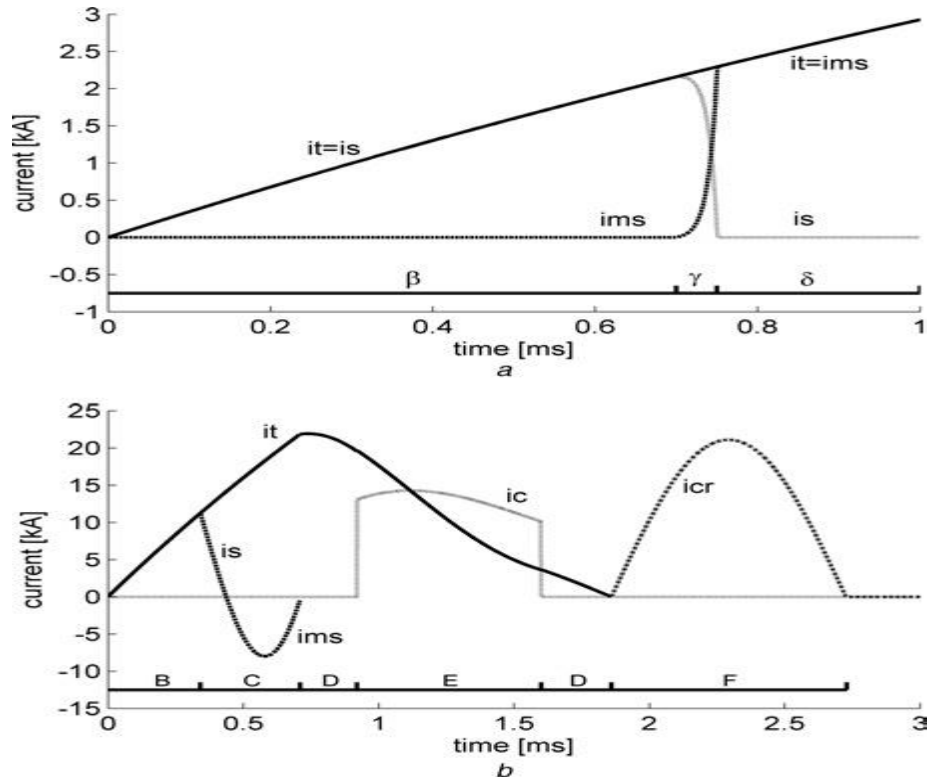


Fig. A4.5 Typical main currents (analytically determined via linear equivalent circuits)

and the following component parameters:

Grid: $R1 = 37 \text{ m}\Omega$, $L1 = 100 \text{ }\mu\text{H}$; ZVS: $L\sigma = 0.35 \text{ }\mu\text{H}$,
 $rT = 0.36 \text{ m}\Omega$, $uT = 4 \text{ V}$; ZCS: $C7 = 1170 \text{ }\mu\text{F}$, $L7 = 25 \text{ }\mu\text{H}$,
 $L9 = 40 \text{ }\mu\text{H}$, $R8 = 445 \text{ m}\Omega$, Chopper hysteresis settings $\frac{1}{4}$
 [5.9–4.5 kV a for ZVS commutation b ZCS turn-off]

The main stack has been developed to turn-off currents up to 2 kA with a maximum arcing time of 100 μs . Using A10, this results in a di/dt of at least $20\text{A}/\mu\text{s}$ or equivalently a stray inductance smaller than $0.4 \text{ }\mu\text{H}$. Stray inductance calculations have been done with the method described in shows the calculated arcing times as a function of the turn-off current (dotted line). Besides our own measurements, above parameters.

5.4 Theory of Rectifying process

The preliminary designing of soft starter basically depends on the two basic theories ; Kirchhoff's Law and the current commutation concepts du/dt & di/dt . For simplifying these two principles, the following diagrams which explain these concepts;

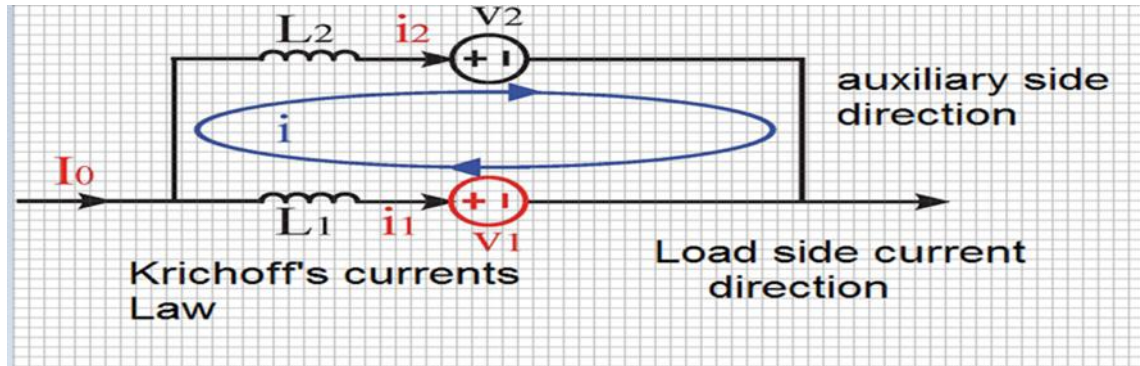


Fig. A4.6 Single line diagram of Kirchhoff's Law

$$I_0 = i_1 + i_2 \dots (A4.4)$$

$$V_1 + L_1 \frac{di_1}{dt} = V_2 + L_2 \frac{di_2}{dt} \dots (A4.5)$$

Commutation can be done by either a mechanical vacuum switching or a semiconductor switching here my designing uses LTT . The commutation begins at $t=0$ and ends at $t=T$, the total current remains I_0 as shown in fig. A4.5 and fig. A4.5 :

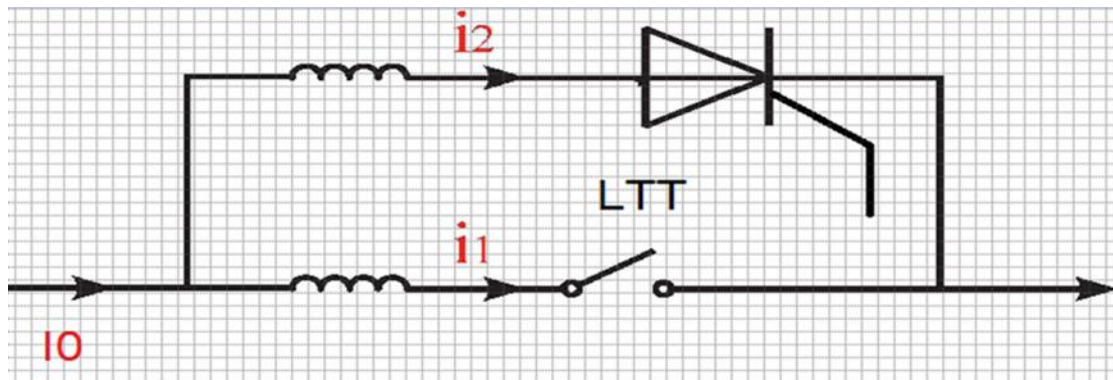


Fig. A4.7 Fabricated of LTT damping attenuation

REFERENCES

- [1] Xu Yao, Zeng Xiangjun, *Member IEEE*, Liu Zhanglei, Yi Wentao, “Novel Control Techniques of Petersen-coil” Electrical & Information Engineering, Changsha University of Science and Technology Changsha, Hunan Province, 410076, China; 978-1-4244-1706-3/08/\$25.00 ©2008 IEEE.
- [2] G.R. MITCHELL “ The high current vacuum arcs and its relevance to circuit interrupter” – PhD thesis , London university polytechnic , 1976.
- [3] Harris . L.P in LAFFERTY “ A mathematical model for cathode spot operation”13th international symposium on Discharges and electrical insulation in Vacuum , Albuquerque NM,USA 1978 .
- [4] Paul .G. Slade ,and. Mienko Braunovic : Electrical contacts, fundamentals , applications and technology .book.
- [5] J.P . Eichenberg , H. Hennenfent, “ Multiple Re-strikes Phenomenon when using Vacuum Circuit Breakers to start Refiner Motors”, IEEE 1998, pp. 266-273.
- [6] Shaoyong Cheng Jimei Wand, “Book Study of High- Current Vacuum Arc Characteristics Under Self – generated Axial Magnetic field of Contact at a long Contact Gap for H.V Vacuum Interrupter”, (0093-38/\$25.00@2008IEEE).
- [7] M. Carabok , R, Jackson , “ An investigation into an insulation failures associated with frequent operated vacuum circuit breakers” , CIRED 1.09.1, 1995.
- [8] M. Murano, S. Yanabu, “ Current chopping Phenomena of medium voltage circuit breakers” IEEE vol 96. Pp243,1977.
- [9] R.P.P .Smeets, “The origin of chopping current” IEEE on Plasma science vol 17,No.2,1989.
- [10] J.F.Perkins; Evaluation of switching surge over voltages on medium voltage power systems, Westinghouse electric corporation , switchgear division , East Pittsburgh Pennsylvania, IEEE1982.
- [11] J.P .Eichenberg , H. Hennenfent & L.Liljestrang ;”ABB Corporate Research Center , Västerås ,Sweden “ Multiple Re-Strikes Phenomenon when Using Vacuum Breaker to Start Refiner Motors” 1998IEEE.
- [12] Wolfhard Merz, Monty Grimes ; “ Fast opening switch approach for high-voltage vacuum tube protection application , Behlke Power Electronic LLC978-1-4673-1225-7/12/\$31.00©2012IEEE.
- [13] Ansgar Mueller, Dieter . Saemann ; switching phenomena in medium voltage systems –good engineering practice on the application of vacuum circuit breakers and contactors SIEMENS power engineering.
- [14] B. R. Pelly .. Research and development Laboratories /Westinghouse Electric Corporation Pittsburg , Pennsylvania .
- [15] Heinrich J.Boening , John W.Schwartzebberg, Lawrence J.Willinger ,Dane E. Piccone,Duane A.Lopez , Howard A.Smolleck .; “Design and Testing of High Power

Repetitively Pulsed , Solid-State Closing Switches”IEEE 1997 (Los Alamos National Laboratory ,MSE536, Los Alamos , NM87545.

- [16] Susan. E. CHILDS , Allan .N. GREENWOOD ; “Events associated with zero current passage during the rapid commutation of a vacuum arc”IEEE1983.General Electric Co.(0093-3813/83/0900-18\$01.00©1983IEEE).
- [17] MIETEK GLINKOWSKI & ALLAN GREENWOOD, “Some interruption criteria for short high frequency vacuum arcs” [0093-3813/89/1000-0741\\$1.00©1989IEEE](#)
- [18] J .Dom, U. Kellner, F.J.Neidemostheide, H .J . Schuldze , “State of the Art Light Triggered Thyristors with Integrated Protection Functions”. Power Electronics Europe Issue 2, 2002,pp29-35
- [19] High Power Directed –light –Triggered Thyrsitor valve Technology . The basis for advanced power electronics ,solutions in transmission systems – SIEMENS.
- [20] F.J.Niedemostheide , H.J.Schulze, U.Kellner –Werdehausen , “ Self protected High Power Thyrsitors” PCIM 2001, Power Conversion (Nurnberg , Germany), pp51-56.
- [21] W. Merz, J.P. Jensen „Light Triggered ThyristorCrowbar for Klystron Protection Application”,Proceedings of the PAC 2003, pp. 749-751.
- [22] W. Merz, DESY, Hamburg, Germany “ High Charge Transfer Operation of LTT Light Triggered Thyristor – Crowbars”; IEEE -Particle Accelerator Conference, 2003. PAC 2003.
- [23] J.P. Eichenberg, QUNO Corporation, Thorold , Ontario, Canada , H.Hennenfent , Avenor Inc., Thunder Bay, Ontario , Canada , L.Liljestrang , ABB Corporate Research , Västerås , Sweden, “ Multiple Re-Strike Phenomenon when Using Vacuum Circuit Breakers to Start Refiner Motors” 1998IEEE P.P 266- 273.
- [24] MATLAB/SIMULINK software application for Fourier series currents explanation and experiments for vacuum research project .
- [25] Erwin Kreyszig “ Fourier series, Euler’s Formulas” switching application technique of vacuum interrupter , section 8.2 P.P 431-485. Advanced Engineering Mathematic.
- [26] Erwin Keryszig" Periodic Functions of Laplace Transform " chapter 4.PP192-234.
- [27] Shaoyong Cheng Jimei Wand, “Study of High- Current Vacuum Arc Characteristics Under Self – generated Axial Magnetic field of Contact at a long Contact Gap for H.V Vacuum Interrupter”, (0093-38/\$25.00@2008IEEE).
- [28] Shaker Jassem Gatan ; “Algorithmic Application for Calculation of Chopping Currents and High Transient over-Voltages for a New Vacuum Interrupter” ISSN: 2603-3259 --(ICEST 2017) p,p 341-34 IEEE-2016.
- [29] G. Ecker and I. Paulus, “The short vacuum arc-Part 2: model and theoretical aspects,” IEEE Trans. Plasma Sci., vol. 16, no. 3, pp. 348–351,Jun. 1988.
- [30] Milenko Braunovic , “ Contacts material book” page 42.
- [31] Reference 18, p.137-145 ; Milenko Braunovic , “ Contacts material book”.

- [32] Reference 19, p. 221-281 ; Milenko Braunovic , “ Contacts material book.
- [33] Paul .G. Slade ,and Dr. Mienko Braunovic : Electrical contacts, fundamentals , applications and technology.
- [34] YOUNG , A.F.B :” Some researchers in current chopping in high voltage circuit breakers” IEEE .1953,100,p337.
- [35] Richardson ,O,W; “ Emission of electricity from hot bodies” Proc, Cambridge Philos, Soc 1901,11,p.286.
- [36] Shottky. W .: “ Emission of electron from an incandescent filament under the action of a retarding potential” Ann.Phy. 1914,P1011 .
- [37] Murrphy , E, L, and Good , R,H,: “ Thermionic emission , field emission and transition” ,Phy, Rev , 1956 102 , p. 1464.
- [38] LEE, T.H and Greenwood . A:” Theory for the cathode mechanism in metal vapor arcs” J, Appl. Phys. 1961,32. 916-923.
- [39] Reference 1, p.225, (*Prof.Gunther Ecker*).
- [40] Ecker .G.in Lafferty , J.M .(ED.): “ Vacuum arcs- theory and application”(Wiley, 1980) page 229.
- [41] Harris, L . P: “ A mathematical model for cathode spot operation” , proceeding of 8th international symposium on discharges and electrical installation in vacuum , Albuquerque NM.USA 1978.
- [42] ZALICKI,Z, and KUTZNER,J.: ‘ Stream od neutral particles reflected from the anode in vacuum arc’, Proceeding of the 5th international symposium on discharges and electrical insulation in vacuum, 1972.
- [43] LITTLE .R.P., and WHITENY ,W.T.: ‘ Electron emission preceding electrical breakdown in vacuum , J.App.Phys. , 1963,34,pp. 2430-2434.
- [44] MILLER H.C., and FARRALL ,G.A.: ‘ Polarity effect in vacuum breakdown electrode conditioning’ J.App. phys., 1965,36,pp. 1338-1344
- [45] GRANBURG, L .: ‘ The initiation of electrical breakdown in vacuum’ ,J.App.phys., 1952,23,p.518 .
- [46] OLENDZKAYA, N.F.: ‘Vacuum breakdown with transfer of conducting particles between electrodes’ ,Radio Eng . Electron phys., 1963,8,p.423
- [47] P.A., and BIRADAR, P.I.: ‘Micro particle processes occurring prior to vacuum breakdown’ , Z. Angew Phys., 1970,30,p.163
- [48] ROZANOVA,N.B., and GRANOVSKII, V.L.: ‘ On the initiation of electrical break down of a high vacuum gap’ ,Sov.phys.Tech.phys., 1956,1,p.471.
- [49] MILLER H.C and FARRALI .G.A “ Polarity effect in vacuum breakdown electrode conditioning” J.App, Physic,1965. 36, pp 1338-1344.
- [50] BOUCHARD, K,G.: ‘Vacuum breakdown strength of persion-strengthened vs. oxygen-free, high-conductivity copper’ ,J,Vac.Sci.Tevhnol., 1970.7,p..358.

- [51] MCCOY ,F,COENRAADS,C and THYAYER,M.: ‘ Some effects of electrode metallurgy and field emission voltage strength in vacuum’, proceedings of 1st international symposium on High voltages in vacuum, Cambridge, MA,USA, 1964.
- [52] B. Roodenburg, A. Taffone, E. Gilardi, S.M. Tenconi, B.H. Evenblij and M.A.M. Kaanders “ Combined ZVS–ZCS topology for high-current direct current hybrid switches: design aspects and first measurements” IET Electr. Power Appl., 2007, 1, (2), pp. 183–192 183.
- [53] Greitzke, S., and Lindmayer, M.: “*Commutation and erosion in hybrid contactor systems, components, hybrids, and manufacturing technology*”, IEEE Tran. Compon., Packag. Manuf. Technol. A, B,C, 1985, 8, (1), pp. 34–39.
- [54] Roodenburg, B., Huijser, T., and Evenblij, B.H.: “*Simulation of an electro-magnetic (EM) drive for a fast opening circuit breaker contact*”. IEE Pulsed Power Symp., Basingstoke, UK, 8 September 2005, ISBN 0-86341-558-x, pp. 4/1–4/6.
- [55] REECE,M.P.: “ The vacuum switch part-1 properties of the vacuum proc. IEE ,1963 ,110, pp.793-802,1999.
- [56] Luhui Liu, Jinwu Zhuang, Chen Wang, Zhuangxian Jiang, Jin Wu, and Bo Chen. “ A Hybrid Vacuum Circuit Breaker for Medium Voltage: Principle and First Measurements” 0885-8977 © 2014 IEEE.
- [57] D. Lorenzi, G. Taddia, and V. Teigo, “Design and tests the 50 kA-18 kV thyristor making switches for the RFX experiment,” Fusion Eng.Design, vol. 58–59, pp. 23–27, Nov. 2001.
- [58] [one line] Available www.abb.com/semiconductors .
- [59] Wolfhard Merz, Monty Grimes ; “ Fast opening switch approach for high-voltage vacuum tube protection application , Behlke Power Electronic LLC.
- [60] J.P .Eichenberg , H. Hennenfent & L.Liljestrang ;”ABB Corporate Research Center , Västerås ,Sweden “ Multiple Re-Strikes Phenomenon when Using Vacuum Breaker to Start Refiner Motors” 1998IEEE.
- [61] Roman A. Serebrov, Boris E. Fridma , Alexey A. Khapugin and valentin A. Martynenko " Development and Research of Heavy Pulse Current LTT Switches"003-3813©2016.
- [62] B.Fridman , T.Enikeev, N.Kovrizhnykh , A. Pekhotnyi , A. Roshal, R.Serebrov, K.kharcheva,” Capacitor bank for fast discharge unit of ITER Facility” .D.V. Efremov Institute of Electrophysical Apparatus , Metalloscopy , St. Petersburg, Russia 978-1-4673-3/13/\$31.00©2013IEEE.
- [63] B.Fridman , R. Enikeev, K.kharcheva, , N.Kovrizhnykh, R.Serebrov,”Counter pulse capacitor bank for 70KA, 10KV Commutation system” D.V. Efremov Institute of Electrophysical Apparatus , Metalloscopy , St. Petersburg. 978-1-4673-5168-3/13/\$31.00© 2013IEEE

- [64] Chang Peng, Alex Q. Huang, Xiaoqing Song, “ Current Commutation in A Medium Voltage Hybrid DC Circuit Breaker using 15 kV Vacuum Switch and SiC Devices” 978-1-4 799-6735-3/15/\$31.00 ©20 15 IEEE.
- [65] Allan Greenwood, T.H.Lee , “ Generalized damping curves and Their use in solving power switching transients”, IEEE August 1963.
- [66] Emmanuel Kwaku Amankwah, “*A Parallel Hybrid Modular Multilevel Converter for High Voltage DC Applications*” Submitted to the University of Nottingham for the degree of Doctor of Philosophy, August, 2013.
- [67] ZHU Liying¹; QIAO Ming¹; WU Jianwen²; CUI Bo¹, “Splitting of Vacuum Arc Column in Transverse Magnetic Field Contacts at Intermediate-Frequency” 978-1-4673-7414-9/15/\$31.00 ©2015 IEEE.
- [68] Shaker Jassem Gatan ; “Algorithmic Application for Calculation of Chopping Currents and High Transient over-Voltages for a New Vacuum Interrupter” ISSN: 2603-3259 --(ICEST 2017) p,p 341-34 IEEE-2016.
- [69] R. L. Boxman, Gerby Eli, Goldsmith, “Behavior of a High Current Vacuum Arc between Hollow Cylindrical Electrodes in a Radial Magnetic Field S”. IEEE Transactions on Plasma Science, vol.8,no.4,pp.308-313, 1980.
- [70] Wolf C, Kurrat M, Lindmayer M, et al. “*Arcing behavior on TMF contacts at high-current interrupting operations*”, International Symposium on Discharges and Electrical Insulation in Vacuum, ISDEIV, Braunschweig, Germany,2010.
- [71] Falkingham L.T., K. Cheng. 1998, “Further experiments in high current switching using small contact gaps”, International Symposium on Discharges and Electrical Insulation in Vacuum, Eindhoven, Netherland.
- [72] Zhu Liying, Wu Jianwen, Liu Bin, et al, “The Dynamic Volt-Ampere Characteristics of a Vacuum Arc at Intermediate-Frequency Under a Transverse Magnetic Field”. Plasma science and technology, vol.15, no.1, pp.30-36, January 2013.
- [73] Zhu Liying, Wu Jianwen, and Zhang Xueming, “Arc Movement of Intermediate-Frequency Vacuum Arc on TMF Contacts” IEEE Transactions on Power Delivery, vol.28, no.4, pp. 2014-2020, October2013.
- [74] Harris, L. P. (1983). "Transverse Forces and Motions at Cathode Spots in Vacuum Arcs." IEEE Transactions on Plasma Science,vol.PS-11,no.(3), pp.94-102, 1983.
- [75] B. Fridman, R. Enikeev, K. Kharcheva, N. Kovrizhnykh, andR. Serebrov, “*Counter pulse capacitor bank for 70 kA, 10 kV commutation system,*” in IEEE PPC Dig. Tech. Papers, Jun. 2013, pp. 1–6.
- [76] B. E. Fridman, “*Transients in pulsed electrical circuits with massive conductors,*” IEEE Trans. Plasma Sci., vol. 34, no. 5, pp. 1938–1943,May 2006.

- [77] Sentaurus Device User Guide, Synopsys Inc., Mountain View, CA, USA, 2014.
- [78] R. A. Serebrov, R. S. Enikeev, and B. E. Fridman, "Semiconductor switches in a counterpulse capacitor bank," *IEEE Trans. Plasma Sci.*, vol. 41, no. 1, pp. 250–256, Jan. 2013.
- [79] A. Greenwood and T. Lee, "Theory and application of the commutation principle for HVDC circuit breakers," *IEEE Trans. Power App. Syst.*, vol. PAS-91, no. 4, pp. 1570–1574, Jul. 1972.
- [80] W. Premerlani, "Forced commutation performance of vacuum switches for HVDC breaker application," *IEEE Trans. Power App. Syst.*, vol. PAS-101, no. 8, pp. 2721–2726, Aug. 1982.
- [81] Y. Niwa, T. Funahashi, K. Yokokura, J. Matsuzaki, M. Homma, and E. Kaneko, "Basic investigation of a high-speed vacuum circuit breaker and its vacuum arc characteristics," *Proc. Inst. Elect. Eng. Transm. Distrib.*, vol. 153, no. 1, pp. 11–15, Jan. 2006.
- [82] A. Yaniv, A. Pokryvailo, E. Shviro, and A. S. Kesar, "Implementation aspects of dc hybrid opening switch," in *Proc. Int. Power Modulators High Voltage Conf.*, Las Vegas, NV, USA, May 27–31, 2008, pp. 507–510.
- [83] D. Alferov, A. Budovsky, D. Evsin, V. Ivanov, V. Sidorov, and V. Yagnov, "DC vacuum circuit-breaker," in *Proc. 23rd Int. Symp. Discharges Elect. Insul. Vacuum*, Bucharest, Romania, Sep. 15–19, 2008, pp. 173–176.
- [84] X. Song, Z. Shi, C. Liu, H. Yang, M. Ma, S. Jia, and L. Wang, "Experimental investigation on the characteristics of drawn vacuum arc in initial expanding stage and in forced current-zero stage," *IEEE Trans. Plasma Sci.*, vol. 39, no. 6, pp. 1330–1335, Jun. 2011.
- [85] M. B. Schulman and P. G. Slade, "Sequential modes of drawn vacuum arcs between butt contacts for currents in the 1 kA to 16kA range," *IEEE Trans. Compon. Packag. Manuf. Technol. A*, vol. 18, no. 2, pp. 417–422, Jun. 1995.
- [86] M. B. Schulman, "Separation of spiral contacts and motion of vacuum arcs at high currents," *IEEE Trans. Plasma Sci.*, vol. 21, no. 2, pp. 484–488, Oct. 1993.
- [87] M. B. Schulman, "The behavior of vacuum arcs between spiral contacts with small gaps," *IEEE Trans. Plasma Sci.*, vol. 23, no. 2, pp. 915–918, Dec. 1995.
- [88] M. B. Schulman, P. G. Slade, and J. V. R. Heberlein, "Effect of an axial magnetic-field upon the development of the vacuum-arc between opening electric contacts," *IEEE Trans. Compon. Packag. Manuf. Technol. A*, vol. 16, no. 2, pp. 180–189, Mar. 1993.
- [89] G. Ecker and I. Paulus, "The short vacuum arc-Part 2: model and theoretical aspects," *IEEE Trans. Plasma Sci.*, vol. 16, no. 3, pp. 348–351, Jun. 1988.
- [90] Z. Jiang, J. Zhuang, C. Wang, L. Liu, and C. Dai, "Simulation analysis and design of a high speed contact mechanism based on electro-magnetic repulsion mechanism," *Trans. China Electrotech. Soc.*, vol. 26, no. 8, pp. 172–177, Aug. 2011.

- [91] A. D. Lorenzi, G. Taddia, and V. Teigo, "Design and tests the 50 kA-18kV thyristor making switches for the RFX experiment," *Fusion Eng.Design*, vol. 58–59, pp. 23–27, Nov. 2001.
- [92] S. Tamura, Y. Kito, R. Shimada, Y. Kanai, H. Koike, and H. Ikeda, "Parallel interruption of heavy direct current by vacuum circuit breakers," *IEEE Trans. Power App. Syst.*, vol. PAS-99, no. 3, pp.1119–1129, May/Jun. 1980.
- [93] L. Novello, F. Baldo, A. Ferro, A. Maistrello, and E. Gaio, "Development and testing of a 10-kA hybrid mechanical-static dc circuitbreaker," *IEEE Trans. Appl. Supercond.*, vol. 21, no. 6, pp. 3621–3627, Dec. 2011.
- [94] S. Cheng et al., "Study on a new single coil type axial magnetic field contact for high voltage vacuum interrupters," *IEEE Trans. Plasma Sci.*, vol. 35, no. 2, pp. 425–433, Apr. 2007.
- [95] Siemens-Sustainable Energy <http://www.energy.siemens.com>.
- [96] H. Zimmer, J. Dragon, J. Hanson, "Basic design considerations for a mechanically switched capacitor with damping network (MSCDN) within a high-voltage-grid"
- [97] IEC 61000-3-6, *Assessment of emission limits for the connection of distorting installations to MV, HV and EHV power systems*, 2008.
- [98] R. C. Campos, D. O. Lacerda and M. F. Alves, Mechanically Switched Capacitor with Damping Network(MSCDN) - Engineering Aspects of Application, Design and Protection , 2010 IEEE/PES Transmission and Distribution Conference and Exposition: Latin America.
- [99] G. Balzer, Switching Phenomena in Medium-voltage Power Systems and Their Consideration in Project Planning, *Brown Boveri Review*, Volume 73, 5/1986, pages 270-278
- [100] H. Hamid, N. Harid, Transient Analysis during Switching of Mechanically Switched Capacitor and Damping Network (MSCDN), 2010 45th International Universities Power Engineering Conference (UPEC).
- [101] Anton V. Schneider, Sergey A. Popov, Alexander V. Batrakov, and Valery A. Lavrinovich, " High-Current Vacuum Arc Shunted by a Semiconductor Switch on Kiloampere Current Interruption" 0093-3813 © 2016 IEEE.
- [102] V. V. Mitsun, L. N. Lenskaya, and V. I. Golub, "Efficiency of diodes for switching inductive loads," (in Russian), *Vopr. Radioelektron., TPS Ser.*, no. 4, pp. 59–67, 1973.
- [103] D. F. Alferov, D. V. Evsin, and V. P. Ivanov, "Study of the current transfer between a diode valve and vacuum arc-quenching chamber," in *Proc. 9th Symp. Elect. Eng. 2030*, report 5.16, Moscow region, Russia, May 2007.
- [104] G. A. Kukekov, *High-Voltage AC Switches*, (in Russian). Moscow, Russia: Energia, 1972.
- [105] N. M. Batlov and B. P. Petrov, *Traction Electrical Devices*, (in Russian). Moscow, Russia: Energia, 1969, p. 240.
- [106] P. G. Slade, *The Vacuum Interrupter: Theory, Design, and Application*. New York, NY, USA: CRC Press, 2008, ch. 2.
- [107] J. M. Lafferty, Ed., *Vacuum Arcs: Theory and Application*. New York, NY, USA: Wiley, 1980.

- [108] J. Hastings, J. Zuercher, and E. Hetzmanseder, “Electrical arcing and material ignition levels,” SAE Tech. Paper 2004-01-1565, 2004.
- [109] R. L. Boxman, D. M. Sanders, and P. J. Martin, Eds., *Handbook of Vacuum Arc Science & Technology: Fundamentals and Applications*. Park Ridge, NJ, USA: Noyes, 1995, p. 742.
- [110] N. A. Kolechitskaya, N. S. Lazarev, R. A. Lytaev, and M. V. Frolova, “Some features of the choice of FACST fault current limitation devices,” in Proc. 9th Symp. Elect. Eng. 2030, report 1.13, Moscow region, Russia, May 2007.
- [111] A. Schneider, S. Popov, V. Durakov, B. Dampilon, S. Dehonova, and A. Batrakov, “On breaking capacity of the CuCr25 composite material produced with electron-beam cladding,” in Proc. 25th ISDEIV, Tomsk, Russia, Sep. 2012, pp. 269–271. Interruption” 0093-3813 © 2016 IEEE.
- [112] [Online]. Available: <http://www.amsc.com>. [Online]. Available: <http://www.superpower-inc.com>.
- [113] Sastry Pamidi, Jozef Kvitkovic, Ulf Trociewitz, Sasha Ishmael, Rainer Meinke, and Gerry Stelzer “A Novel Magnet for AC Loss Measurements on 2G Superconductor Rings and Coils in Axial and Radial Magnetic Fields” 1051-8223/\$26.00 © 2011 IEEE.
- [114] V. V. Mitsun, L. N. Lenskaya, and V. I. Golub, “Efficiency of diodes for switching inductive loads,” (in Russian), *Vopr. Radioelektron.*, TPS Ser.,no. 4, pp. 59–67, 1973.
- [115] D. F. Alferov, D. V. Evsin, and V. P. Ivanov, “Study of the currenttransfer between a diode valve and vacuum arc-quenching chamber,” inProc. 9th Symp. Elect. Eng. 2030, report 5.16, Moscow region, Russia,May 2007.
- [116] G. A. Kukekov, *High-Voltage AC Switches*, (in Russian). Moscow,Russia: Energia, 1972.
- [117] N. M. Batlov and B. P. Petrov, *Traction Electrical Devices*, (in Russian).Moscow, Russia: Energia, 1969, p. 240.
- [118] P. G. Slade, *The Vacuum Interrupter: Theory, Design, and Application*.New York, NY, USA: CRC Press, 2008, ch. 2.